

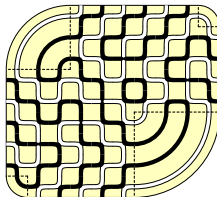
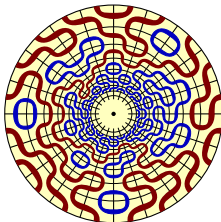
Around the Razumov-Stroganov correspondence



UNIVERSITÀ DEGLI STUDI
DI MILANO

Andrea Sportiello

65th Séminaire Lotharingien de Combinatoire
Strobl (Austria) – 13-15 September 2010



A scheme of the lectures

Lecture 1

O(1) Dense Loop Model, Fully Packed Loops, Plane Partitions

statement of the Razumov-Stroganov correspondence
FPL, ASM, TSSCPP and all that (with plenty of bijections)

Lecture 2

Proof of the Razumov-Stroganov correspondence

lemmas from Yang-Baxter integrability
lemmas from the generalized Wieland gyration

Lecture 3

Asymptotics of large Alternating Sign Matrices

rederivation of the Colomo-Pronko arctic curve
arctic curve for the triangloid domain

General bibliography on background topics

D.M. Bressoud and J. Propp,

How the Alternating Sign Matrix Conjecture was solved

Notices of the American Mathematical Society **46** 637-646 (1999)

D.M. Bressoud, *Proofs and Confirmations:*

the Story of the Alternating Sign Matrix Conjecture

Lecture Notes of Les Houches Summer School, session 89, July 2008

Exact Methods in Low-dim. Statistical Physics and Quantum Computing

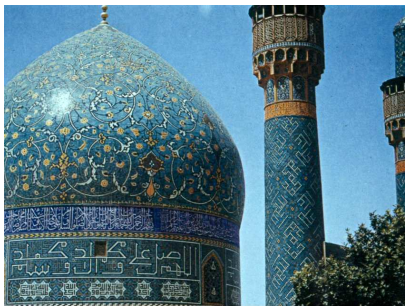
- 6 B. Nienhuis *Loop models*
- 7 N. Reshetikhin *Integrability of the 6-vertex model*
- 12 R. Kenyon *The dimer model*
- 17 P. Zinn-Justin *Integrability and combinatorics: selected topics*

➡ P. Zinn-Justin, *HDR Report*, arXiv: math-ph/0901.0665

➡ Tiago Fonseca, *PhD Thesis*

Stating the Razumov-Stroganov correspondence

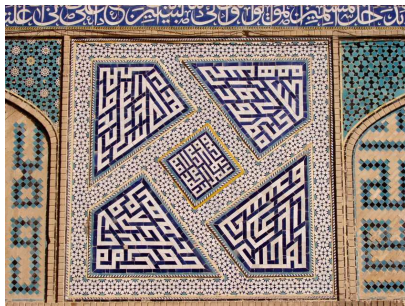
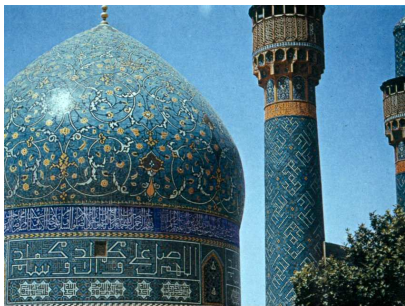
A prolog in Eastern Arts. . .



For hystorical and religious reasons, there has been a flourishing of geometrical tilings in Eastern Arts and Architecture...

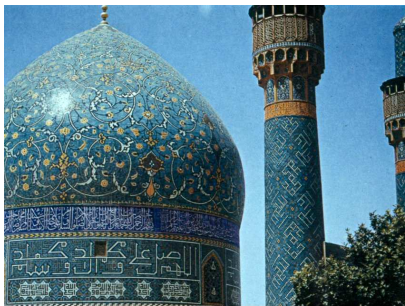
(photos are of Isfahan)

A prolog in Eastern Arts. . .



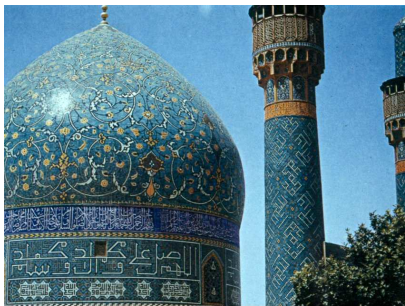
...Here you see, besides **regular** tilings, also **random** tilings of the plane...

A prolog in Eastern Arts. . .

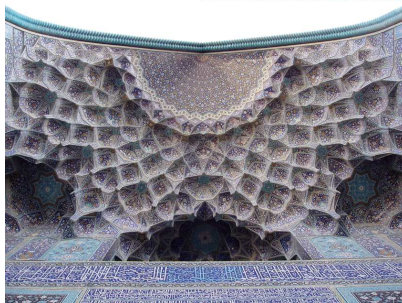


...Here you see, besides **regular** tilings, also **random** tilings of the plane...

A prolog in Eastern Arts. . .



...and well, ok, this is not a Plane Partitions, but...



Three Random Tiling Problems

O(1) Dense Loop Model

XXZ Quantum Spin Chain at $\Delta = -\frac{1}{2}$

Potts Model at edge-percolation

–

Fully-Packed Loops (FPL) in a square

Alternating Sign Matrices (ASM)

Six-Vertex Model at $\Delta = +\frac{1}{2}$ (Ice Model)

“Gog” triangles

–

TSSCPP (Plane Partitions)

Dimer coverings / Lozenge tilings

NILP (Non-intersecting Lattice Paths)

“Magog” triangles

Three Random Tiling Problems

► **O(1) Dense Loop Model**

XXZ Quantum Spin Chain at $\Delta = -\frac{1}{2}$

Potts Model at edge-percolation

–

Fully-Packed Loops (FPL) in a square

Alternating Sign Matrices (ASM)

Six-Vortex Model at $\Delta = +\frac{1}{2}$ (Ice Model)

“Gog” triangles

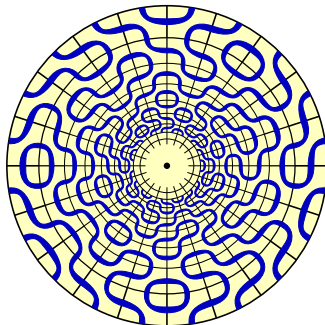
–

TSSCPP (Plane Partitions)

Dimer coverings / Lozenge tilings

NILP (Non-intersecting Lattice Paths)

“Magog” triangles



Three Random Tiling Problems

O(1) Dense Loop Model

XXZ Quantum Spin Chain at $\Delta = -\frac{1}{2}$

Potts Model at edge-percolation

–

- ➔ **Fully-Packed Loops** (FPL) in a square
- Alternating Sign Matrices (ASM)
- Six-Vortex Model at $\Delta = +\frac{1}{2}$ (Ice Model)
- “Gog” triangles

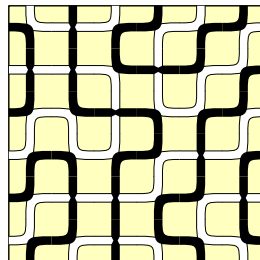
–

TSSCPP (Plane Partitions)

Dimer coverings / Lozenge tilings

NILP (Non-intersecting Lattice Paths)

“Magog” triangles



Three Random Tiling Problems

O(1) Dense Loop Model

XXZ Quantum Spin Chain at $\Delta = -\frac{1}{2}$

Potts Model at edge-percolation

–

Fully-Packed Loops (FPL) in a square

Alternating Sign Matrices (ASM)

Six-Vortex Model at $\Delta = +\frac{1}{2}$ (Ice Model)

“Gog” triangles

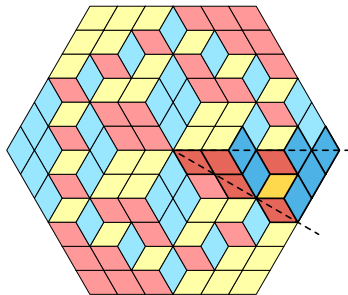
–

➔ **TSSCPP** (Plane Partitions)

Dimer coverings / Lozenge tilings

NILP (Non-intersecting Lattice Paths)

“Magog” triangles



Three Random Tiling Problems

O(1) Dense Loop Model

XXZ Quantum Spin Chain at $\Delta = -\frac{1}{2}$

Potts Model at edge-percolation

–

Fully-Packed Loops (FPL) in a square

Alternating Sign Matrices (ASM)

Six-Vortex Model at $\Delta = +\frac{1}{2}$ (Ice Model)

“Gog” triangles

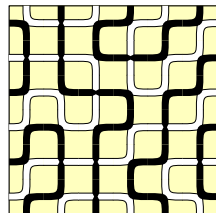
–

TSSCPP (Plane Partitions)

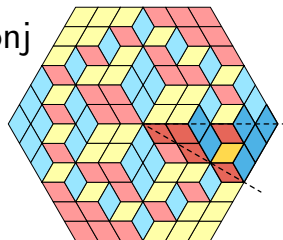
Dimer coverings / Lozenge tilings

NILP (Non-intersecting Lattice Paths)

“Magog” triangles



ASM-conj



Three Random Tiling Problems

O(1) Dense Loop Model

XXZ Quantum Spin Chain at $\Delta = -\frac{1}{2}$

Potts Model at edge-percolation

–

Fully-Packed Loops (FPL) in a square

Alternating Sign Matrices (ASM)

Six-Vortex Model at $\Delta = +\frac{1}{2}$ (Ice Model)

“Gog” triangles

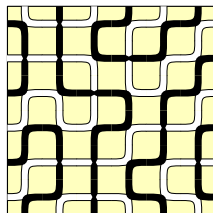
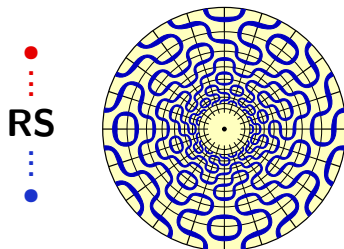
–

TSSCPP (Plane Partitions)

Dimer coverings / Lozenge tilings

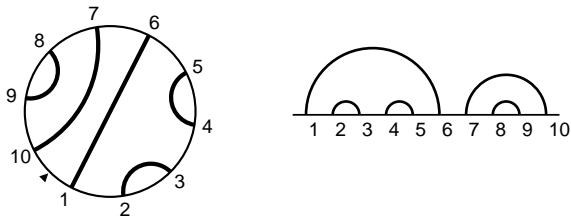
NILP (Non-intersecting Lattice Paths)

“Magog” triangles



Link patterns

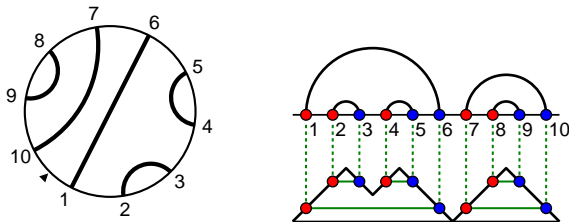
A **link pattern** $\pi \in \mathcal{LP}(n)$ is a pairing of $\{1, 2, \dots, 2n\}$ having no pairs $(a, c), (b, d)$ such that $a < b < c < d$ (i.e., the drawing consists of n **non-crossing** arcs).



They are $C_n = \frac{1}{n+1} \binom{2n}{n}$ (the n -th *Catalan number*),

Link patterns

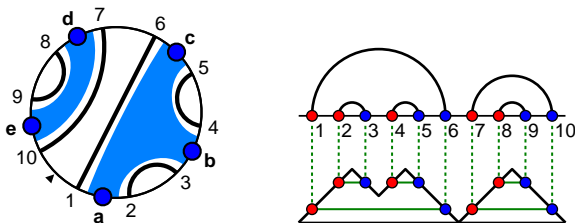
A **link pattern** $\pi \in \mathcal{LP}(n)$ is a pairing of $\{1, 2, \dots, 2n\}$ having no pairs $(a, c), (b, d)$ such that $a < b < c < d$ (i.e., the drawing consists of n **non-crossing** arcs).



They are $C_n = \frac{1}{n+1} \binom{2n}{n}$ (the n -th *Catalan number*),
are in easy bijection with **Dyck Paths** of length $2n$

Link patterns

A **link pattern** $\pi \in \mathcal{LP}(n)$ is a pairing of $\{1, 2, \dots, 2n\}$ having no pairs $(a, c), (b, d)$ such that $a < b < c < d$ (i.e., the drawing consists of n **non-crossing** arcs).

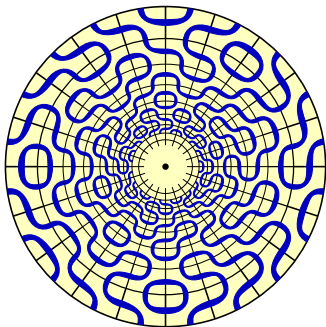


They are $C_n = \frac{1}{n+1} \binom{2n}{n}$ (the n -th *Catalan number*), are in easy bijection with **Dyck Paths** of length $2n$ and with **non-crossing partitions** of n elements.

...and many other things...

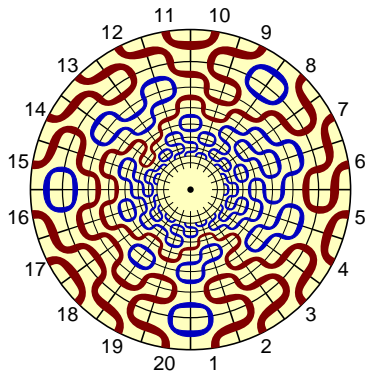
Link patterns in the Dense Loop Model

To a **dense-loop** configuration on a semi-infinite cylinder, a **link pattern** π is naturally associated, as the connectivity pattern for the points on the boundary.



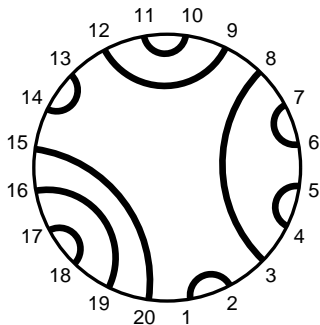
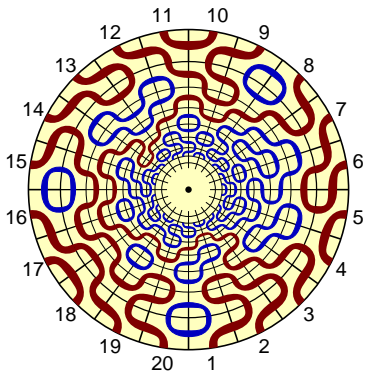
Link patterns in the Dense Loop Model

To a **dense-loop** configuration on a semi-infinite cylinder, a **link pattern** π is naturally associated, as the connectivity pattern for the points on the boundary.



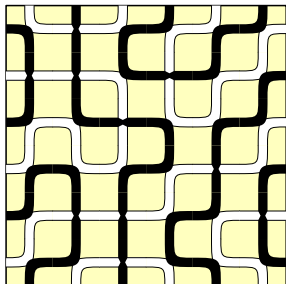
Link patterns in the Dense Loop Model

To a **dense-loop** configuration on a semi-infinite cylinder, a **link pattern** π is naturally associated, as the connectivity pattern for the points on the boundary.



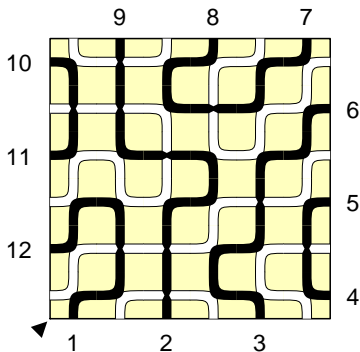
Link patterns in Fully-Packed Loops

To a **Fully-Packed Loop** configuration, a **link pattern** π is naturally associated, from connectivities among the black terminations on the boundary.



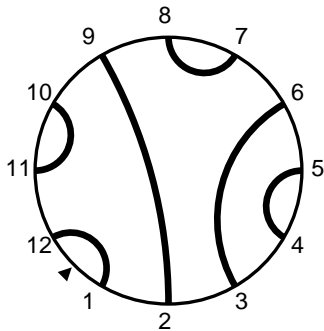
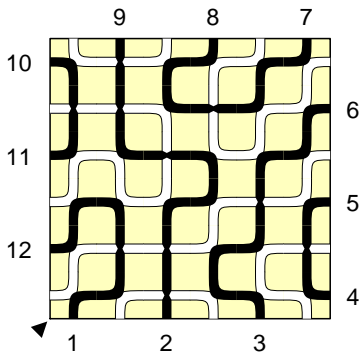
Link patterns in Fully-Packed Loops

To a **Fully-Packed Loop** configuration, a **link pattern** π is naturally associated, from connectivities among the black terminations on the boundary.

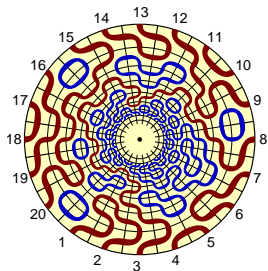


Link patterns in Fully-Packed Loops

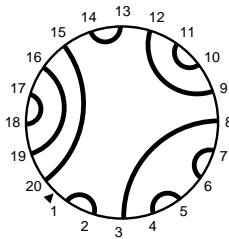
To a Fully-Packed Loop configuration, a link pattern π is naturally associated, from connectivities among the black terminations on the boundary.



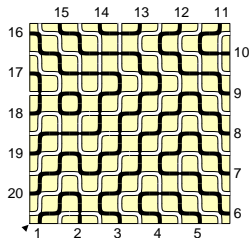
The Razumov-Stroganov correspondence



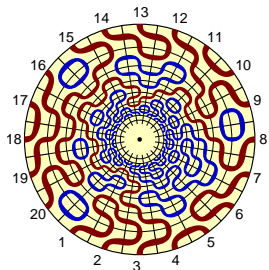
$\tilde{\Psi}_n(\pi)$: probability of π
in the $O(1)$ Dense Loop Model
in the $\{1, \dots, 2n\} \times \mathbb{N}$ cylinder



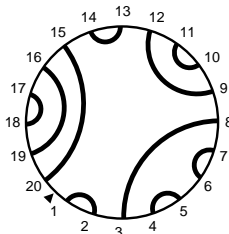
$\Psi_n(\pi)$: probability of π
for FPL with uniform measure
in the $n \times n$ square



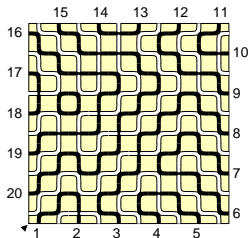
The Razumov-Stroganov correspondence



$\tilde{\Psi}_n(\pi)$: probability of π
in the $O(1)$ Dense Loop Model
in the $\{1, \dots, 2n\} \times \mathbb{N}$ cylinder



$\Psi_n(\pi)$: probability of π
for FPL with uniform measure
in the $n \times n$ square



Razumov-Stroganov correspondence

(conjecture: Razumov Stroganov, 2001; proof: AS Cantini, 2010)

$$\tilde{\Psi}_n(\pi) = \Psi_n(\pi)$$

Dihedral symmetry of FPL

A corollary of the Razumov-Stroganov correspondence. . .

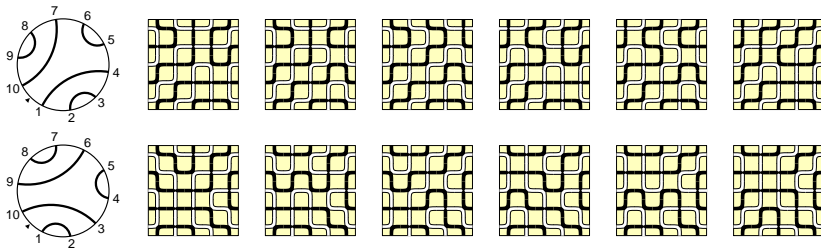
(. . . that was known *before* the Razumov-Stroganov conjecture)

call R the operator that rotates a link pattern by one position

Dihedral symmetry of FPL

(proof: Wieland, 2000)

$$\Psi_n(\pi) = \Psi_n(R\pi)$$



Deconstructing* the Razumov-Stroganov correspondence

* Deconstruction is an approach, introduced by Jacques Derrida, which rigorously pursues the meaning of a text to the point of exposing the contradictions and internal oppositions upon which it is apparently founded and showing that those foundations are irreducibly unstable, or impossible.

(Wikipedia: Deconstruction)

General protocol for random structures

Positions $x \in V$, in a graph $\mathcal{G} = (V, E)$

Local variables $\phi(x)$, attached to positions.

E.g., $\phi : V \rightarrow \{\blacksquare, \square\} \cong \{1, 0\}$

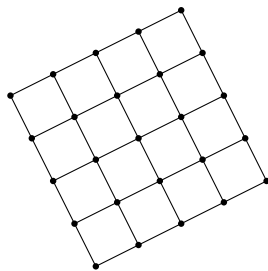
Unnormalized measure $\mu(\phi)$ (encoded by \mathcal{G})

Generating function $Z = \sum_{\phi} \mu(\phi)$.

Expectation on local k -point events:

$$\langle \phi(x_1) \cdots \phi(x_k) \rangle := \frac{1}{Z} \sum_{\phi} \mu(\phi) \phi(x_1) \cdots \phi(x_k)$$

...non-local observables...



General protocol for random structures

Positions $x \in V$, in a graph $\mathcal{G} = (V, E)$

Local variables $\phi(x)$, attached to positions.

E.g., $\phi : V \rightarrow \{\blacksquare, \square\} \cong \{1, 0\}$

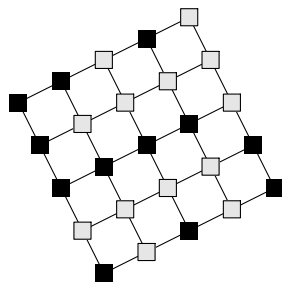
Unnormalized measure $\mu(\phi)$ (encoded by \mathcal{G})

Generating function $Z = \sum_{\phi} \mu(\phi)$.

Expectation on local k -point events:

$$\langle \phi(x_1) \cdots \phi(x_k) \rangle := \frac{1}{Z} \sum_{\phi} \mu(\phi) \phi(x_1) \cdots \phi(x_k)$$

...non-local observables...



General protocol for random structures

Positions $x \in V$, in a graph $\mathcal{G} = (V, E)$

Local variables $\phi(x)$, attached to positions.

E.g., $\phi : V \rightarrow \{\blacksquare, \square\} \cong \{1, 0\}$

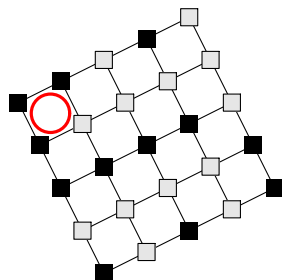
Unnormalized measure $\mu(\phi)$ (encoded by \mathcal{G})

Generating function $Z = \sum_{\phi} \mu(\phi)$.

Expectation on local k -point events:

$$\langle \phi(x_1) \cdots \phi(x_k) \rangle := \frac{1}{Z} \sum_{\phi} \mu(\phi) \phi(x_1) \cdots \phi(x_k)$$

...non-local observables...



General protocol for random structures

Positions $x \in V$, in a graph $\mathcal{G} = (V, E)$

Local variables $\phi(x)$, attached to positions.

E.g., $\phi : V \rightarrow \{\blacksquare, \square\} \cong \{1, 0\}$

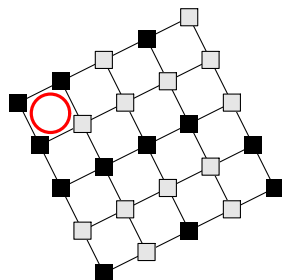
Unnormalized measure $\mu(\phi)$ (encoded by \mathcal{G})

Generating function $Z = \sum_{\phi} \mu(\phi)$.

Expectation on local k -point events:

$$\langle \phi(x_1) \cdots \phi(x_k) \rangle := \frac{1}{Z} \sum_{\phi} \mu(\phi) \phi(x_1) \cdots \phi(x_k)$$

...non-local observables...



General protocol for random structures

Positions $x \in V$, in a graph $\mathcal{G} = (V, E)$

Local variables $\phi(x)$, attached to positions.

E.g., $\phi : V \rightarrow \{\blacksquare, \square\} \cong \{1, 0\}$

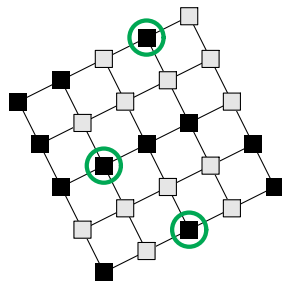
Unnormalized measure $\mu(\phi)$ (encoded by \mathcal{G})

Generating function $Z = \sum_{\phi} \mu(\phi)$.

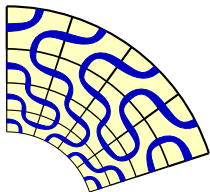
Expectation on local k -point events:

$$\langle \phi(x_1) \cdots \phi(x_k) \rangle := \frac{1}{Z} \sum_{\phi} \mu(\phi) \phi(x_1) \cdots \phi(x_k)$$

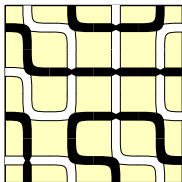
...non-local observables...



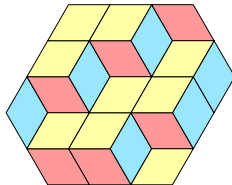
...our three models within this framework...



$O(1)$ Dense Loops

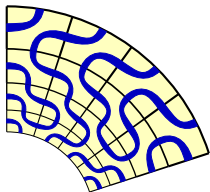


FPL

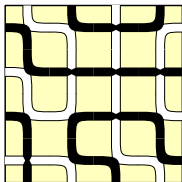


Plane Partitions

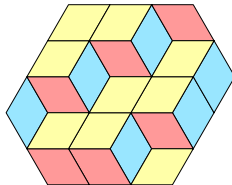
...our three models within this framework...



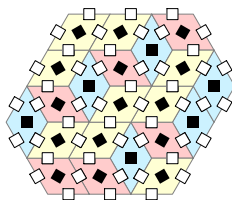
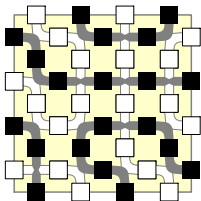
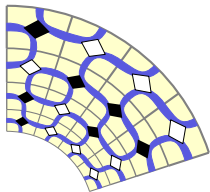
$O(1)$ Dense Loops



FPL



Plane Partitions



A hierarchy of problems

- Independent (Bernoulli) processes – percolation models
 - Determinantal processes – fermionic models
 - Yang-Baxter–Integrable systems
-

A hierarchy of problems

- Independent (Bernoulli) processes – percolation models
- Determinantal processes – fermionic models
- Yang-Baxter–Integrable systems


- ❖ $\mu(\phi) = \prod_{1 \leq i \leq n} \mu_i(\phi(x_i))$


- ❖ all k -point functions are trivial, as the 1-point fn. encodes them all!

- ❖ $Z = \prod_{1 \leq i \leq n} (a_i + b_i)$

$$\langle \phi(x_1) \cdots \phi(x_k) \rangle = \prod_{1 \leq i \leq k} \langle \phi(x_i) \rangle = \prod_{1 \leq i \leq k} \frac{a_{x_i}}{a_{x_i} + b_{x_i}}$$


- ❖ the only non-trivial probabilistic events are non-local (e.g., for percolation, Cardy formula)


 G.R. Grimmett, *Percolation*, Springer GMW-321, 1999 Vol. 321

 W. Werner, *Lectures on two-dimensional critical percolation*, lect. notes IAS-Park City summer school 2007 arXiv:0710.0856

A hierarchy of problems


- Independent (Bernoulli) processes – percolation models
 - **Determinantal processes – fermionic models**
 - Yang-Baxter–Integrable systems
- ❖ Examples: Ising Model, Dimers, Spanning Trees, Abelian Sandpile. . .
 - ❖ $Z = \det L$ for a certain $n \times n$ matrix L (or even smaller)
 - ❖ k -point fn. are the determinant of a $k \times k$ matrix $G(x_1, \dots, x_k)$, whose entries are a “kernel function”
 $G_{ij} = \mathcal{K}(x_i, x_j) \propto (L^{-1})_{x_i x_j}$: the 2-point fn. encodes them all!
 - ❖ closed expression for Z even for $\mathcal{O}(n)$ local weights

 B.J. Hough, M. Krishnapur, Y. Peres and B. Virag,
Zeros of Gaussian Analytic Functions and Determinantal Point Processes,
stat-www.berkeley.edu/~peres/GAF_book.pdf


 K. Johansson, *The arctic circle boundary and the Airy process*,
Annals of Prob. **33** 1-30 (2005) [arXiv:math/0306216](https://arxiv.org/abs/math/0306216)

A hierarchy of problems

- Independent (Bernoulli) processes – percolation models
- Determinantal processes – fermionic models
- **Yang-Baxter–Integrable systems**
 - ❖ YB eq. leads to remarkable exchange properties
 - ❖ allows for only $\mathcal{O}(\sqrt{n})$ weights, attached to the *spectral lines*
 - ❖ on the cylinder, Z is solved in terms of Bethe equations
 - ❖ Z and few special k -point fns. may have simple expressions (and possibly a determinant)
 - ❖ specific percolation and fermionic systems are often special points on the YB-integrable manifold.

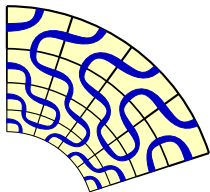
 R.J. Baxter, *Exactly Solved Models in Statistical Mechanics*, Academic Press (1982)

<http://tpsrv.anu.edu.au/Members/baxter/book>

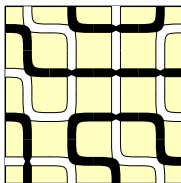
 C. Gómez, M. Ruiz-Altaba and G. Sierra, *Quantum Groups in Two dimensional Physics*, Cambridge UP (1996)

A hierarchy of problems

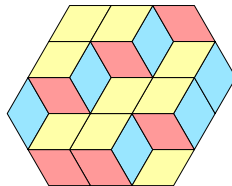
- Independent (Bernoulli) processes – percolation models
- Determinantal processes – fermionic models
- Yang-Baxter–Integrable systems



Bernoulli



Y-B Integrable



Determinantal

Exact Sampling and bijections

Consider the **computational complexity** $T_\phi(n)$ for sampling configs of size n from the measure $\mu(\phi)$

This concept is “robust” under bijections and combinatorial rewritings of the problem:

if $X : \phi \rightarrow \psi$ is a map implemented with complexity $T_X(n)$,

$$T_\phi(n) - T_{X^{-1}}(n) \leq T_\psi(n) \leq T_\phi(n) + T_X(n)$$

Exact Sampling and bijections

Consider the **computational complexity** $T_\phi(n)$ for sampling configs of size n from the measure $\mu(\phi)$

This concept is “robust” under bijections and combinatorial rewritings of the problem:

if $X : \phi \rightarrow \psi$ is a map implemented with complexity $T_X(n)$,

$$T_\phi(n) - T_{X^{-1}}(n) \leq T_\psi(n) \leq T_\phi(n) + T_X(n)$$

If, for large n , $T_{X^{\pm 1}}(n) \ll T_\psi(n), T_\phi(n)$, then $T_\psi(n) \sim T_\phi(n)$.

Exact Sampling and bijections

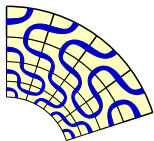
Consider the **computational complexity** $T_\phi(n)$ for sampling configs of size n from the measure $\mu(\phi)$

This concept is “robust” under bijections and combinatorial rewritings of the problem:

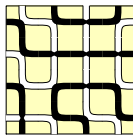
if $X : \phi \rightarrow \psi$ is a map implemented with complexity $T_X(n)$,

$$T_\phi(n) - T_{X^{-1}}(n) \leq T_\psi(n) \leq T_\phi(n) + T_X(n)$$

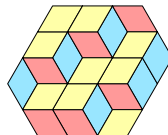
If, for large n , $T_{X^{\pm 1}}(n) \ll T_\psi(n), T_\phi(n)$, then $T_\psi(n) \sim T_\phi(n)$.



Bernoulli



Y-B Integrable



Determinantal

Exact Sampling and bijections

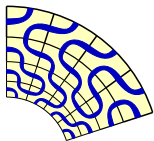
Consider the **computational complexity** $T_\phi(n)$ for sampling configs of size n from the measure $\mu(\phi)$

This concept is “robust” under bijections and combinatorial rewritings of the problem:

if $X : \phi \rightarrow \psi$ is a map implemented with complexity $T_X(n)$,

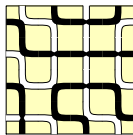
$$T_\phi(n) - T_{X^{-1}}(n) \leq T_\psi(n) \leq T_\phi(n) + T_X(n)$$

If, for large n , $T_{X^{\pm 1}}(n) \ll T_\psi(n), T_\phi(n)$, then $T_\psi(n) \sim T_\phi(n)$.

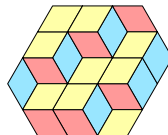


Bernoulli

$T_\phi(n) \sim n$
(obvious)



Y-B Integrable



Determinantal

Exact Sampling and bijections

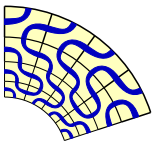
Consider the **computational complexity** $T_\phi(n)$ for sampling configs of size n from the measure $\mu(\phi)$

This concept is “robust” under bijections and combinatorial rewritings of the problem:

if $X : \phi \rightarrow \psi$ is a map implemented with complexity $T_X(n)$,

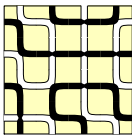
$$T_\phi(n) - T_{X^{-1}}(n) \leq T_\psi(n) \leq T_\phi(n) + T_X(n)$$

If, for large n , $T_{X^{\pm 1}}(n) \ll T_\psi(n), T_\phi(n)$, then $T_\psi(n) \sim T_\phi(n)$.

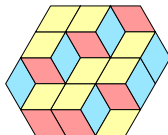


Bernoulli

$T_\phi(n) \sim n$
(obvious)



Y-B Integrable



Determinantal

$T_\phi(n) \lesssim n^4$
by divide&conquer

Exact Sampling and bijections

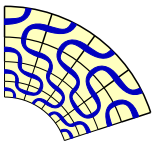
Consider the **computational complexity** $T_\phi(n)$ for sampling configs of size n from the measure $\mu(\phi)$

This concept is “robust” under bijections and combinatorial rewritings of the problem:

if $X : \phi \rightarrow \psi$ is a map implemented with complexity $T_X(n)$,

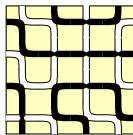
$$T_\phi(n) - T_{X^{-1}}(n) \leq T_\psi(n) \leq T_\phi(n) + T_X(n)$$

If, for large n , $T_{X^{\pm 1}}(n) \ll T_\psi(n), T_\phi(n)$, then $T_\psi(n) \sim T_\phi(n)$.



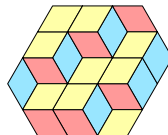
Bernoulli

$T_\phi(n) \sim n$
(obvious)



Y-B Integrable

No guarantee
(but often CFTP!)



Determinantal

$T_\phi(n) \lesssim n^4$
by divide&conquer

Reconstructing the Razumov-Stroganov correspondence

The 6-Vertex Model

A famous Yang-Baxter–integrable system is the **6-Vertex Model**:

- you have a degree-4 graph \mathcal{G} ,
- variables are **edge-orientations**,
- weights are on the **vertices**,

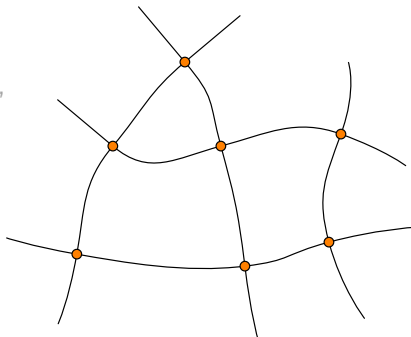
depend on the four arrows,
through **spectral parameters**
attached to the lines,
and a **global parameter q**

The 6-Vertex Model

A famous Yang-Baxter–integrable system is the **6-Vertex Model**:

- you have a degree-4 graph \mathcal{G} ,
- variables are **edge-orientations**,
- weights are on the **vertices**,

depend on the four arrows,
through **spectral parameters**
attached to the lines,
and a **global parameter q**

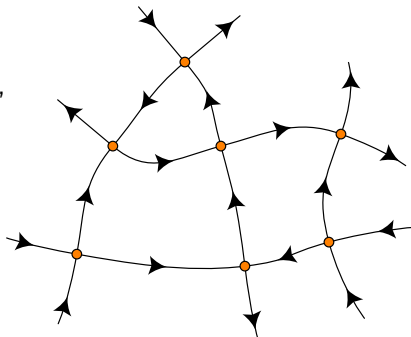


The 6-Vertex Model

A famous Yang-Baxter–integrable system is the **6-Vertex Model**:

- you have a degree-4 graph \mathcal{G} ,
- variables are **edge-orientations**,
- weights are on the **vertices**,

depend on the four arrows,
through **spectral parameters**
attached to the lines,
and a **global parameter q**

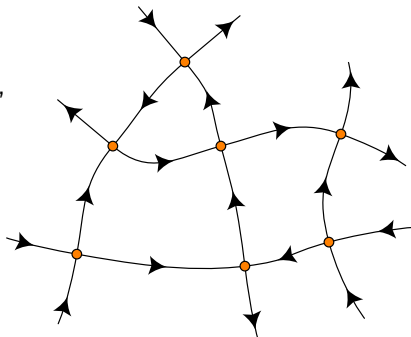


The 6-Vertex Model

A famous Yang-Baxter–integrable system is the **6-Vertex Model**:

- you have a degree-4 graph \mathcal{G} ,
- variables are **edge-orientations**,
- weights are on the **vertices**,

depend on the four arrows,
through **spectral parameters**
attached to the lines,
and a **global parameter q**

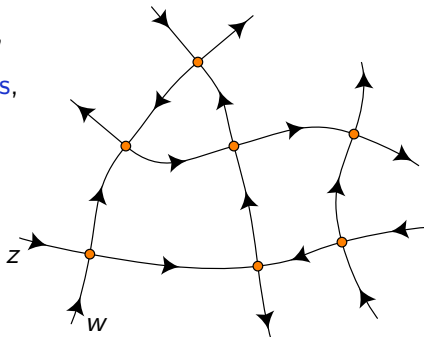


The 6-Vertex Model

A famous Yang-Baxter–integrable system is the **6-Vertex Model**:

- you have a degree-4 graph \mathcal{G} ,
- variables are **edge-orientations**,
- weights are on the **vertices**,

depend on the four arrows,
through **spectral parameters**
attached to the lines,
and a **global parameter q**

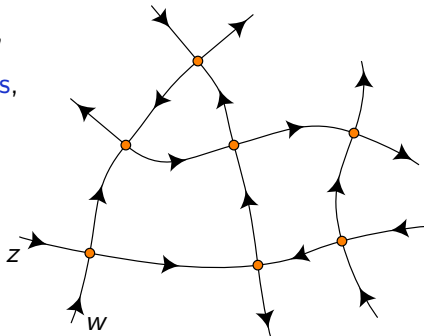


The 6-Vertex Model

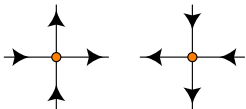
A famous Yang-Baxter–integrable system is the **6-Vertex Model**:

- you have a degree-4 graph \mathcal{G} ,
- variables are **edge-orientations**,
- weights are on the **vertices**,

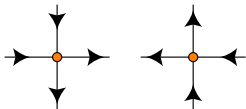
depend on the four arrows,
through **spectral parameters**
attached to the lines,
and a **global parameter q**



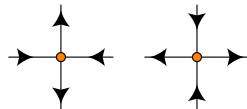
$$a = zq - w/q$$



$$b = z - w$$



$$c = (1/q - q)\sqrt{zw}$$



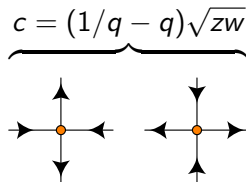
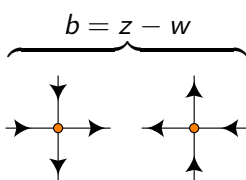
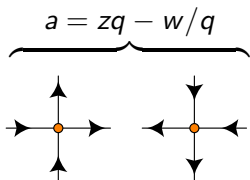
The 6-Vertex Model

A famous Yang-Baxter-integrable system is the **6-Vertex Model**:

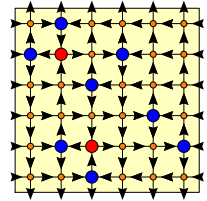
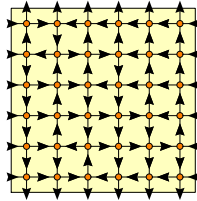
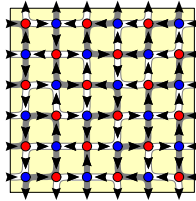
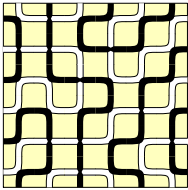
- you have a degree-4 graph \mathcal{G} ,
- variables are **edge-orientations**,
- weights are on the **vertices**,

depend on the four arrows,
through **spectral parameters**
attached to the lines,
and a **global parameter q**

$$\Delta = \frac{a^2 + b^2 - c^2}{2ab} = \frac{1}{2} \left(q + \frac{1}{q} \right)$$

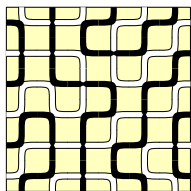


Fully-Packed Loops \Rightarrow 6VM \Rightarrow Alternating Sign Matrices

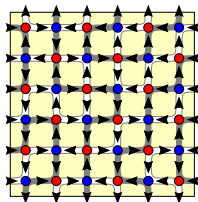


FPL
config

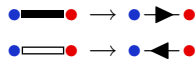
Fully-Packed Loops \Rightarrow 6VM \Rightarrow Alternating Sign Matrices



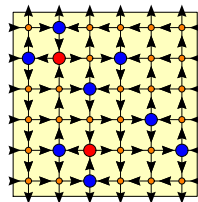
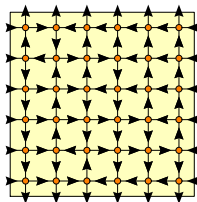
FPL
config



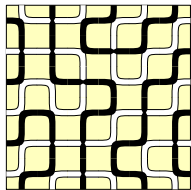
• or • according
to parity;



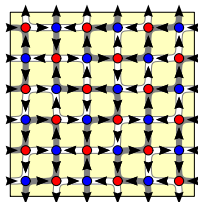
Forget parity;



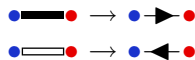
Fully-Packed Loops \Rightarrow 6VM \Rightarrow Alternating Sign Matrices



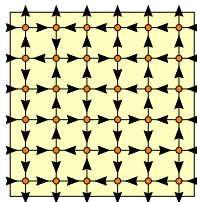
FPL
config



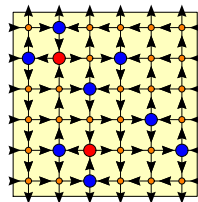
● or ● according
to parity;



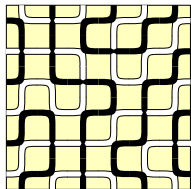
Forget parity;



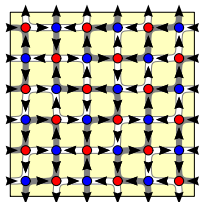
6-vertex
config
(DWBC)



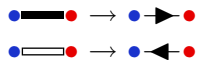
Fully-Packed Loops \Rightarrow 6VM \Rightarrow Alternating Sign Matrices



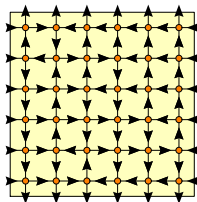
FPL
config



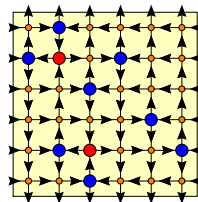
• or • according
to parity;



Forget parity;

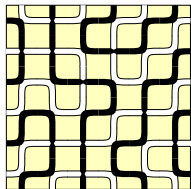


6-vertex
config
(DWBC)

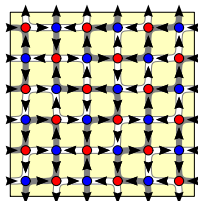


Arrow directions
along rows/cols
get flipped at •, •

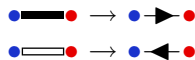
Fully-Packed Loops \Rightarrow 6VM \Rightarrow Alternating Sign Matrices



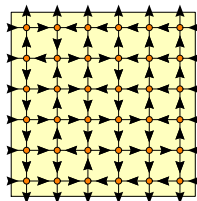
FPL
config



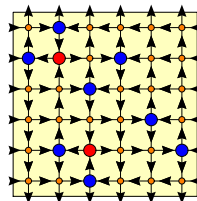
• or • according
to parity;



Forget parity;



6-vertex
config
(DWBC)

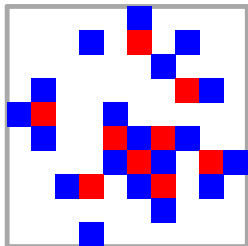
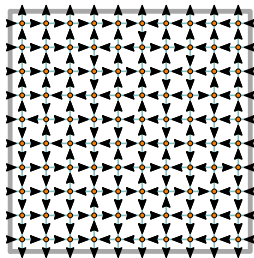


Arrow directions
along rows/cols
get flipped at •, •

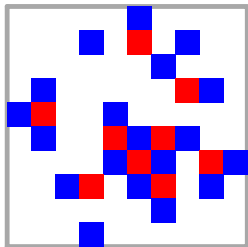
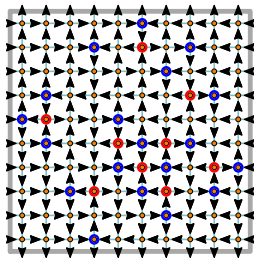
ASM config

0	+1	0	0	0	0
+1	-1	0	+1	0	0
0	0	+1	0	0	0
0	0	0	0	+1	0
0	+1	-1	0	0	+1
0	0	+1	0	0	0

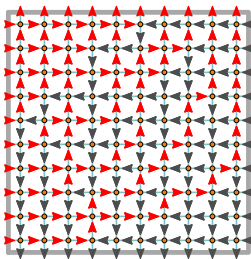
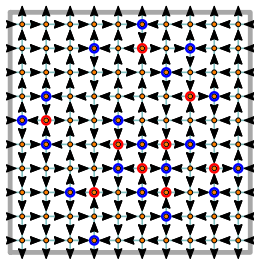
6VM \rightarrow permutation, height function, monotone triangle



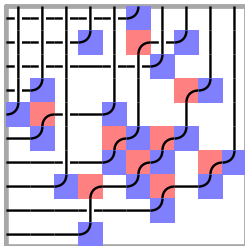
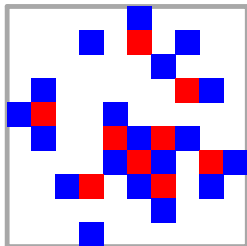
6VM \rightarrow permutation, height function, monotone triangle



6VM \rightarrow permutation, height function, monotone triangle

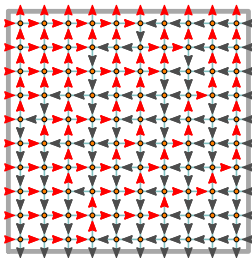
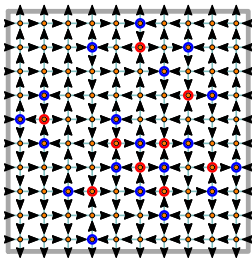


mark **east**- and
north-bound
arrows...

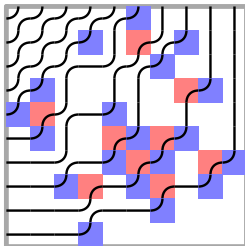
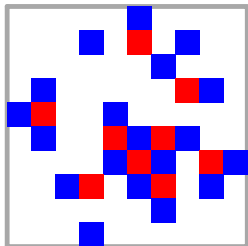


...you see a
permutation of
row/column-indices
(crossings count the
inversion number)

6VM \rightarrow permutation, height function, monotone triangle

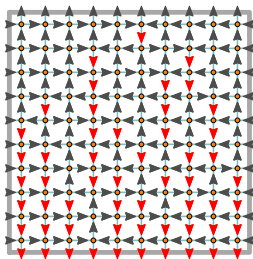
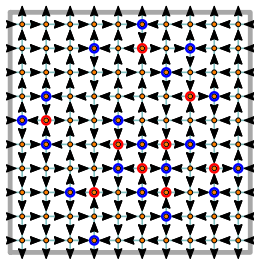


mark **east-** and
north-bound
arrows...

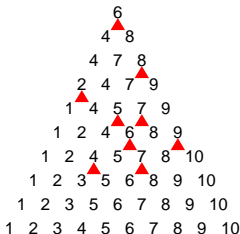
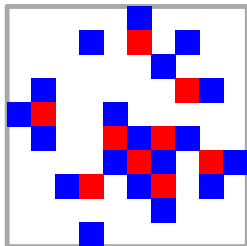


...or **directed**
non-crossing paths,
which are **not** of
Gessel-Viennot
type...

6VM \rightarrow permutation, height function, monotone triangle

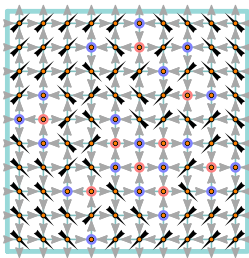
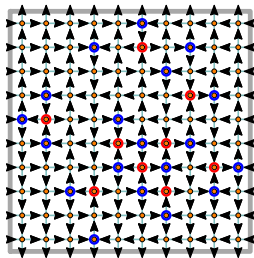


mark **south-bound** arrows, and read column positions...

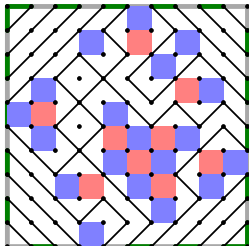
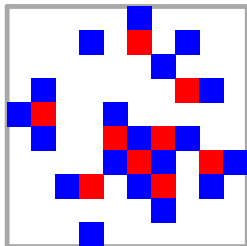


...you get a **monotone triangle**,
 base = $(1, 2, \dots, n)$,
 strict horizontally
 and weak elsewhere

6VM \rightarrow permutation, height function, monotone triangle

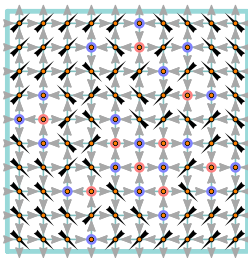
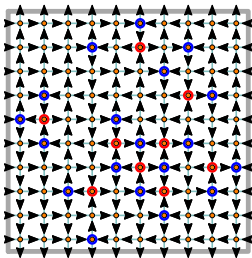


draw a line for a coherent flow...

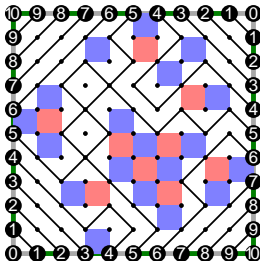
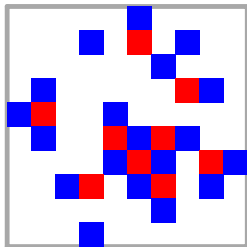


...you get an Eulerian graph,
regions can be 2-coloured resp.
boundaries

6VM \rightarrow permutation, height function, monotone triangle

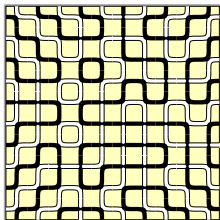


draw a line for a coherent flow...

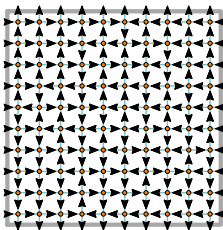


...they're also level lines of a height function, with ± 1 -slope b.c.

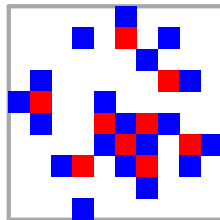
...in summary...



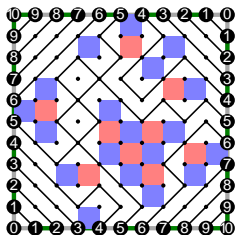
FPL



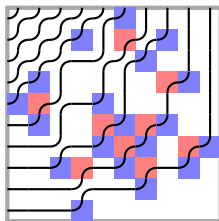
6-vertex



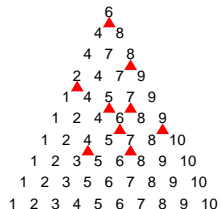
ASM



height function



quasi-NILP



monotone triangle

Alternating Sign Matrices: some history

Alternating Sign Matrices arose in combinatorics through the work of **Mills, Robbins and Rumsey** ('80s)... they took the old **Dodgson** Condensation Algorithm (1866)

$$\det M = \frac{\det M_{1,1} \det M_{n,n} - \det M_{1,n} \det M_{n,1}}{\det M_{1n,1n}}$$

and defined a **λ -determinant** algorithmically, as

$$\det_{\lambda} M = \frac{\det_{\lambda} M_{1,1} \det_{\lambda} M_{n,n} - \lambda \det_{\lambda} M_{1,n} \det_{\lambda} M_{n,1}}{\det_{\lambda} M_{1n,1n}}$$

The result is (surprisingly) a **Laurent polynomial** in entries m_{ij} : “old” permutations take a λ^k factor, “new” terms are the non-trivial ASM, and have also $(1 - \lambda)^h$ factors. . .

...a 3×3 example:

$$\det M = m_{11}m_{22}m_{33} + m_{12}m_{23}m_{31} + m_{13}m_{21}m_{32}$$



$$- m_{11}m_{23}m_{32} - m_{12}m_{21}m_{33} - m_{13}m_{22}m_{31}$$



 J. Propp: *Lambda-determinants and Domino Tilings*, 2005

...a 3×3 example:

$$\det_{\lambda} M = m_{11}m_{22}m_{33} + \lambda^2 m_{12}m_{23}m_{31} + \lambda^2 m_{13}m_{21}m_{32}$$



$$-\lambda m_{11}m_{23}m_{32} - \lambda m_{12}m_{21}m_{33} - \lambda^3 m_{13}m_{22}m_{31}$$



$$-\lambda(1 - \lambda) \frac{m_{12}m_{21}m_{23}m_{32}}{m_{22}}$$



 J. Propp: *Lambda-determinants and Domino Tilings*, 2005

λ -determinants, years later...

... Now this **Laurent phenomenon**, i.e. the λ -determinant being a Laurent polynomial in matrix entries, is well understood in the wider frame of **Fomin-Zelevinsky Cluster Algebras**

📖 S. Fomin, A. Zelevinsky: *The Laurent Phenomenon*, 2002

📖 Ph. Di Francesco, R. Kedem: *Q-system, Cluster Algebras, Paths and Total Positivity*, 2010

...and the λ -determinant is an integrable DWBC 6-Vertex partition function (with “electric fields”) at a fermionic point

$$a = -\lambda \quad a' = 1 \quad b = 1 \quad b' = 1 \quad c = m_{ij} \quad c' = \frac{1 - \lambda}{m_{ij}}$$

$$a'/a = -\lambda; \quad b'/b = 1; \quad \Delta = \frac{aa' + bb' - cc'}{2\sqrt{aa'bb'}} = 0; \quad t = \sqrt{\frac{bb'}{aa'}} = \sqrt{-\lambda}.$$

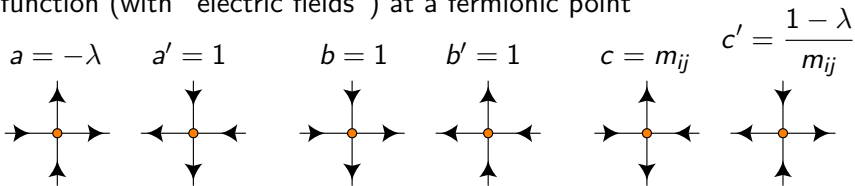
λ -determinants, years later...

... Now this **Laurent phenomenon**, i.e. the λ -determinant being a Laurent polynomial in matrix entries, is well understood in the wider frame of **Fomin-Zelevinsky Cluster Algebras**

📖 S. Fomin, A. Zelevinsky: *The Laurent Phenomenon*, 2002

📖 Ph. Di Francesco, R. Kedem: *Q-system, Cluster Algebras, Paths and Total Positivity*, 2010

...and the λ -determinant is an integrable DWBC 6-Vertex partition function (with “electric fields”) at a fermionic point

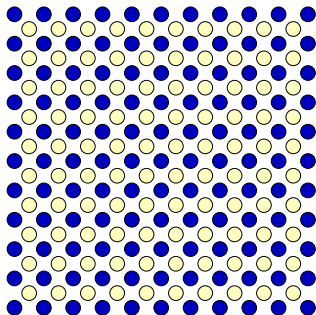


$$a'/a = -\lambda; \quad b'/b = 1; \quad \Delta = \frac{aa' + bb' - cc'}{2\sqrt{aa'bb'}} = 0; \quad t = \sqrt{\frac{bb'}{aa'}} = \sqrt{-\lambda}.$$

$O(n)$ Dense Loops, Potts Model and Temperley-Lieb

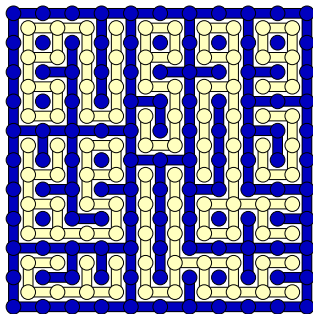


$O(n)$ Dense Loops, Potts Model and Temperley-Lieb



interlace a “blue” and a “white” square grids of points

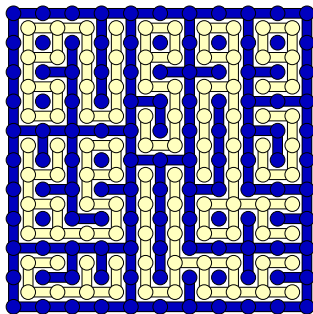
$O(n)$ Dense Loops, Potts Model and Temperley-Lieb



for every square plaquette e , either connect the blue opposite endpoints (with weight w_e), or the white ones (with weight $1/w_e$)

$$\begin{array}{c} \circ \\ \circ \\ \circ \\ \circ \end{array} = w_e \begin{array}{c} \circ \\ \text{---} \\ \circ \\ \text{---} \\ \circ \end{array} + \frac{1}{w_e} \begin{array}{c} \circ \\ \text{---} \\ \circ \\ \text{---} \\ \circ \end{array}$$

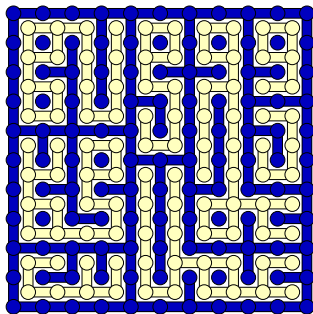
$O(n)$ Dense Loops, Potts Model and Temperley-Lieb



include the overall “topological” factors: a λ per blue connected component (i.e., white independent cycle), and a ρ per white connected component (i.e., blue independent cycle)

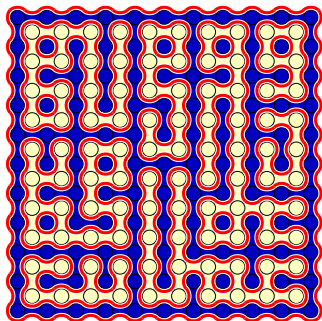
in 2D: independent cycle \equiv no chords

$O(n)$ Dense Loops, Potts Model and Temperley-Lieb



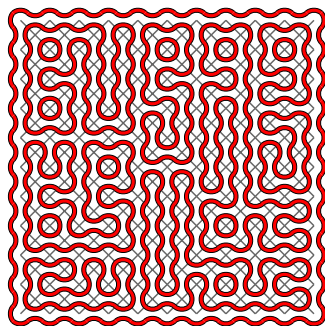
the generating function is the Q -state Potts Model on the square lattice, with local weights w_e , and $Q = \lambda\rho$

$O(n)$ Dense Loops, Potts Model and Temperley-Lieb



Consider now the contours of white/blue domains...

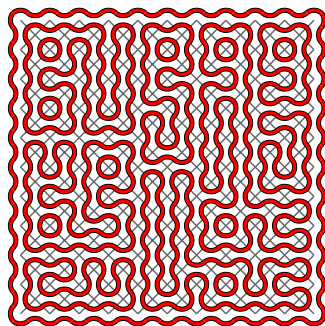
$O(n)$ Dense Loops, Potts Model and Temperley-Lieb



...they produce a dense packing of loops, for tiling the (45-degree rotated) square lattice with the two **Temperley-Lieb** tiles

$$\begin{array}{c} \circ \\ \diagup \quad \diagdown \\ \circ \quad \circ \\ \diagdown \quad \diagup \\ \circ \end{array} = w_e \begin{array}{c} \circ \\ \diagup \quad \diagdown \\ \text{red} \quad \text{blue} \\ \diagdown \quad \diagup \\ \circ \end{array} + \frac{1}{w_e} \begin{array}{c} \circ \\ \diagup \quad \diagdown \\ \text{blue} \quad \text{red} \\ \diagdown \quad \diagup \\ \circ \end{array}$$

$O(n)$ Dense Loops, Potts Model and Temperley-Lieb



include a “topological” factor n per cycle
this correspond to the $O(n)$ Dense Loop Model,
for $n^2 = Q = \lambda\rho$

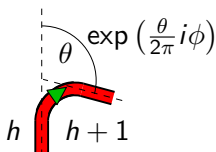
$O(n)$ Dense Loops: height representation

In $2D$, we have a **2nd order phase transition** only in the range


$$-2 \leq n \leq 2 \quad 0 \leq Q \leq 4$$

Set $n = 2 \cos \phi$, and make n local, using complex numbers:

$$2 \cos \phi \text{ (loop) } = e^{i\phi} \text{ (loop with arrow) } + e^{-i\phi} \text{ (loop with arrow) }$$



height representation \longrightarrow **Coulomb Gas techniques**

 B. Nienhuis, *Two-dimensional critical phenomena and the Coulomb Gas*, in *Phase Transitions and Critical Phenomena* vol. 11, 1987

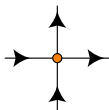
Loops \leftrightarrow Oriented Loops \leftrightarrow Arrows

The formulation as **Oriented Loops** has simultaneously degrees of freedom for **Temperley-Lieb plaquettes** and for **arrows**

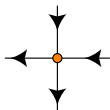
We can now sum over the plaquette d.o.f., and find a **6-Vertex Model**



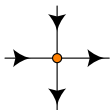
$$a = 1$$



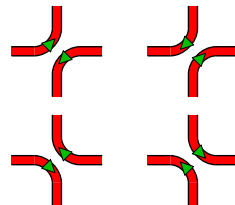
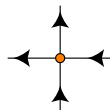
$$a' = 1$$



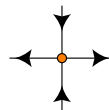
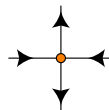
$$b = 1$$



$$b' = 1$$



$$c = c' = 2 \cos(\phi/2)$$



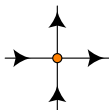
Loops \leftrightarrow Oriented Loops \leftrightarrow Arrows

The formulation as **Oriented Loops** has simultaneously degrees of freedom for **Temperley-Lieb plaquettes** and for **arrows**

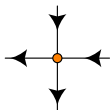
We can now sum over the plaquette d.o.f., and find a **6-Vertex Model**



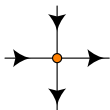
$$a = 1$$



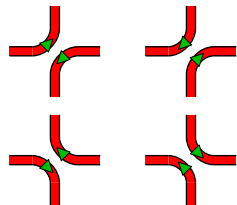
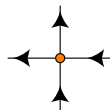
$$a' = 1$$



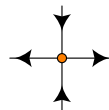
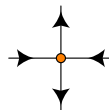
$$b = 1$$



$$b' = 1$$



$$c = c' = 2 \cos(\phi/2)$$



$$n = \omega - 2 = -\Delta/2$$

Integer Partitions and Plane Partitions

Take a 2D quadrant \mathbb{N}^2 ,

Pile squares (subject to “gravity” along the $(1, 1)$ axis).

That is, produce subsets $\pi \subset \mathbb{N}^2$ such that, if $(x, y) \in \pi$, then

$$\{(x', y')\}_{\substack{1 \leq x' \leq x \\ 1 \leq y' \leq y}} \subseteq \pi$$

Call $|\pi|$ the number of squares in π

Related to [partitions of an integer](#):

$$|\pi| = a_1 + a_2 + \dots + a_k$$

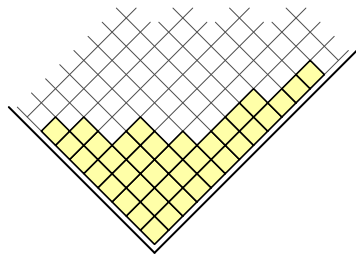
with $a_1 \geq a_2 \geq \dots \geq a_k$,

and thus with a long history

([Euler](#), [Sylvester](#), [Frobenius](#), [Hardy-Ramanujan](#),...)

Also related to [Random Walk on \$\mathbb{Z}\$](#)

Generating function:
$$\sum_{\pi} q^{|\pi|} = \prod_{j \geq 1} \frac{1}{1 - q^j}$$



Integer Partitions and Plane Partitions

Take a 2D quadrant \mathbb{N}^2 ,

Pile squares (subject to “gravity” along the $(1, 1)$ axis).

That is, produce subsets $\pi \subset \mathbb{N}^2$ such that, if $(x, y) \in \pi$, then

$$\{(x', y')\}_{\substack{1 \leq x' \leq x \\ 1 \leq y' \leq y}} \subseteq \pi$$

Call $|\pi|$ the number of squares in π

Related to [partitions of an integer](#):

$$|\pi| = a_1 + a_2 + \dots + a_k$$

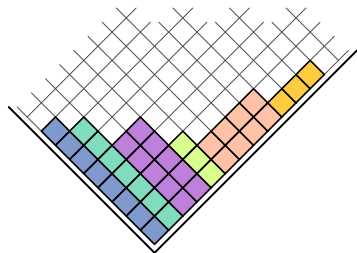
with $a_1 \geq a_2 \geq \dots \geq a_k$,

and thus with a long history

([Euler](#), [Sylvester](#), [Frobenius](#), [Hardy-Ramanujan](#),...)

Also related to [Random Walk on \$\mathbb{Z}\$](#)

Generating function:

$$\sum_{\pi} q^{|\pi|} = \prod_{j \geq 1} \frac{1}{1 - q^j}$$


Unrestricted Plane Partitions

Take the 3D octant \mathbb{N}^3 .

Pile cubes (subject to “gravity” along the $(1, 1, 1)$ axis).

That is, produce subsets $\pi \subset \mathbb{N}^3$ such that, if $(x, y, z) \in \pi$, then

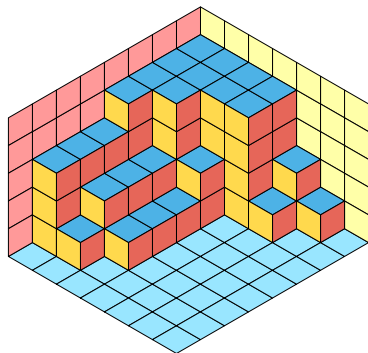
$$\{(x', y', z')\}_{\substack{1 \leq x' \leq x \\ 1 \leq y' \leq y \\ 1 \leq z' \leq z}} \subseteq \pi$$

Call $|\pi|$ the number of cubes in π

Generating fn.: (MacMahon, 1912)

$$\sum_{\pi} q^{|\pi|} = \prod_{j \geq 1} \frac{1}{(1 - q^j)^j}$$

Meaningful for $q \in \mathbb{C}$, $|q| < 1$



Unrestricted Plane Partitions

Take the 3D octant \mathbb{N}^3 .

Pile cubes (subject to “gravity” along the $(1, 1, 1)$ axis).

That is, produce subsets $\pi \subset \mathbb{N}^3$ such that, if $(x, y, z) \in \pi$, then

$$\{(x', y', z') \mid \begin{array}{l} 1 \leq x' \leq x \\ 1 \leq y' \leq y \\ 1 \leq z' \leq z \end{array}\} \subseteq \pi$$

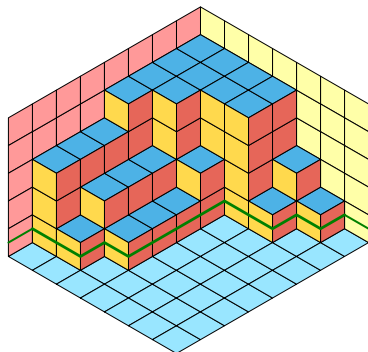
Call $|\pi|$ the number of cubes in π

Generating fn.: (MacMahon, 1912)

$$\sum_{\pi} q^{|\pi|} = \prod_{j \geq 1} \frac{1}{(1 - q^j)^j}$$

Meaningful for $q \in \mathbb{C}$, $|q| < 1$

Can be sliced into a string of integer partitions, ordered w.r.t. inclusion



Unrestricted Plane Partitions

Take the 3D octant \mathbb{N}^3 .

Pile cubes (subject to “gravity” along the $(1, 1, 1)$ axis).

That is, produce subsets $\pi \subset \mathbb{N}^3$ such that, if $(x, y, z) \in \pi$, then

$$\{(x', y', z')\}_{\substack{1 \leq x' \leq x \\ 1 \leq y' \leq y \\ 1 \leq z' \leq z}} \subseteq \pi$$

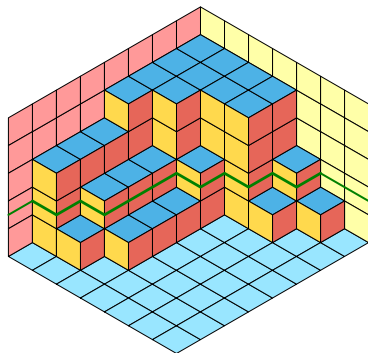
Call $|\pi|$ the number of cubes in π

Generating fn.: (MacMahon, 1912)

$$\sum_{\pi} q^{|\pi|} = \prod_{j \geq 1} \frac{1}{(1 - q^j)^j}$$

Meaningful for $q \in \mathbb{C}$, $|q| < 1$

Can be sliced into a string of integer partitions, ordered w.r.t. inclusion



Unrestricted Plane Partitions

Take the 3D octant \mathbb{N}^3 .

Pile cubes (subject to “gravity” along the $(1, 1, 1)$ axis).

That is, produce subsets $\pi \subset \mathbb{N}^3$ such that, if $(x, y, z) \in \pi$, then

$$\{(x', y', z')\}_{\substack{1 \leq x' \leq x \\ 1 \leq y' \leq y \\ 1 \leq z' \leq z}} \subseteq \pi$$

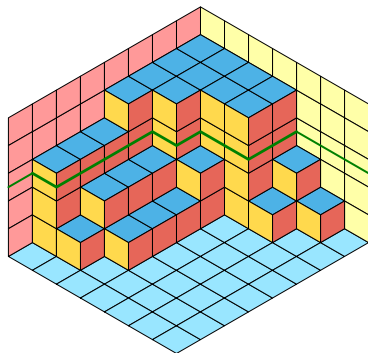
Call $|\pi|$ the number of cubes in π

Generating fn.: (MacMahon, 1912)

$$\sum_{\pi} q^{|\pi|} = \prod_{j \geq 1} \frac{1}{(1 - q^j)^j}$$

Meaningful for $q \in \mathbb{C}$, $|q| < 1$

Can be sliced into a string of integer partitions, ordered w.r.t. inclusion



Unrestricted Plane Partitions

Take the 3D octant \mathbb{N}^3 .

Pile cubes (subject to “gravity” along the $(1, 1, 1)$ axis).

That is, produce subsets $\pi \subset \mathbb{N}^3$ such that, if $(x, y, z) \in \pi$, then

$$\{(x', y', z')\}_{\substack{1 \leq x' \leq x \\ 1 \leq y' \leq y \\ 1 \leq z' \leq z}} \subseteq \pi$$

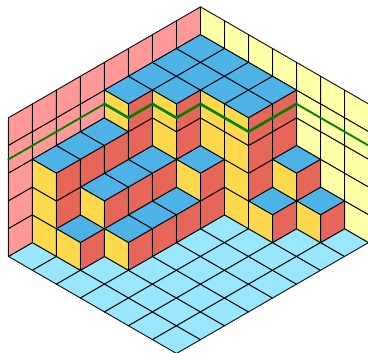
Call $|\pi|$ the number of cubes in π

Generating fn.: (MacMahon, 1912)

$$\sum_{\pi} q^{|\pi|} = \prod_{j \geq 1} \frac{1}{(1 - q^j)^j}$$

Meaningful for $q \in \mathbb{C}$, $|q| < 1$

Can be sliced into a string of integer partitions,
ordered w.r.t. inclusion



Unrestricted Plane Partitions

Take the 3D octant \mathbb{N}^3 .

Pile cubes (subject to “gravity” along the $(1, 1, 1)$ axis).

That is, produce subsets $\pi \subset \mathbb{N}^3$ such that, if $(x, y, z) \in \pi$, then

$$\{(x', y', z')\}_{\substack{1 \leq x' \leq x \\ 1 \leq y' \leq y \\ 1 \leq z' \leq z}} \subseteq \pi$$

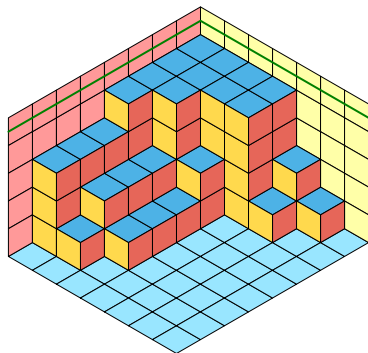
Call $|\pi|$ the number of cubes in π

Generating fn.: (MacMahon, 1912)

$$\sum_{\pi} q^{|\pi|} = \prod_{j \geq 1} \frac{1}{(1 - q^j)^j}$$

Meaningful for $q \in \mathbb{C}$, $|q| < 1$

Can be sliced into a string of integer partitions, ordered w.r.t. inclusion



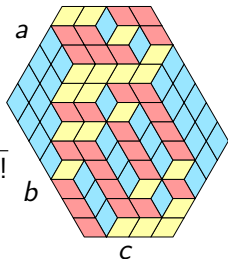
Plane Partitions in a box

In a compact box, can push q to the “combinatorial point” $q = 1$

No symmetry:

P.A. MacMahon (1915)

$$M_{a,b,c} = \prod_{\substack{0 \leq i < a \\ 0 \leq j < b \\ 0 \leq k < c}} \frac{i+j+k+2}{i+j+k+1} = \prod_{0 \leq j < c} \frac{j!(j+a+b)!}{(j+a)!(j+b)!}$$

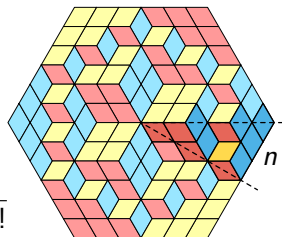


... various symmetry classes ...

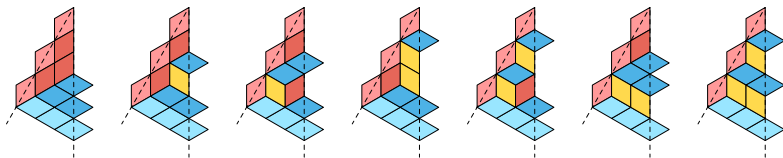
Maximally symmetric (TSSCPP):

G. Andrews (1994)

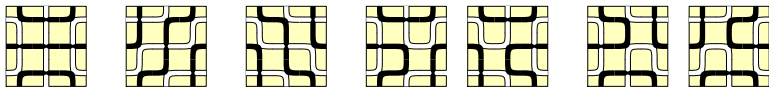
$$A_n = \prod_{0 \leq j < n} \frac{(3j+1)!}{(n+j)!} = \prod_{0 \leq j < n} \frac{j!(3j+1)!}{(2j)!(2j+1)!}$$



Plane Partitions and Fully-Packed Loops

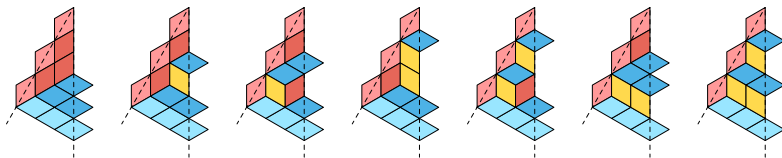


TSSCPP in a hexagon of side $2n$ = # FPL in a square of side n

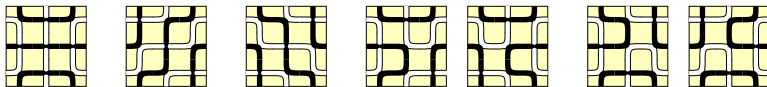


(Proof: Zeilberger 1996, with generating functions and much more;
Kuperberg 1996, specializing results from the Six-vertex model)

Plane Partitions and Fully-Packed Loops



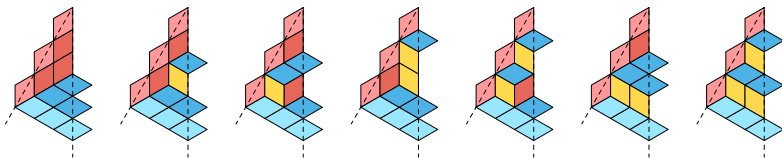
TSSCPP in a hexagon of side $2n$ = # FPL in a square of side n



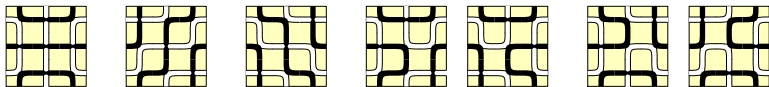
(Proof: Zeilberger 1996, with generating functions and much more;
Kuperberg 1996, specializing results from the Six-vertex model)

We have **no bijectorial clue** of why this is true

Plane Partitions and Fully-Packed Loops



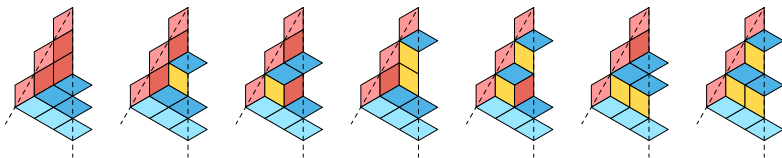
TSSCPP in a hexagon of side $2n$ = # FPL in a square of side n



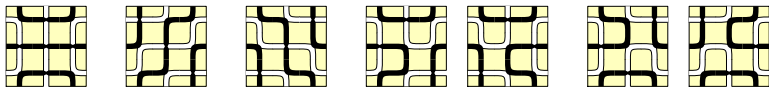
(Proof: Zeilberger 1996, with generating functions and much more;
Kuperberg 1996, specializing results from the Six-vertex model)

We have **no bijectional clue** of why this is true
We have no TSSCPP candidate for **FPL link pattern classes**

Plane Partitions and Fully-Packed Loops



TSSCPP in a hexagon of side $2n$ = # FPL in a square of side n

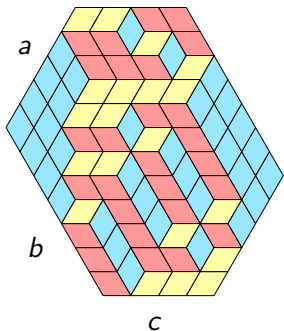



(Proof: Zeilberger 1996, with generating functions and much more;
Kuperberg 1996, specializing results from the Six-vertex model)

We have **no bijectional clue** of why this is true
We have no TSSCPP candidate for **FPL link pattern classes**
But a natural **τ -enumeration** for TSSCPP
is also natural for the $O(1)$ Dense Loop Model

Boxed Plane Partitions as Non-Intersecting Lattice Paths

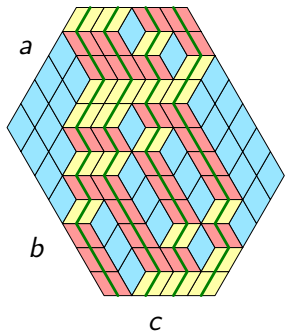
Let's go back to the $a \times b \times c$ boxed Plane Partition, and see why lozenge occupations are a determinantal process...




 I. Gessel and G. Viennot, *Binomial determinants, paths, and hook length formulae*, 1985

Boxed Plane Partitions as Non-Intersecting Lattice Paths

Let's go back to the $a \times b \times c$ boxed Plane Partition, and see why lozenge occupations are a determinantal process...

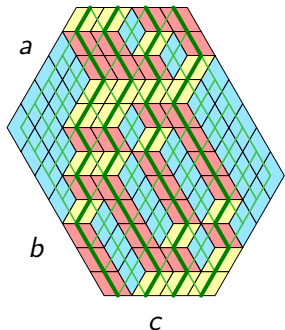


We have c directed paths on the square lattice, connecting top and bottom sides, which do not intersect (NILP)


 I. Gessel and G. Viennot, *Binomial determinants, paths, and hook length formulae*, 1985

Boxed Plane Partitions as Non-Intersecting Lattice Paths

Let's go back to the $a \times b \times c$ boxed Plane Partition, and see why lozenge occupations are a determinantal process...

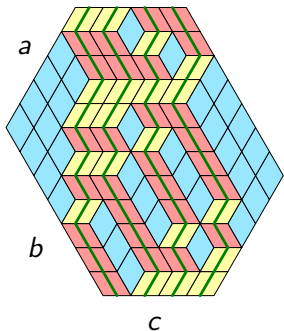


We have c directed paths on the square lattice, connecting top and bottom sides, which do not intersect (NILP)


 I. Gessel and G. Viennot, *Binomial determinants, paths, and hook length formulae*, 1985

Boxed Plane Partitions as Non-Intersecting Lattice Paths

Let's go back to the $a \times b \times c$ boxed Plane Partition, and see why lozenge occupations are a determinantal process...

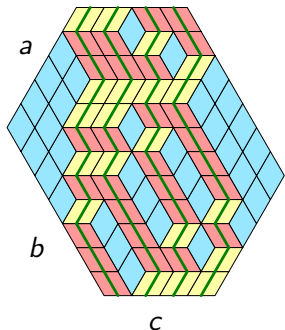


If it weren't for the non-intersecting constraint, the number of path configs would just be $\binom{a+b}{a}^c$, that is....

 I. Gessel and G. Viennot, *Binomial determinants, paths, and hook length formulae*, 1985


Boxed Plane Partitions as Non-Intersecting Lattice Paths

Let's go back to the $a \times b \times c$ boxed Plane Partition, and see why lozenge occupations are a determinantal process...



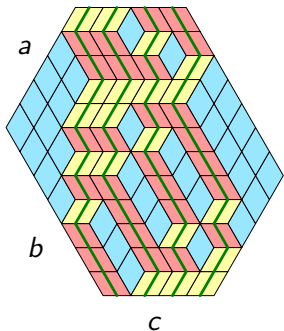
If it weren't for the non-intersecting constraint, the number of path configs would just be $\binom{a+b}{a}^c$, that is....

$$\det \begin{pmatrix} \binom{a+b}{a} & 0 & 0 & 0 \\ 0 & \binom{a+b}{a} & 0 & 0 \\ 0 & 0 & \binom{a+b}{a} & 0 \\ 0 & 0 & 0 & \binom{a+b}{a} \end{pmatrix}$$


 I. Gessel and G. Viennot, *Binomial determinants, paths, and hook length formulae*, 1985

Boxed Plane Partitions as Non-Intersecting Lattice Paths

Let's go back to the $a \times b \times c$ boxed Plane Partition, and see why lozenge occupations are a determinantal process...

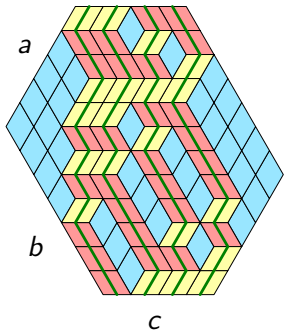


The non-intersecting constraint, through a magic cancellation coming from configs with “the wrong pairing”, leads to the formula...

 I. Gessel and G. Viennot, *Binomial determinants, paths, and hook length formulae*, 1985


Boxed Plane Partitions as Non-Intersecting Lattice Paths

Let's go back to the $a \times b \times c$ boxed Plane Partition, and see why lozenge occupations are a determinantal process...



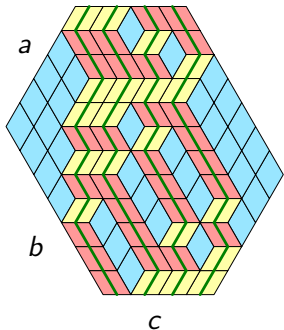
The non-intersecting constraint, through a magic cancellation coming from configs with “the wrong pairing”, leads to the formula...

$$\det \begin{pmatrix} \binom{a+b}{a} & \binom{a+b}{a+1} & \binom{a+b}{a+2} & \binom{a+b}{a+3} \\ \binom{a+b}{a-1} & \binom{a+b}{a} & \binom{a+b}{a+1} & \binom{a+b}{a+2} \\ \binom{a+b}{a-2} & \binom{a+b}{a-1} & \binom{a+b}{a} & \binom{a+b}{a+1} \\ \binom{a+b}{a-3} & \binom{a+b}{a-2} & \binom{a+b}{a-1} & \binom{a+b}{a} \end{pmatrix}$$

 I. Gessel and G. Viennot, *Binomial determinants, paths, and hook length formulae*, 1985

Boxed Plane Partitions as Non-Intersecting Lattice Paths


Let's go back to the $a \times b \times c$ boxed Plane Partition, and see why lozenge occupations are a determinantal process...



The non-intersecting constraint, through a magic cancellation coming from configs with “the wrong pairing”, leads to the formula...

$$\det \begin{pmatrix} \binom{a+b}{a} & \binom{a+b}{a+1} & \binom{a+b}{a+2} & \binom{a+b}{a+3} \\ \binom{a+b}{a-1} & \binom{a+b}{a} & \binom{a+b}{a+1} & \binom{a+b}{a+2} \\ \binom{a+b}{a-2} & \binom{a+b}{a-1} & \binom{a+b}{a} & \binom{a+b}{a+1} \\ \binom{a+b}{a-3} & \binom{a+b}{a-2} & \binom{a+b}{a-1} & \binom{a+b}{a} \end{pmatrix}$$

Why?

 I. Gessel and G. Viennot, *Binomial determinants, paths, and hook length formulae*, 1985

Passing through gates

Consider a collection of gates, of width 1.

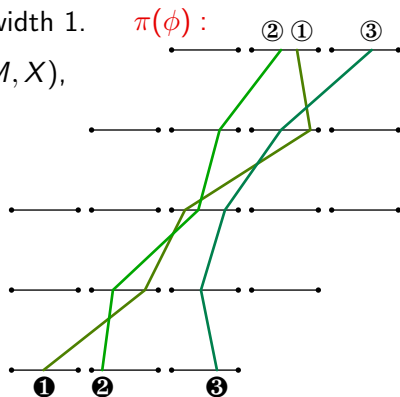
We consider configurations $\phi = (M, X)$, composed of n directed paths, going through the gates.

A matrix $M = \{m_i^{(j)}\}$ encodes the indices of the gates visited by the paths.

A matrix $X = \{x_i^{(j)}\}$ encodes the positions $x \in [0, 1]$ at which the gates are crossed.

Paths go through neighbouring gates, i.e. $m_{i+1}^{(j)} - m_i^{(j)} \in \{0, 1\}$

The measure is $d\mu(\phi) = \epsilon(\pi(\phi)) \prod_{i,j} dx_i^{(j)} f(m_{i+1}^{(j)}, m_i^{(j)})$



Passing through gates

Consider a collection of gates, of width 1.

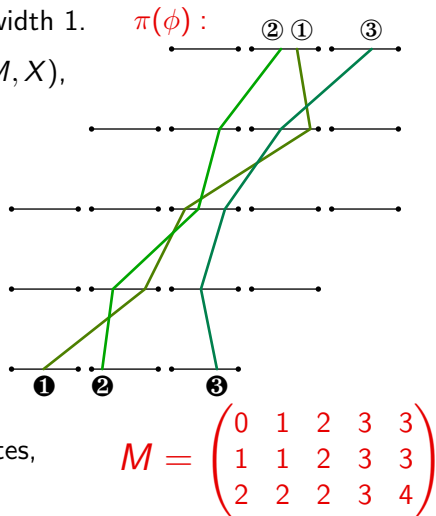
We consider configurations $\phi = (M, X)$, composed of n directed paths, going through the gates.

A matrix $M = \{m_i^{(j)}\}$ encodes the indices of the gates visited by the paths.

A matrix $X = \{x_i^{(j)}\}$ encodes the positions $x \in [0, 1]$ at which the gates are crossed.

Paths go through neighbouring gates, i.e. $m_{i+1}^{(j)} - m_i^{(j)} \in \{0, 1\}$

The measure is $d\mu(\phi) = \epsilon(\pi(\phi)) \prod_{i,j} dx_i^{(j)} f(m_{i+1}^{(j)}, m_i^{(j)})$



Passing through gates

Consider a collection of gates, of width 1.

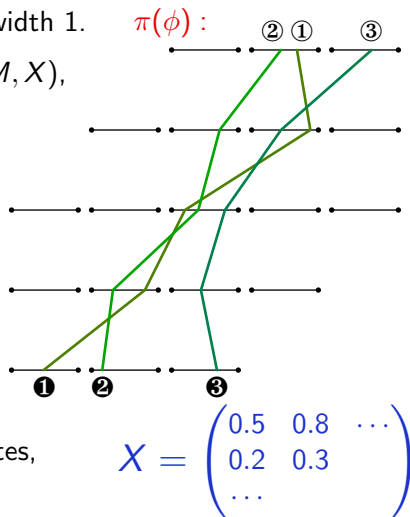
We consider configurations $\phi = (M, X)$, composed of n directed paths, going through the gates.

A matrix $M = \{m_i^{(j)}\}$ encodes the indices of the gates visited by the paths.

A matrix $X = \{x_i^{(j)}\}$ encodes the positions $x \in [0, 1]$ at which the gates are crossed.

Paths go through neighbouring gates, i.e. $m_{i+1}^{(j)} - m_i^{(j)} \in \{0, 1\}$

The measure is $d\mu(\phi) = \epsilon(\pi(\phi)) \prod_{i,j} dx_i^{(j)} f(m_{i+1}^{(j)}, m_i^{(j)})$



Passing through gates

Recall the form of the measure:

$$d\mu(\phi) = \epsilon(\pi(\phi)) \prod_{i,j} dx_i^{(j)} f(m_{i+1}^{(j)}, m_i^{(j)})$$

Calculate the generating function

$$Z = \int d\mu(\phi)$$

The local weights $f(\dots)$

depend on M only.

The entries of X

can be exchanged freely.

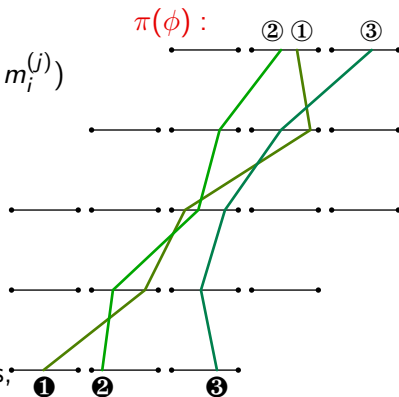
If in ϕ a gate is crossed by k paths,

symmetrize the contribution to Z

summing over the $k!$ rewirings

The relative weight from different ϕ' only comes

from the factor $\epsilon(\pi(\phi'))$ in $d\mu(\phi')$



Passing through gates

and gives an overall factor

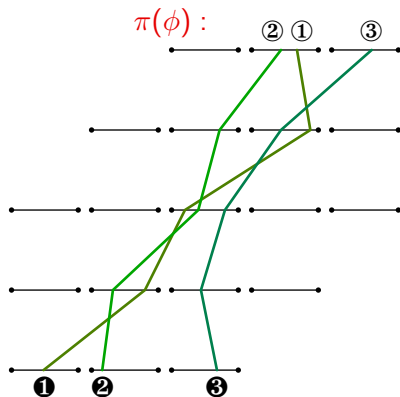
$$\sum_{\sigma \in \mathfrak{S}_k} \epsilon(\sigma) = \begin{cases} 1 & k = 0, 1 \\ 0 & k \geq 2 \end{cases}$$

Thus, the symmetrized contribution of ϕ is **zero** if any gate is crossed two or more times...

now you can integrate over X , and get the desired NILP, i.e., lozenge tilings.

General principle:

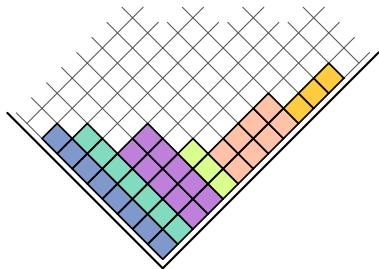
\pm exchange rule \rightarrow involution lemmas \rightarrow 0-1 occupations!



Unrestricted Plane Partitions as an independent process

A picture-reminder of integer partitions and plane partitions...

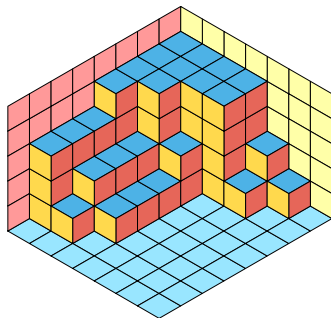
Integer Partitions



Generating function:

$$\sum_{\pi} q^{|\pi|} = \prod_{j \geq 1} \frac{1}{1 - q^j}$$

(Unrestricted) Plane Partitions



Generating function:

$$\sum_{\pi} q^{|\pi|} = \prod_{j \geq 1} \frac{1}{(1 - q^j)^j}$$

Unrestricted Plane Partitions as an independent process

For integer partitions $\mathbf{a} = (a_1, \dots, a_k)$

we have a unique decomposition as $\mathbf{a} = (\dots, \underbrace{k, k, \dots, k}_{\nu_k}, \dots)$

If we consider the measure $\mu(\mathbf{a}) \propto q^{|\mathbf{a}|} = \prod_k (q^k)^{\nu_k}$,

we recognize an independent process for the variables ν_k

Consequences:

Exact Sampling: the ν_k 's are independent geometric variables,

$$\nu_k \stackrel{d}{=} \left\lfloor \frac{\ln \text{rand}(0, 1)}{k \ln q} \right\rfloor$$

Analyticity of Z : the generating function factorizes,

$$Z(q) = \sum_{\mathbf{a}} q^{|\mathbf{a}|} = \prod_k Z_k(q) = \prod_k \frac{1}{1 - q^k}$$

the zeroes of $Z(q)$ for $q \in \mathbb{C}$ are union of the zeroes of the $Z_k(q)$'s

Unrestricted Plane Partitions as an independent process

This is very much like what happens for the **integers**:

For **integers** $n \in \mathbb{N}^+$ we have a **unique prime decomposition**

$$n = \prod_{p \in \mathcal{P}} p^{\nu_p}$$

If we consider the measure $\mu_\alpha(n) \propto n^{-\alpha} = \prod_{p \in \mathcal{P}} (p^{-\alpha})^{\nu_p}$, we recognize an **independent process** for the exponents ν_p

Consequences:

Exact Sampling:

$$\ln n \stackrel{d}{=} \sum_{p \in \mathcal{P}} \ln p \left[-\frac{\ln \text{rand}(0, 1)}{\alpha \ln p} \right]$$

Analyticity of Z : Euler product formula for Riemann ζ function

$$\zeta(\alpha) = \sum_n \frac{1}{n^\alpha} = \prod_{p \in \mathcal{P}} Z_p(\alpha) = \prod_{p \in \mathcal{P}} \frac{1}{1 - p^{-\alpha}}$$

Unrestricted Plane Partitions as an independent process

For Unrestricted Plane Partitions π , MacMahon formula states

$$Z_{\text{PP}}(q) = \sum_{\pi} q^{|\pi|} = \prod_{j \geq 1} \frac{1}{(1 - q^j)^j}$$

Do we have a “**unique prime decomposition**”


$$\pi = p_{1,1}^{\nu_{1,1}} p_{2,1}^{\nu_{2,1}} p_{2,2}^{\nu_{2,2}} p_{3,1}^{\nu_{3,1}} p_{3,2}^{\nu_{3,2}} p_{3,3}^{\nu_{3,3}} \cdots$$

such that the prime object $p_{k,h}$ has k cubes (thus carries a q^k)?

Note: this would imply the formula for $Z_{\text{PP}}(q)$.

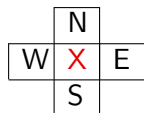
Answer: in a sense, yes... the “primes” are the “hooks”

 Bender and Knuth, *Enumeration of Plane Partitions*, 1972

 I. Pak, *Hook length formula and geometric combinatorics*, 2001

The Pak Algorithm

From the **independent variables** $\nu(x, y) \equiv \nu_{x+y-1, x}$,
to $h(x, y)$, the **height of the pile** of cubes in (x, y)



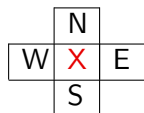
operation A: $X \rightarrow X + \max(N, E)$;

operation B: $X \rightarrow -X + \max(N, E) + \min(S, W)$;

To **clear** (x, y) means to apply A at (x, y) , and B at $(x + z, y + z)_{z \geq 1}$
For $\mathbf{x} = (x, y)$, say $\mathbf{x} \prec \mathbf{x}'$ if $x < x'$ and $y < y'$

1. the input is your $\nu = \{\nu(x, y)\}$.
2. take $S \subset \mathbb{N}^2$, closed under \prec , and $S \supseteq \{(x, y) : \nu(x, y) > 0\}$.
3. clear all $(x, y) \in S$, in a whatever order compatible with \prec
(larger first).
4. the result is your $\mathbf{h} = \{h(x, y)\}$.

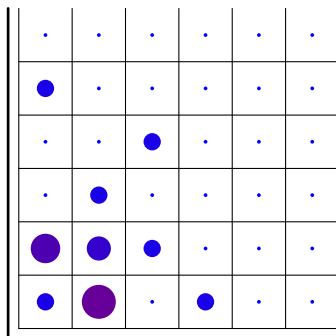
The Pak Algorithm



operation A: $X \rightarrow X + \max(N, E)$;

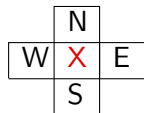
operation B: $X \rightarrow -X + \max(N, E) + \min(S, W)$;

$C(x, y)$: apply A at (x, y) , and B at $(x + z, y + z)_{z \geq 1}$



1. the input is your $\nu = \{\nu(x, y)\}$.

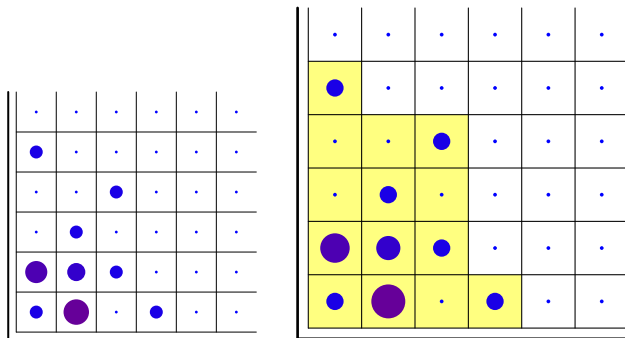
The Pak Algorithm



operation A: $X \rightarrow X + \max(N, E)$;

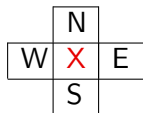
operation B: $X \rightarrow -X + \max(N, E) + \min(S, W)$;

$C(x, y)$: apply A at (x, y) , and B at $(x + z, y + z)_{z \geq 1}$



2. take $S \subset \mathbb{N}^2$, convex and containing all positive ν 's.

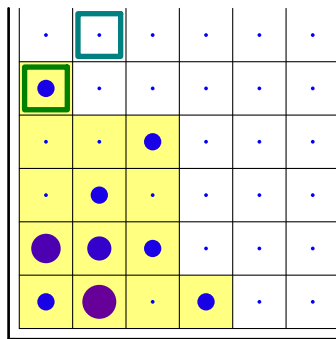
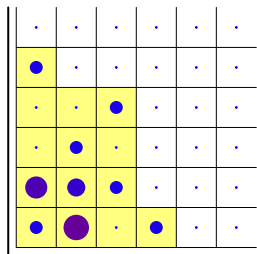
The Pak Algorithm



operation A: $X \rightarrow X + \max(N, E)$;

operation B: $X \rightarrow -X + \max(N, E) + \min(S, W)$;

$C(x, y)$: apply A at (x, y) , and B at $(x + z, y + z)_{z \geq 1}$



3. clear all $(x, y) \in S$, larger first, w.r.t. partial ordering.

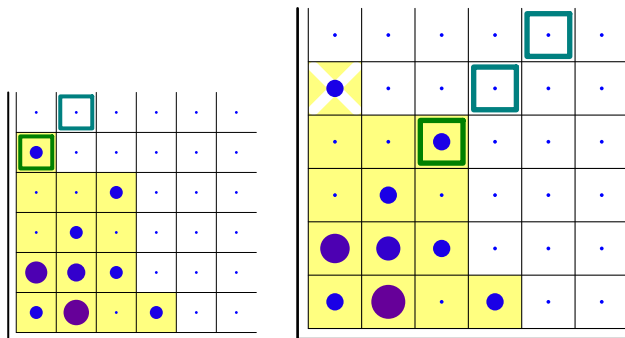
The Pak Algorithm

	N	
W	X	E
	S	

operation A: $X \rightarrow X + \max(N, E)$;

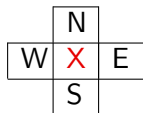
operation B: $X \rightarrow -X + \max(N, E) + \min(S, W)$;

$C(x, y)$: apply A at (x, y) , and B at $(x + z, y + z)_{z \geq 1}$



3. clear all $(x, y) \in S$, larger first, w.r.t. partial ordering.

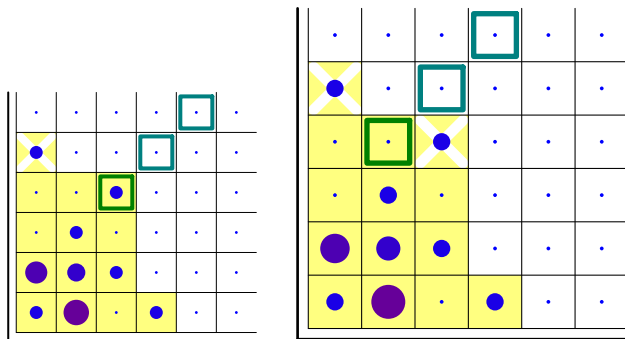
The Pak Algorithm



operation A: $X \rightarrow X + \max(N, E)$;

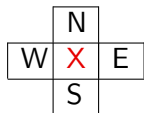
operation B: $X \rightarrow -X + \max(N, E) + \min(S, W)$;

$C(x, y)$: apply A at (x, y) , and B at $(x + z, y + z)_{z \geq 1}$



3. clear all $(x, y) \in S$, larger first, w.r.t. partial ordering.

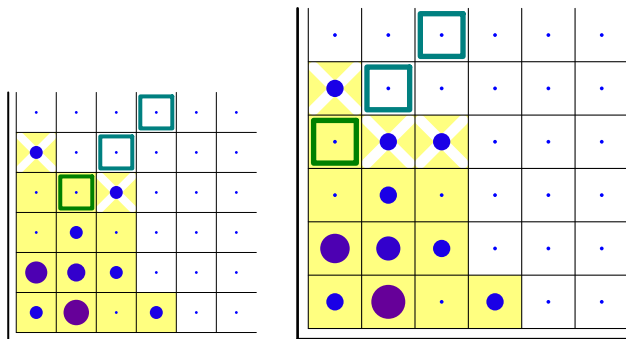
The Pak Algorithm



operation A: $X \rightarrow X + \max(N, E)$;

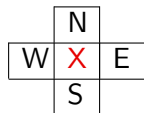
operation B: $X \rightarrow -X + \max(N, E) + \min(S, W)$;

$C(x, y)$: apply A at (x, y) , and B at $(x+z, y+z)_{z \geq 1}$



3. clear all $(x, y) \in S$, larger first, w.r.t. partial ordering.

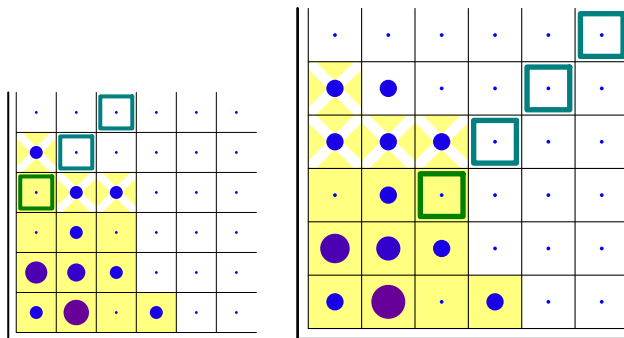
The Pak Algorithm



operation A: $X \rightarrow X + \max(N, E)$;

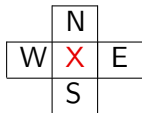
operation B: $X \rightarrow -X + \max(N, E) + \min(S, W)$;

$C(x, y)$: apply A at (x, y) , and B at $(x+z, y+z)_{z \geq 1}$



3. clear all $(x, y) \in S$, larger first, w.r.t. partial ordering.

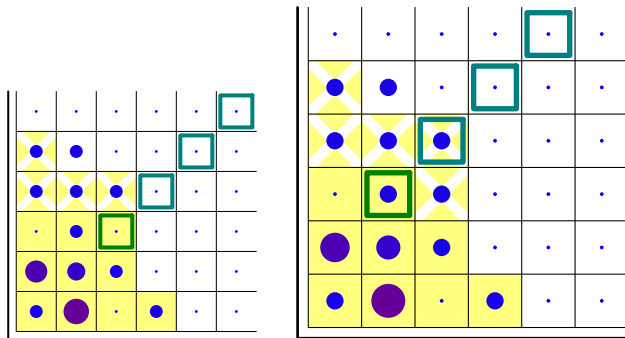
The Pak Algorithm



operation A: $X \rightarrow X + \max(N, E)$;

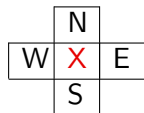
operation B: $X \rightarrow -X + \max(N, E) + \min(S, W)$;

$C(x, y)$: apply A at (x, y) , and B at $(x + z, y + z)_{z \geq 1}$



3. clear all $(x, y) \in S$, larger first, w.r.t. partial ordering.

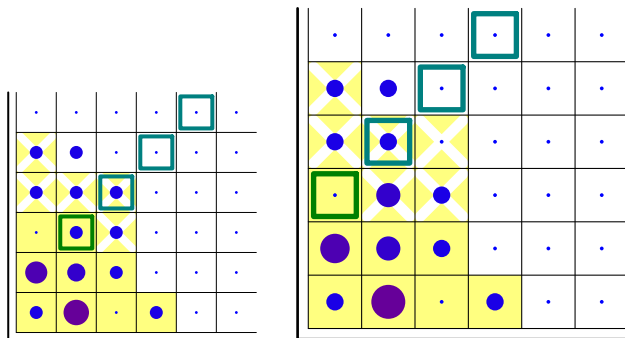
The Pak Algorithm



operation A: $X \rightarrow X + \max(N, E)$;

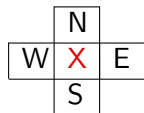
operation B: $X \rightarrow -X + \max(N, E) + \min(S, W)$;

$C(x, y)$: apply A at (x, y) , and B at $(x+z, y+z)_{z \geq 1}$



3. clear all $(x, y) \in S$, larger first, w.r.t. partial ordering.

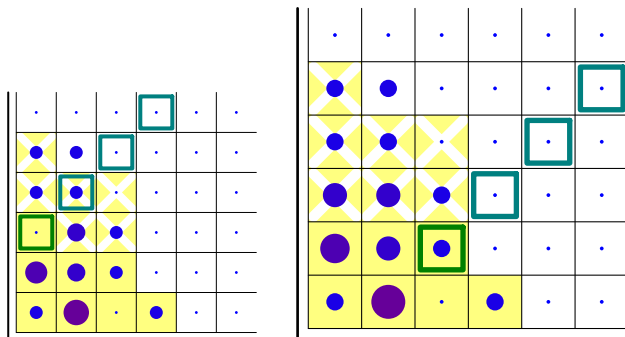
The Pak Algorithm



operation A: $X \rightarrow X + \max(N, E)$;

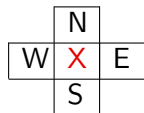
operation B: $X \rightarrow -X + \max(N, E) + \min(S, W)$;

$C(x, y)$: apply A at (x, y) , and B at $(x + z, y + z)_{z \geq 1}$



3. clear all $(x, y) \in S$, larger first, w.r.t. partial ordering.

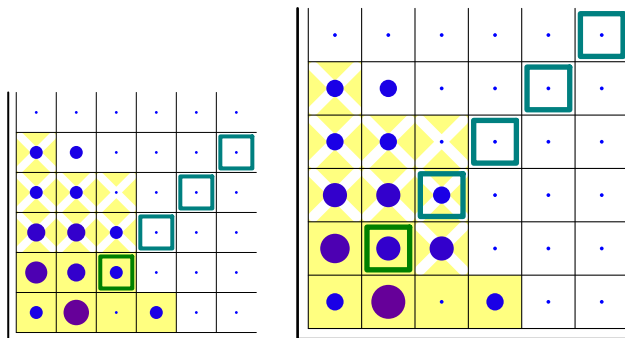
The Pak Algorithm



operation A: $X \rightarrow X + \max(N, E)$;

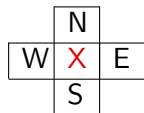
operation B: $X \rightarrow -X + \max(N, E) + \min(S, W)$;

$C(x, y)$: apply A at (x, y) , and B at $(x + z, y + z)_{z \geq 1}$



3. clear all $(x, y) \in S$, larger first, w.r.t. partial ordering.

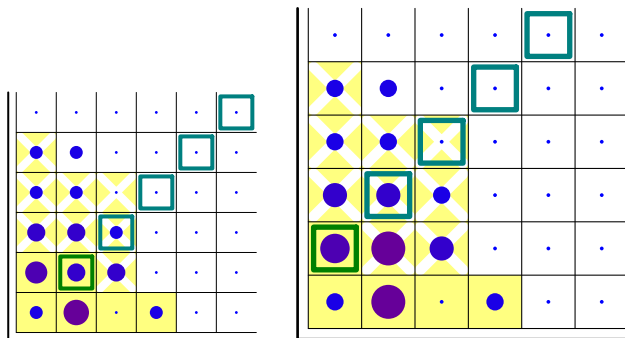
The Pak Algorithm



operation A: $X \rightarrow X + \max(N, E)$;

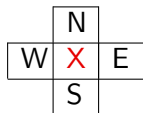
operation B: $X \rightarrow -X + \max(N, E) + \min(S, W)$;

$C(x, y)$: apply A at (x, y) , and B at $(x + z, y + z)_{z \geq 1}$



3. clear all $(x, y) \in S$, larger first, w.r.t. partial ordering.

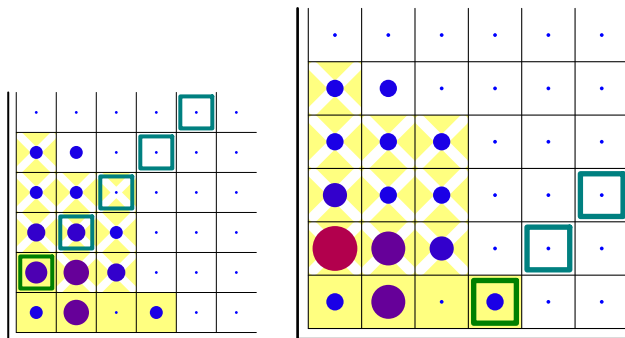
The Pak Algorithm



operation A: $X \rightarrow X + \max(N, E)$;

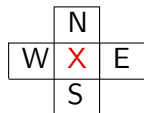
operation B: $X \rightarrow -X + \max(N, E) + \min(S, W)$;

$C(x, y)$: apply A at (x, y) , and B at $(x+z, y+z)_{z \geq 1}$



3. clear all $(x, y) \in S$, larger first, w.r.t. partial ordering.

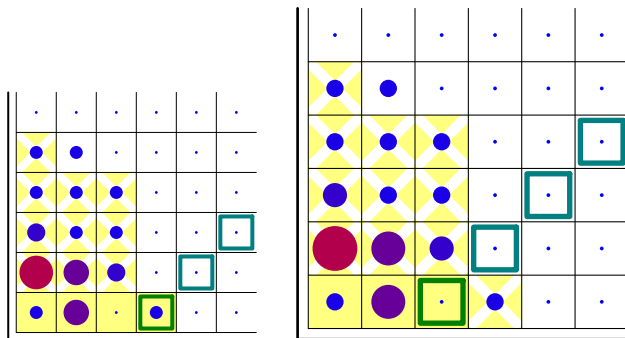
The Pak Algorithm



operation A: $X \rightarrow X + \max(N, E)$;

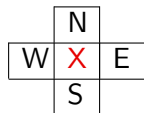
operation B: $X \rightarrow -X + \max(N, E) + \min(S, W)$;

$C(x, y)$: apply A at (x, y) , and B at $(x+z, y+z)_{z \geq 1}$



3. clear all $(x, y) \in S$, larger first, w.r.t. partial ordering.

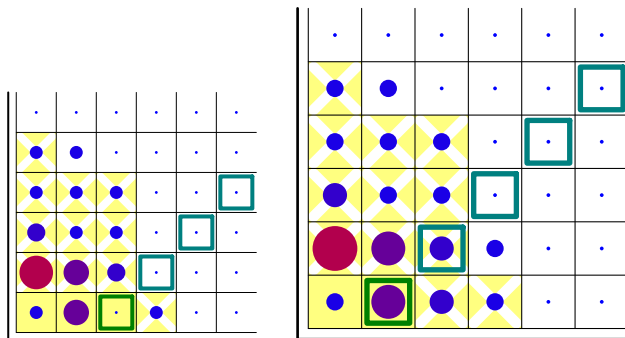
The Pak Algorithm



operation A: $X \rightarrow X + \max(N, E)$;

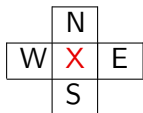
operation B: $X \rightarrow -X + \max(N, E) + \min(S, W)$;

$C(x, y)$: apply A at (x, y) , and B at $(x+z, y+z)_{z \geq 1}$



3. clear all $(x, y) \in S$, larger first, w.r.t. partial ordering.

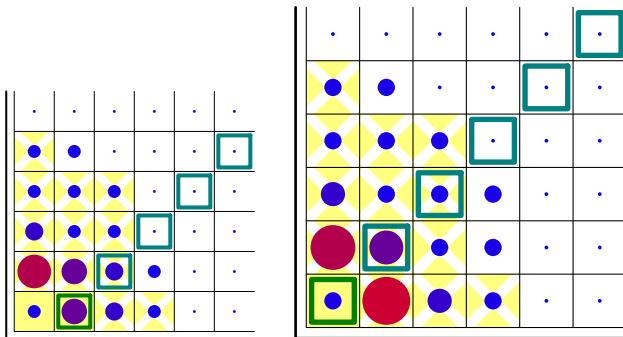
The Pak Algorithm



operation A: $X \rightarrow X + \max(N, E)$;

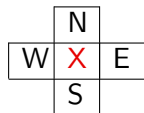
operation B: $X \rightarrow -X + \max(N, E) + \min(S, W)$;

$C(x, y)$: apply A at (x, y) , and B at $(x+z, y+z)_{z \geq 1}$



3. clear all $(x, y) \in S$, larger first, w.r.t. partial ordering.

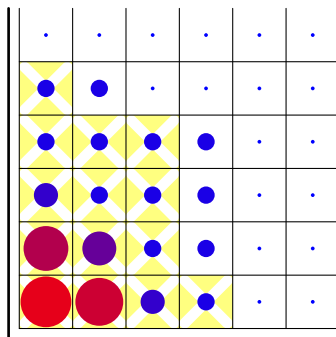
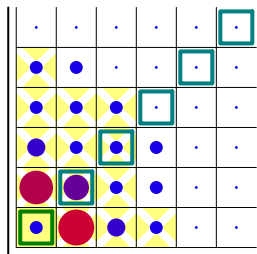
The Pak Algorithm



operation A: $X \rightarrow X + \max(N, E)$;

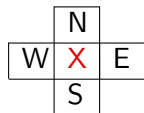
operation B: $X \rightarrow -X + \max(N, E) + \min(S, W)$;

$C(x, y)$: apply A at (x, y) , and B at $(x + z, y + z)_{z \geq 1}$



- clear all $(x, y) \in S$, larger first, w.r.t. partial ordering.

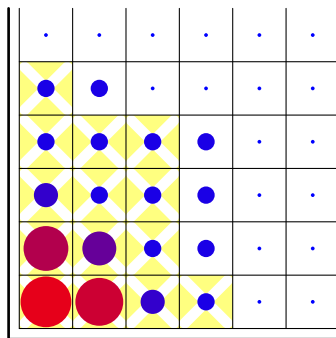
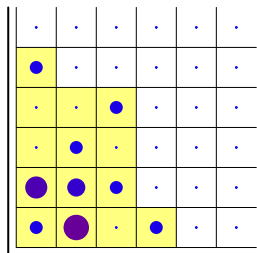
The Pak Algorithm



operation A: $X \rightarrow X + \max(N, E)$;

operation B: $X \rightarrow -X + \max(N, E) + \min(S, W)$;

$C(x, y)$: apply A at (x, y) , and B at $(x + z, y + z)_{z \geq 1}$

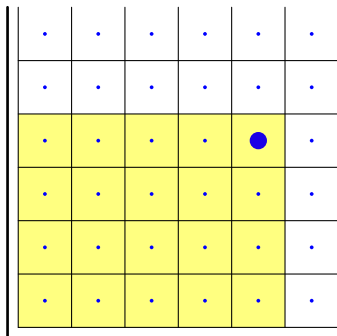


4. the result is your $\mathbf{h} = \{h(x, y)\}$.

The Pak Algorithm

A bit hard to follow... Let's see some simpler cases:

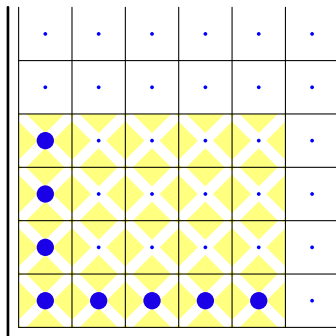
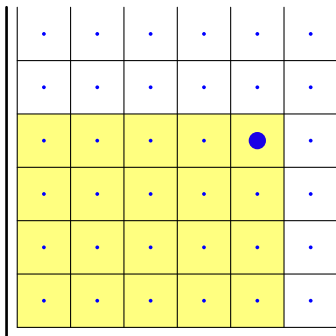
1. A single $\nu_{x,y} > 0$ makes a height- ν hook-shaped height function



The Pak Algorithm

A bit hard to follow... Let's see some simpler cases:

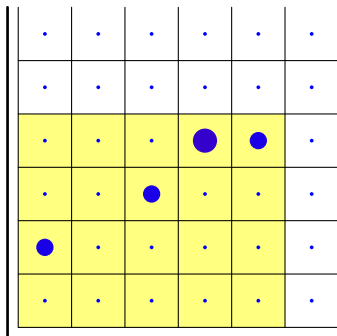
1. A single $\nu_{x,y} > 0$ makes a height- ν hook-shaped height function



The Pak Algorithm

A bit hard to follow... Let's see some simpler cases:

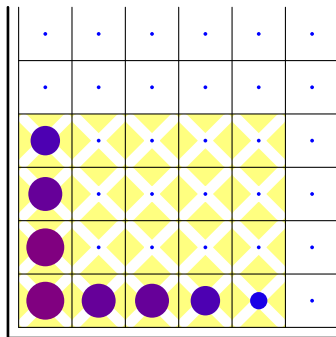
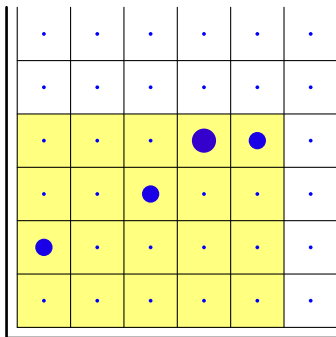
2. A chain of $\nu_{x_i, y_i} > 0$, for $(x_1, y_1) \prec (x_2, y_2) \prec \dots$, leads to the sum of the previous hook-shaped height functions



The Pak Algorithm

A bit hard to follow... Let's see some simpler cases:

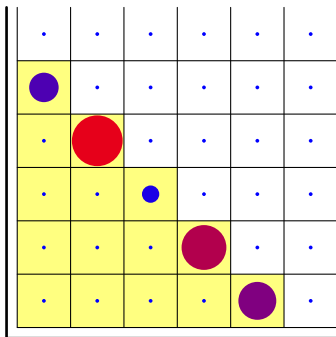
2. A chain of $\nu_{x_i, y_i} > 0$, for $(x_1, y_1) \prec (x_2, y_2) \prec \dots$, leads to the sum of the previous hook-shaped height functions



The Pak Algorithm

A bit hard to follow... Let's see some simpler cases:

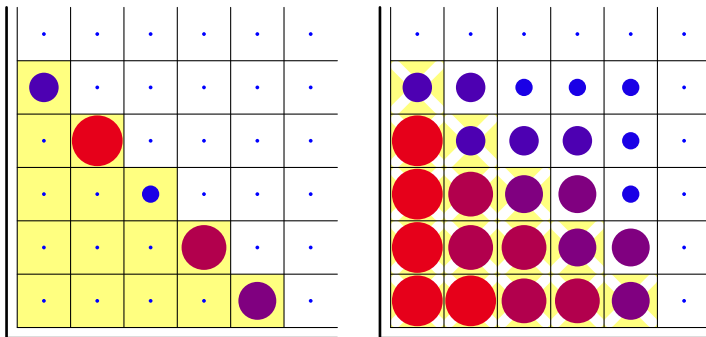
3. A diagonal of $\nu_{x_i, y_i} > 0$, for (x_i, y_i) not ordered w.r.t. \prec , makes the hooks to stack one on top of the other, the higher values of ν are stacked before



The Pak Algorithm

A bit hard to follow... Let's see some simpler cases:

3. A diagonal of $\nu_{x_i, y_i} > 0$, for (x_i, y_i) not ordered w.r.t. \prec , makes the hooks to stack one on top of the other, the higher values of ν are stacked before

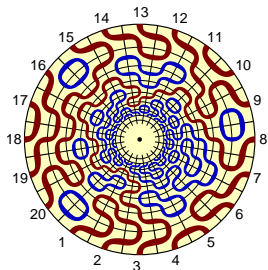


THIS SHOULD BE THE END OF THE FIRST LECTURE...

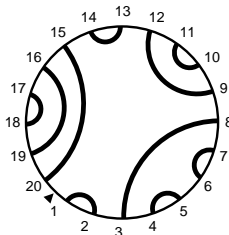
Lecture 2

Proof of the Razumov-Stroganov correspondence

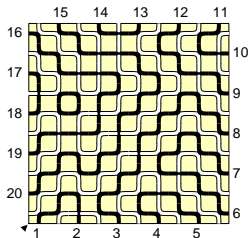
The Razumov-Stroganov correspondence... a reminder



$\tilde{\Psi}_n(\pi)$: probability of π
in the $O(1)$ Dense Loop Model
in the $\{1, \dots, 2n\} \times \mathbb{N}$ cylinder



$\Psi_n(\pi)$: probability of π
for FPL with uniform measure
in the $n \times n$ square



Razumov-Stroganov correspondence

(conjecture: Razumov Stroganov, 2001; proof: AS Cantini, 2010)

$$\tilde{\Psi}_n(\pi) = \Psi_n(\pi)$$

Dihedral symmetry of FPL

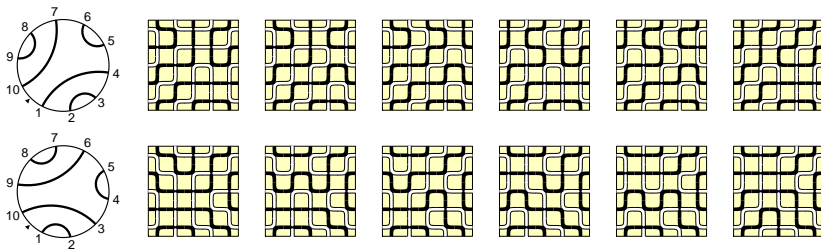
We stated yesterday that the surprising corollary of the Razumov-Stroganov 2001 conjecture, on [dihedral symmetry](#) of FPL $\psi_n(\pi)$ enumerations, was already a theorem by then...

call R the operator that rotates a link pattern by one position

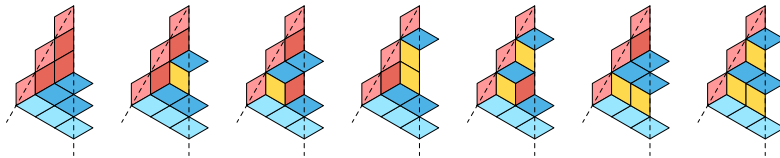
Dihedral symmetry of FPL

(proof: Wieland, 2000)

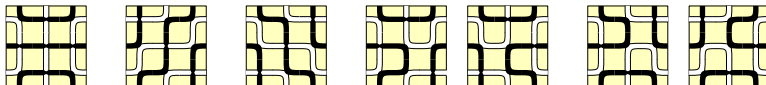
$$\Psi_n(\pi) = \Psi_n(R\pi)$$



Plane Partitions and Fully-Packed Loops




TSSCPP in a hexagon of side $2n$ = # FPL in a square of side n



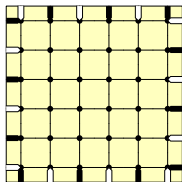
(Proof: Zeilberger 1996, with generating functions and much more;
Kuperberg 1996, specializing results from the Six-vertex model)

We have **no bijectional clue** of why this is true

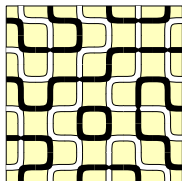
 D.M. Bressoud and J. Propp, *How the Alternating Sign Matrix Conjecture was solved*, (1999)

FPL in fancy domains...

We considered so far FPL in the $n \times n$ square domain, with alternating boundary conditions, i.e. consistent fillings of this:

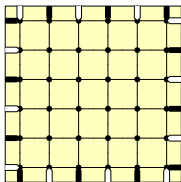


into things like this:

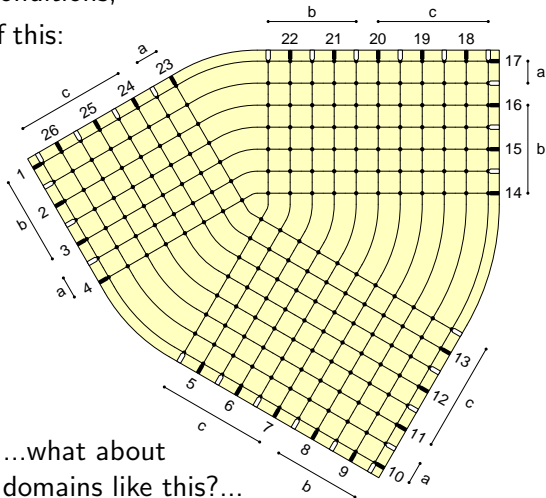
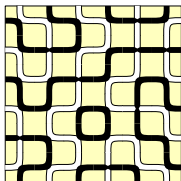


FPL in fancy domains...

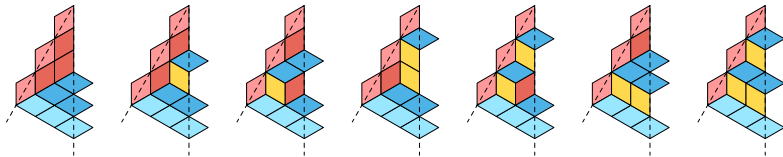
We considered so far FPL in the $n \times n$ square domain, with alternating boundary conditions, i.e. consistent fillings of this:



into things like this:



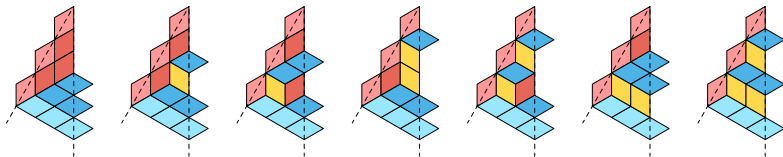
Plane Partitions and Fully-Packed Loops



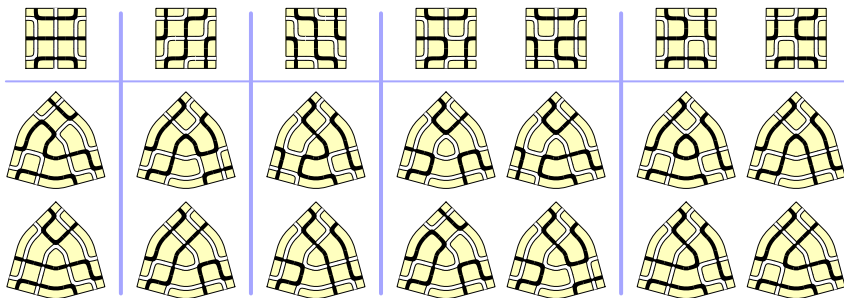
TSSCPP in a hexagon of side $2n$ = # FPL in a square of side n



Plane Partitions and Fully-Packed Loops



TSSCPP in a hexagon of side $2n$ = # FPL in a square of side n



...maybe generalize Razumov-Stroganov before proving it?...

First part of the proof: old facts from integrability

The Temperley-Lieb(1) monoid

Consider the **graphical action** over **link patterns** $\pi \in \mathcal{LP}(n)$
(throw away detached cycles)

$$R : \begin{array}{c} \text{7 strands with crossings} \\ 1 \quad 2 \quad 3 \quad \dots \quad 2n \end{array} \quad e_j : \begin{array}{c} \text{strands } 1, 2, 3, \dots, j, j+1, \dots, 2n \\ \text{with a cap on strands } j, j+1 \end{array}$$

The maps $\{e_j\}_{1 \leq j \leq 2n}$ and $R^{\pm 1}$ generate a **semigroup**

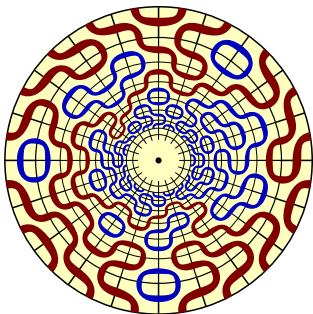
Example:

$$e_1(\pi) : \begin{array}{c} \text{Diagram with crossings and a cap on strands 1, 2} \\ 1 \quad 2 \quad 3 \quad 4 \quad 5 \quad 6 \quad 7 \quad 8 \quad 9 \quad 10 \end{array} = \begin{array}{c} \text{Diagram with a cap on strands 1, 2 and other arcs} \\ 1 \quad 2 \quad 3 \quad 4 \quad 5 \quad 6 \quad 7 \quad 8 \quad 9 \quad 10 \end{array}$$

$$e_2(\pi) : \begin{array}{c} \text{Diagram with crossings and a cap on strands 2, 3} \\ 1 \quad 2 \quad 3 \quad 4 \quad 5 \quad 6 \quad 7 \quad 8 \quad 9 \quad 10 \end{array} = \begin{array}{c} \text{Diagram with a cap on strands 2, 3 and other arcs} \\ 1 \quad 2 \quad 3 \quad 4 \quad 5 \quad 6 \quad 7 \quad 8 \quad 9 \quad 10 \end{array}$$

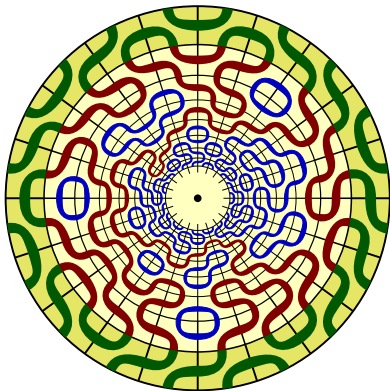
Consider the **linear space** $\mathbb{C}^{\mathcal{LP}(n)}$, linear span of **basis vectors** $|\pi\rangle$.
 Operators e_j and $R^{\pm 1}$ are **linear operators** over $\mathbb{C}^{\mathcal{LP}(n)}$

$O(1)$ dense loop model: the Markov Chain over $\mathcal{LP}(n)$



A config with $t - 1$ layers.

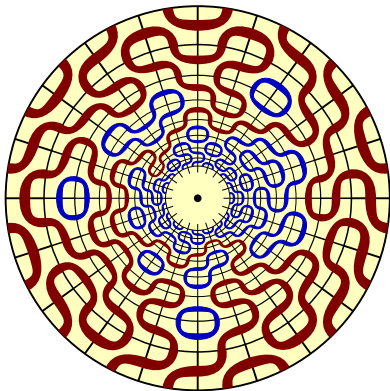
$O(1)$ dense loop model: the Markov Chain over $\mathcal{LP}(n)$



A config with $t - 1$ layers.

Add a new layer, of i.i.d. tiles,
with prob. $p = 1/2 \dots$

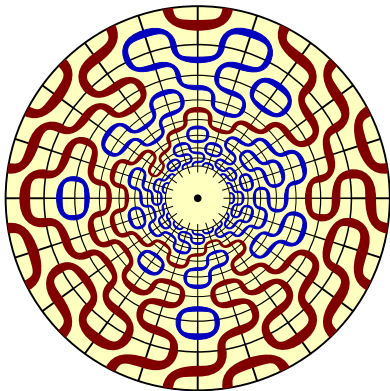
$O(1)$ dense loop model: the Markov Chain over $\mathcal{LP}(n)$



A config with $t - 1$ layers.

Add a new layer, of i.i.d. tiles,
with prob. $p = 1/2$...

$O(1)$ dense loop model: the Markov Chain over $\mathcal{LP}(n)$



A config with $t - 1$ layers.

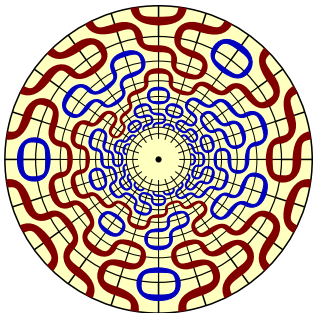
Add a new layer, of i.i.d. tiles, with prob. $p = 1/2$...

Some loops get detached from the boundary. You have a config with t layers, and a new link pattern.

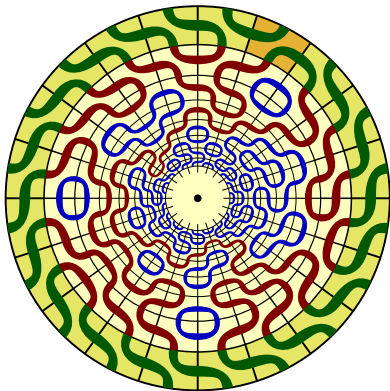
$$\text{Rates } T_{p=1/2}(\pi, \pi')$$

$O(1)$ dense loop model: an example at work

Now repeat the game...



$O(1)$ dense loop model: an example at work

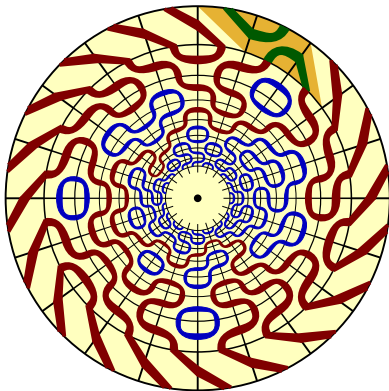


Now repeat the game...

...but add i.i.d. tiles, with prob.

$p \rightarrow 0 \dots$

$O(1)$ dense loop model: an example at work



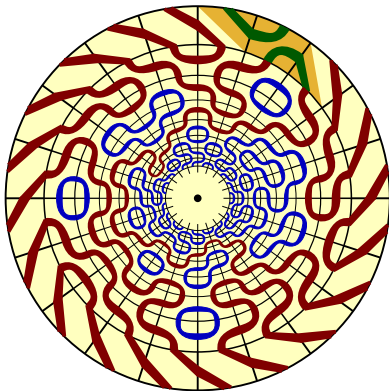
Now repeat the game...

...but add i.i.d. tiles, with prob.
 $p \rightarrow 0$...

For most of the layers you just rotate. From time to time, you have a single non-trivial tile.

$$\text{Rates } T_{p \rightarrow 0}(\pi, \pi')$$

$O(1)$ dense loop model: an example at work



Now repeat the game...

...but add i.i.d. tiles, with prob.
 $p \rightarrow 0$...

For most of the layers you just rotate. From time to time, you have a single non-trivial tile.

Rates $T_{p \rightarrow 0}(\pi, \pi')$

Non-trivial layers look like
operators $R e_j$

Integrability: commutation of Transfer Matrices

Call $T_p(\pi, \pi')$ the matrix of transition rates
(on the space of link patterns $\mathbb{C}^{\mathcal{LP}(n)}$)
for tiling one layer using probability p .

Trivial: $\tilde{\Psi}_p(\pi)$, the steady state, is the **unique** eigenstate of $T_p(\pi, \pi')$ with all positive entries

A magic application of Yang-Baxter: $[T_p, T_{p'}] = 0$

Consequence: $\tilde{\Psi}_p(\pi) \equiv \tilde{\Psi}_{p'}(\pi)$ and we can get $\tilde{\Psi}(\pi) := \tilde{\Psi}_{1/2}(\pi)$ from the study of the easier $T_{p \rightarrow 0}(\pi, \pi')$

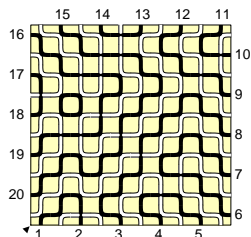
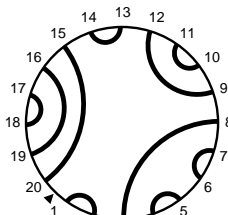
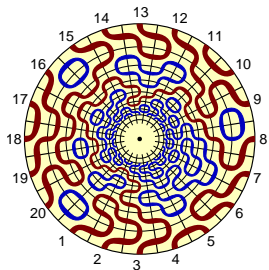
Call $H_n = \sum_{i=1}^{2n} (e_i - 1)$ and $|\tilde{\mathfrak{s}}_n\rangle = \sum_{\pi} \tilde{\Psi}(\pi) |\pi\rangle$.

Realize $R^{-1} T_p = I + pH + \mathcal{O}(p^2)$. We thus have

$$H_n |\tilde{\mathfrak{s}}_n\rangle = 0$$

linear-algebra characterization of $\tilde{\Psi}(\pi)$

The Razumov-Stroganov correspondence: reloaded



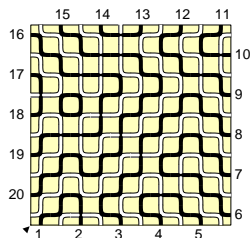
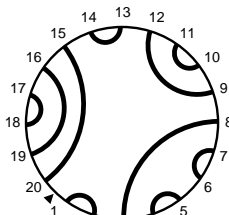
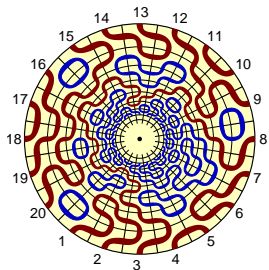
$$|\tilde{s}_n\rangle := \sum_{\pi \in \mathcal{LP}(n)} \tilde{\Psi}_n(\pi) |\pi\rangle$$

$$H_n |\tilde{s}_n\rangle = 0$$

$$|s_n\rangle = \sum_{\phi \in \mathcal{Fpl}(n)} |\pi(\phi)\rangle$$

$$\mathcal{Fpl}(n) = \{ \text{FPL in } n \times n \text{ square} \}$$

The Razumov-Stroganov correspondence: reloaded



$$|\tilde{s}_n\rangle := \sum_{\pi \in \mathcal{L}\mathcal{P}(n)} \tilde{\Psi}_n(\pi) |\pi\rangle$$
$$H_n |\tilde{s}_n\rangle = 0$$

$$|s_n\rangle = \sum_{\phi \in \mathcal{F}pl(n)} |\pi(\phi)\rangle$$
$$\mathcal{F}pl(n) = \{ \text{FPL in } n \times n \text{ square} \}$$

Razumov-Stroganov correspondence

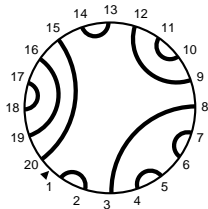
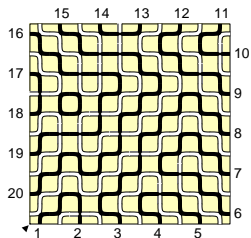
(conjecture: Razumov Stroganov, 2001; proof: AS Cantini, 2010)

$$H_n |s_n\rangle = 0$$

Second part of the proof: new facts from gyration

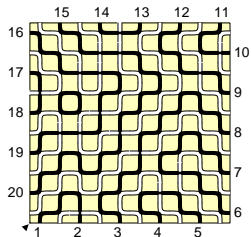
Wieland gyration: how it works

FPL config

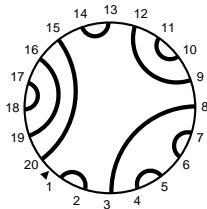
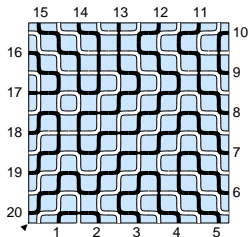


Wieland gyration: how it works



FPL config



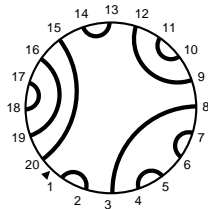
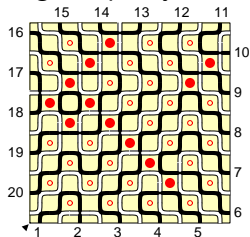
...and its conjugate,
exchanging black and white





Wieland gyration: how it works

Mark faces  and ,

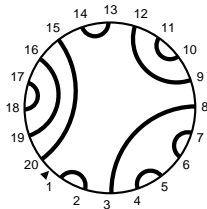
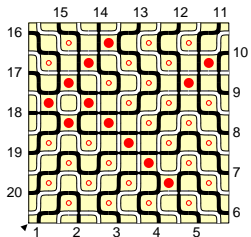
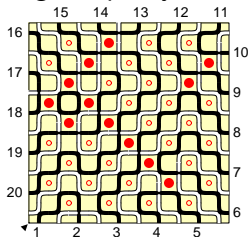
of given parity





Wieland gyration: how it works

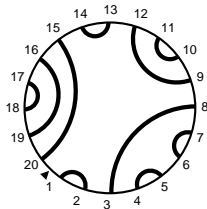
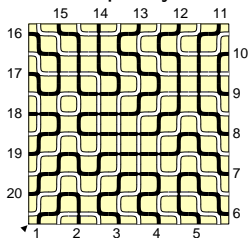
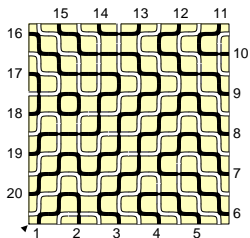
Mark faces  and ,
of given parity

Exchange  \leftrightarrow 





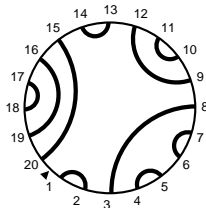
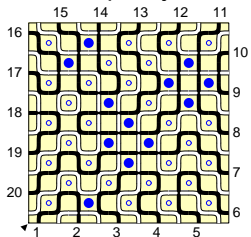
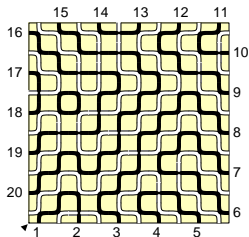
Wieland gyration: how it works

Mark faces  and ,
of other parity







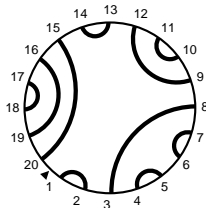
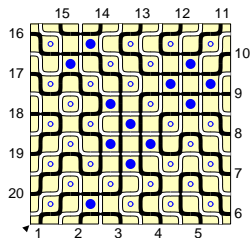
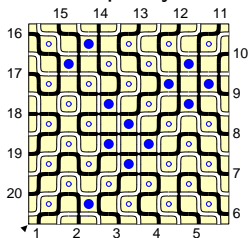
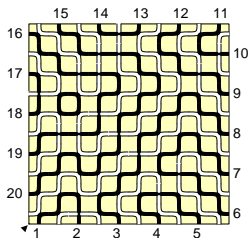
Wieland gyration: how it works

Mark faces  and ,
of other parity

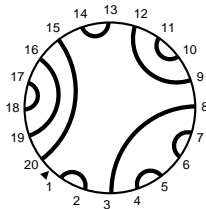
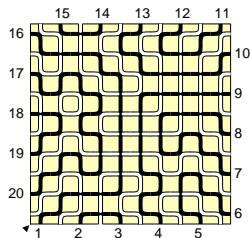
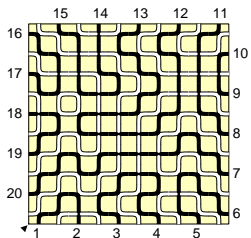
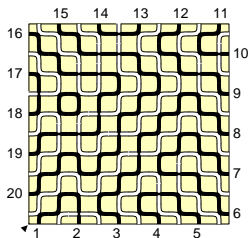


Wieland gyration: how it works

Mark faces  and , Exchange  \leftrightarrow 

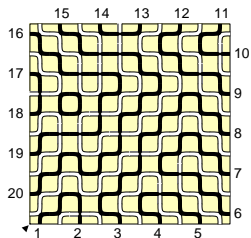


Wieland gyration: how it works

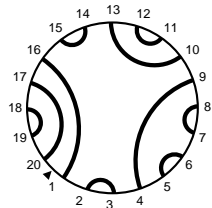
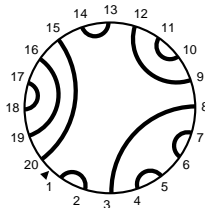
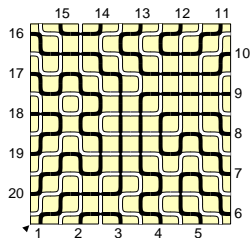
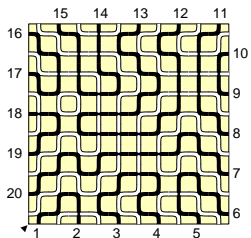


Wieland gyration: how it works

Link pattern $\pi...$

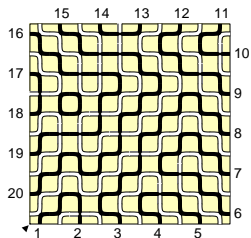


...and $R\pi...$

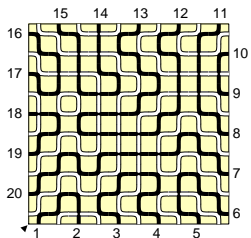


Wieland gyration: how it works

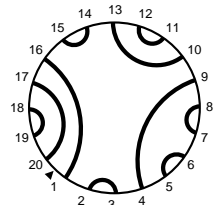
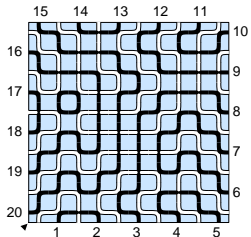
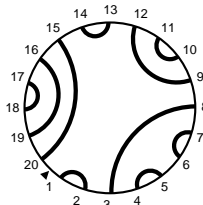
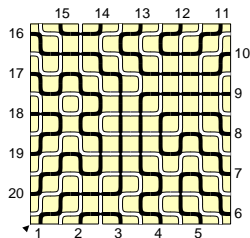
Link pattern $\pi...$



...and, on the conjugate
of the intermediate step...

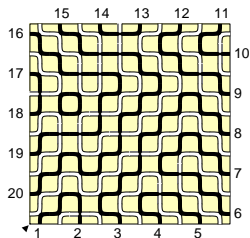


...and $R\pi...$

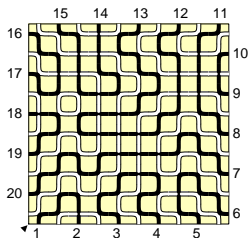


Wieland gyration: how it works

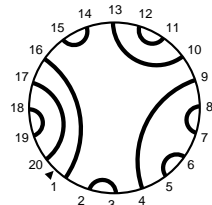
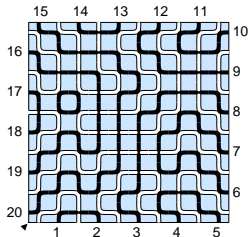
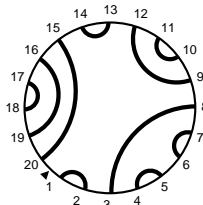
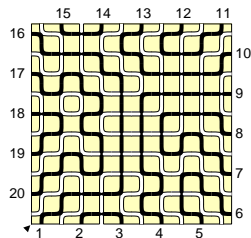
Link pattern $\pi\dots$



$\dots R^{\frac{1}{2}} \pi \dots$



\dots and $R \pi \dots$



An unnoticed lemma on gyration orbits

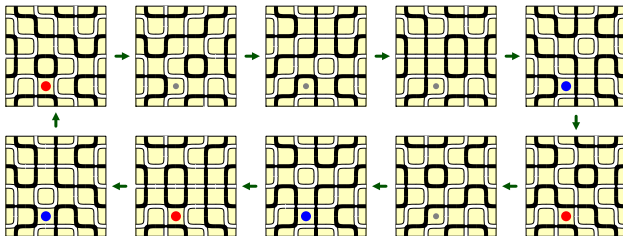
Call $\mathcal{O}(\phi)$ the orbit of ϕ under Wieland gyration.

For a face α , say

$$\mathcal{N}_\alpha(\phi) = \begin{cases} +1 & \text{if you have } \boxed{\blacksquare} \\ -1 & \text{if you have } \boxed{\square} \\ 0 & \text{otherwise} \end{cases}$$

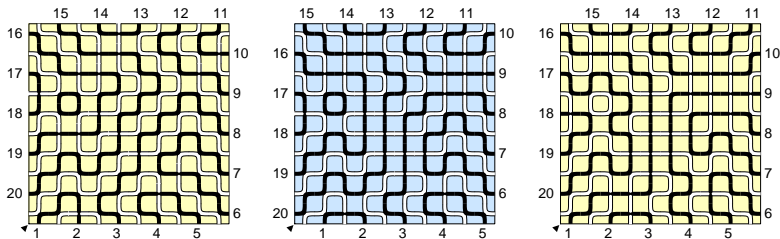
A lemma on \mathcal{N}_α

$$\forall \text{ FPL } \phi, \text{ face } \alpha \quad \sum_{\phi' \in \mathcal{O}(\phi)} \mathcal{N}_\alpha(\phi') = 0$$



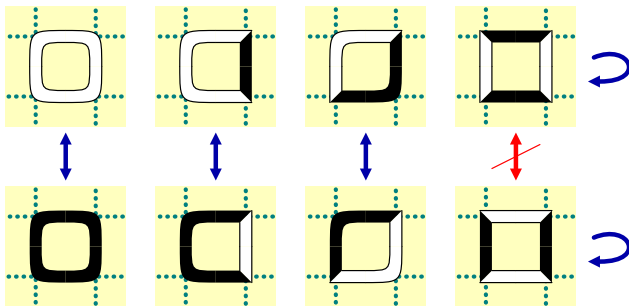
Wieland gyration: why it works

Easier to visualize the $\square \leftrightarrow \square$ exchange on the few \square , \square faces...
...but better use the conjugate config at intermediate step,
and think that \square , \square are **the only faces fixed** in the transformation



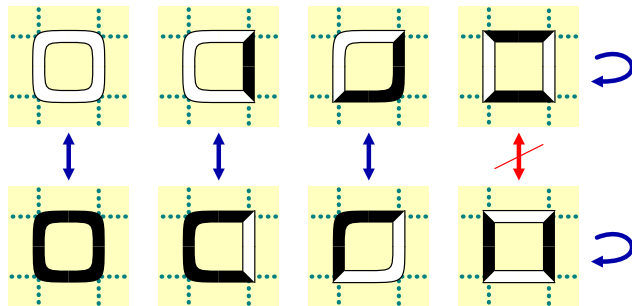
Wieland gyration: why it works

Easier to visualize the $\square \leftrightarrow \square$ exchange on the few \square , \square faces...
...but better use the conjugate config at intermediate step,
and think that \square , \square are **the only faces fixed** in the transformation



Wieland gyration: why it works

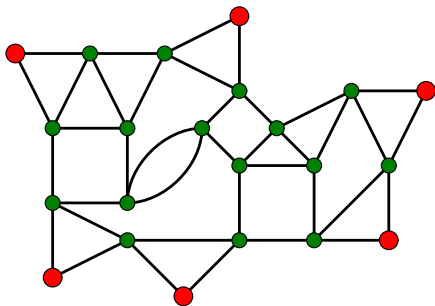
Easier to visualize the $\square \leftrightarrow \square$ exchange on the few \square , \square faces...
...but better use the conjugate config at intermediate step,
and think that \square , \square are **the only faces fixed** in the transformation



This **inverts** $\deg_{\text{black}}(v) \leftrightarrow \deg_{\text{white}}(v)$,
and **preserves** connectivity of open-path endpoints

Wieland gyration: why it works

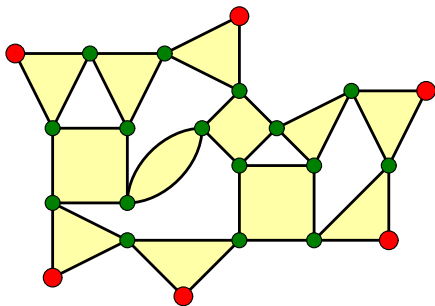
We have seen why Wieland gyration works “in the bulk”: now we see how it works “globally”:



A graph with vertices of degree 2 and 4...

Wieland gyration: why it works

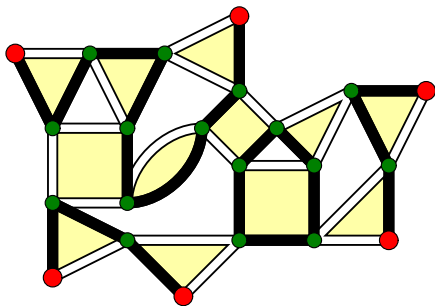
We have seen why Wieland gyration works “in the bulk”: now we see how it works “globally”:



...a decomposition of
the edge-set into cycles
 $\ell \leq 4$

Wieland gyration: why it works

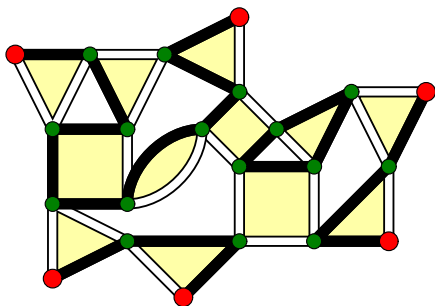
We have seen why Wieland gyration works “in the bulk”: now we see how it works “globally”:





A FPL configuration

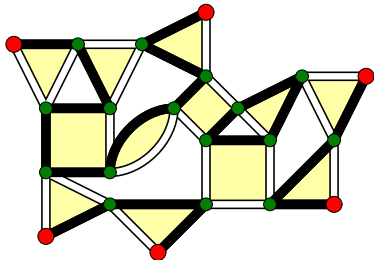
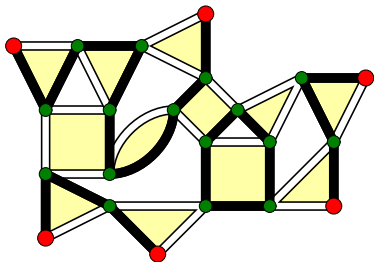
Wieland gyration: why it works

We have seen why Wieland gyration works “in the bulk”: now we see how it works “globally”:



Invert colouration in all faces except  and : same link pattern for open paths (connecting red bullets)

Wieland gyration: why it works



Wieland gyration: where it works

So, the trick is:

- **invert** $\deg_{\text{black}}(v) \leftrightarrow \deg_{\text{white}}(v)$
- **preserve** connectivity of open paths

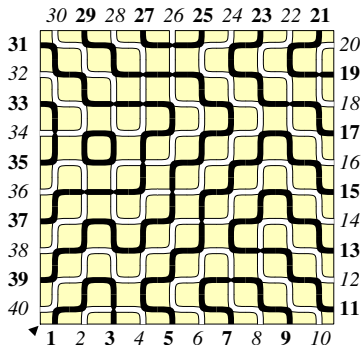
- Works with the Wieland recipe, on faces $\ell = 4$
- Works with just complementation, on faces $\ell = 1, 2, 3$
- Can't work at all on faces $\ell \geq 5$
- At boundaries, pair external legs to produce triangles, and you're within the framework above... **figs in next slide!**

A **single** move exists on plenty of graphs...
but **rotation** comes from **two** moves!

If you want two, you get a very strict **classification theorem**
(essentially, convex planar quadrangulations, and up to 4 triangles)
...however, many more domains than just $n \times n$ squares!

Wieland gyration: where it works

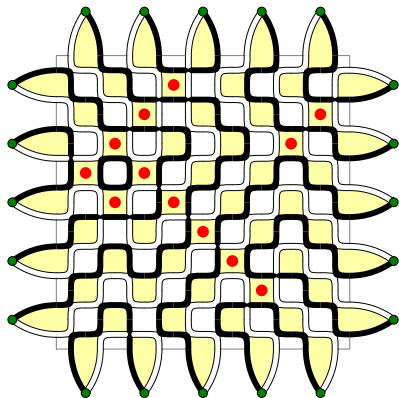
...in the original square domain for FPL we have “external legs” (i.e., vertices of degree 1)... how do we recover the setting above with vertices of degree 2 and 4?



A configuration on (Λ, τ_+)
(i.e., first leg is black)

Wieland gyration: where it works

...in the original square domain for FPL we have “external legs” (i.e., vertices of degree 1)... how do we recover the setting above with vertices of degree 2 and 4?

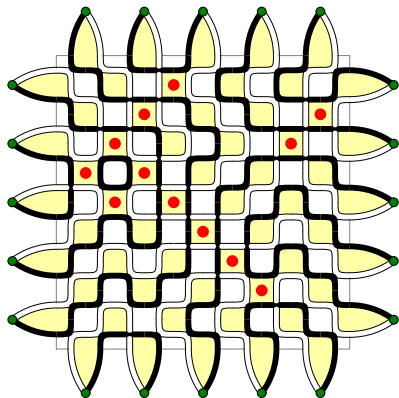


The construction of \mathcal{G}_+ ,
pairing $(2j - 1, 2j)$ legs
(plaquettes are in yellow)

mark in red  and 

Wieland gyration: where it works

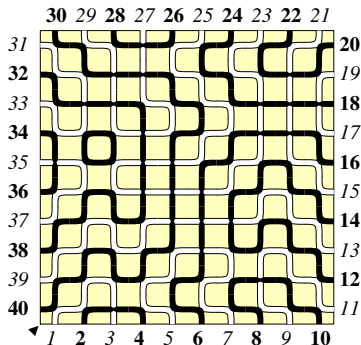
...in the original square domain for FPL we have “external legs” (i.e., vertices of degree 1)... how do we recover the setting above with vertices of degree 2 and 4?



The result of map H_+

Wieland gyration: where it works

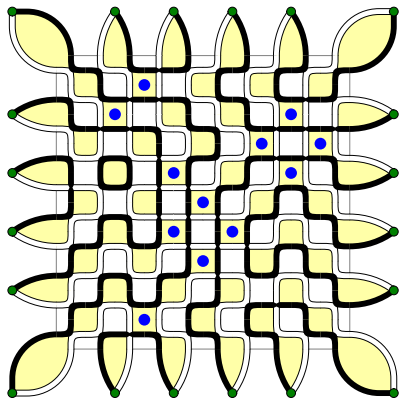
...in the original square domain for FPL we have “external legs” (i.e., vertices of degree 1)... how do we recover the setting above with vertices of degree 2 and 4?





Split auxiliary vertices to recover the (Λ, τ_-) geometry (i.e., first leg is white)

Wieland gyration: where it works

...in the original square domain for FPL we have “external legs” (i.e., vertices of degree 1)... how do we recover the setting above with vertices of degree 2 and 4?

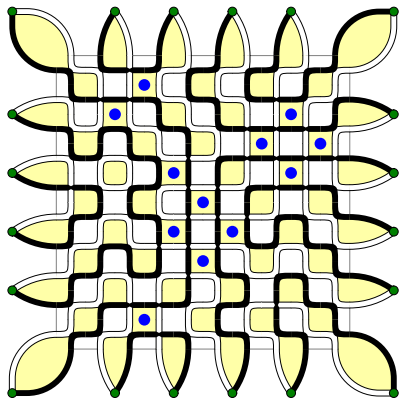


The construction of \mathcal{G}_- ,
pairing $(2j, 2j + 1)$ legs

mark in blue  and 

Wieland gyration: where it works

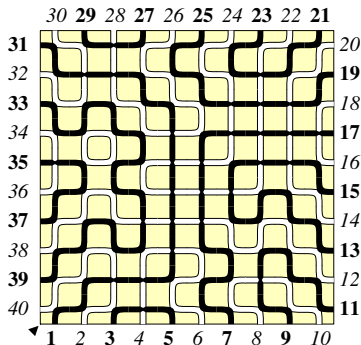
...in the original square domain for FPL we have “external legs” (i.e., vertices of degree 1)... how do we recover the setting above with vertices of degree 2 and 4?



The result of map H_-

Wieland gyration: where it works

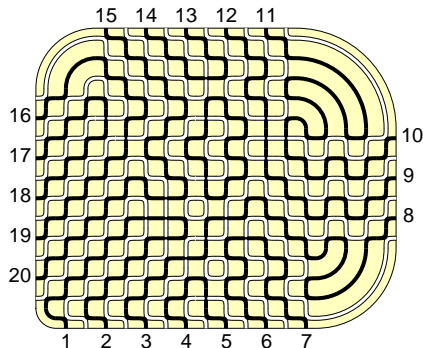
...in the original square domain for FPL we have “external legs” (i.e., vertices of degree 1)... how do we recover the setting above with vertices of degree 2 and 4?



Split auxiliary vertices to recover the (Λ, τ_+) original geometry (with a rotated link pattern)...

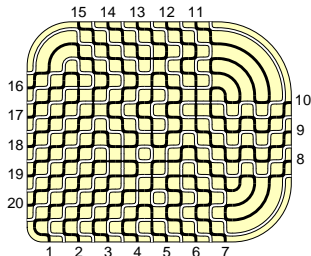
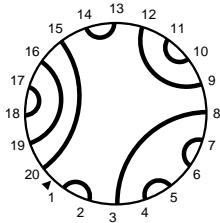
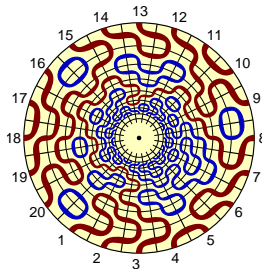
Wieland gyration: where it works

An example of our “convex planar quadrangulations, and up to 4 triangles” general domains...



(bottom line: an **elementary** generalization of Wieland strategy gives **rotational symmetry** for FPL enumerations above)

The Razumov-Stroganov correspondence: generalised



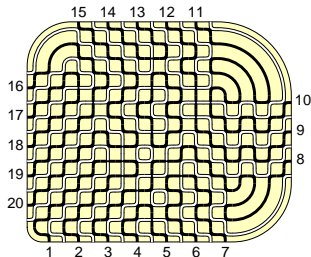
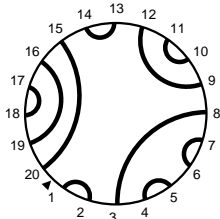
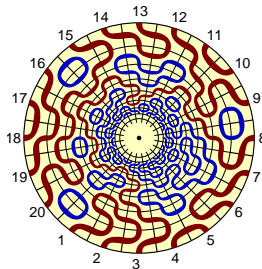
$$|\tilde{s}_n\rangle := \sum_{\pi \in \mathcal{LP}(n)} \tilde{\Psi}_n(\pi) |\pi\rangle$$

$$H_n |\tilde{s}_n\rangle = 0$$

$$|s_\Lambda\rangle = \sum_{\phi \in \mathcal{Fpl}(\Lambda)} |\pi(\phi)\rangle$$

$$\mathcal{Fpl}(\Lambda) = \{ \text{FPL in domain } \Lambda \}$$

The Razumov-Stroganov correspondence: generalised



$$|\tilde{s}_n\rangle := \sum_{\pi \in \mathcal{LP}(n)} \tilde{\Psi}_n(\pi) |\pi\rangle$$

$$H_n |\tilde{s}_n\rangle = 0$$

$$|s_\Lambda\rangle = \sum_{\phi \in \mathcal{Fpl}(\Lambda)} |\pi(\phi)\rangle$$

$$\mathcal{Fpl}(\Lambda) = \{ \text{FPL in domain } \Lambda \}$$

Razumov-Stroganov correspondence on Wieland domains

(proof: AS Cantini, 2010)

$$\tilde{\Psi}_n(\pi) = \Psi_\Lambda(\pi)$$

i.e.

$$H_n |s_\Lambda\rangle = 0$$

Yet one word on gyration... the boundary conditions

We have seen how to generalise the **domain**,
using black/white alternating boundary conditions

What does it happen if we generalise on **boundary conditions**?

Pairing consecutive legs with the same colour produces arcs,
and “**loses link-pattern information**”: gyration holds for
linear combinations of $\Psi(\pi)$, instead of component-wise.

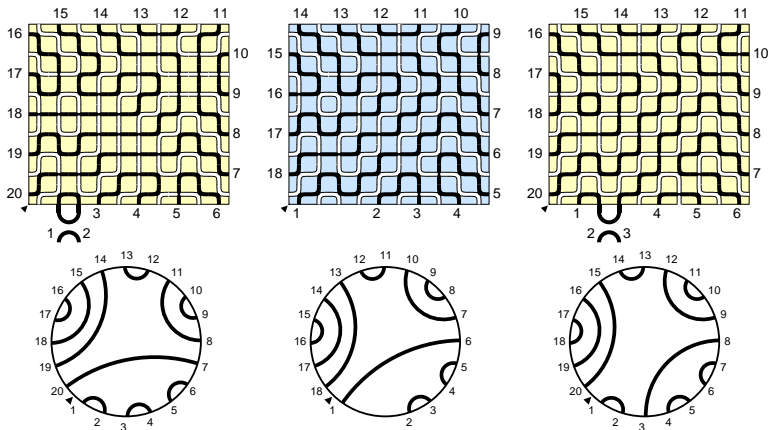
These linear combinations, induced by arcs, are well-described by
Temperley-Lieb operators.

This fact suggested us that gyration on domains
with a “**defect**” in the boundary conditions was related to
Razumov-Stroganov (in its “linear-algebra formulation” ...)

An example with generic boundary conditions

Example: the state $|s_j^c\rangle$ (that we define in the next slide) satisfies

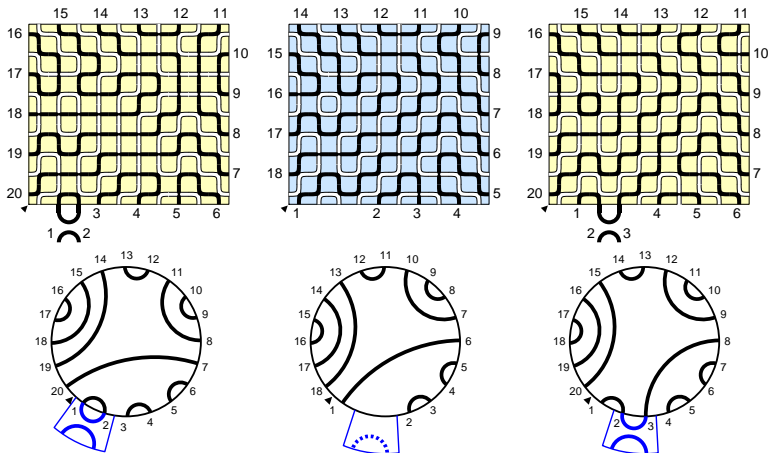
$$(R e_{j-1} - e_j)|s_j^c\rangle = 0$$



An example with generic boundary conditions

Example: the state $|s_j^c\rangle$ (that we define in the next slide) satisfies

$$(R e_{j-1} - e_j)|s_j^c\rangle = 0$$



The structure of the proof

Rewrite the starting $H|s\rangle = 0$ as $\mathbf{S}(e_j - 1)|s\rangle = 0$
 $\mathbf{S} := 1 + R + \dots + R^{2n-1}$

Write “ $|s\rangle = |s_j^a\rangle + |s_j^b\rangle + |s_j^c\rangle$ ”,
i.e., **marginalise** w.r.t. a single matrix entry (on the boundary).

$$\begin{aligned} |s\rangle &= \text{grid} = \text{grid}_1 + \text{grid}_2 + \text{grid}_3 \\ &= \text{grid}_4 + \text{grid}_5 + \text{grid}_6 \\ &= |s_j^a\rangle + |s_j^b\rangle + |s_j^c\rangle \end{aligned}$$

The structure of the proof

Combining **recursion relations** with the new **gyration relations** gives

$$\mathbf{S}(e_j - 1)|s_j^a\rangle = \mathbf{S}(e_{j+1} - 1)(|s_{j+1}^a\rangle + |s_{j+1}^c\rangle)$$

$$\mathbf{S}(e_j - 1)|s_j^b\rangle = \mathbf{S}(e_{j-1} - 1)(|s_{j-1}^b\rangle + |s_{j-1}^c\rangle)$$

Recursion end up at the **corners** of the domain, and you get

$$H|s\rangle = \sum_j \mathbf{S}(e_j - 1)|s_j^c\rangle$$

Note: we have “ $(e_j - 1)|s_j^c\rangle$ ” terms, not “ $(e_j - 1)|s_k^c\rangle$ ”
and a double sum, as in the naïve approach!

The summands are **separately** zero, as seen using the **lemma on \mathcal{N}_α**

What is left to do

- We can deal with ASM, HTASM, QTASM (also refined), all special cases of our generalization
- We get as corollary the translation of integrability results from the spin chain to ASM, and vice versa
- Yet another corollary is the generalization of the “Alternating Sign Matrix conjecture” to the whole family of Wieland domains (at least for what concerns divisibility)

...but we miss:

- The refined conjecture for the monodromy matrix by Ph. Di Francesco in `cond-mat/0407477` (JSTAT 2004, P08009)
- VSASM – USASM – UUSASM – OSASM, refined with boundary parameters, and Razumov-Stroganov correspondence for the *closed* spin chain and *symplectic* characters

An example of our generalized ASM–TSSCPP Theorem

From Zeilberger / Kuperberg, we know that $\# \text{TSSCPP}$ of size $2n$ equals A_n , i.e. $\# \text{FPL}$ of size n .

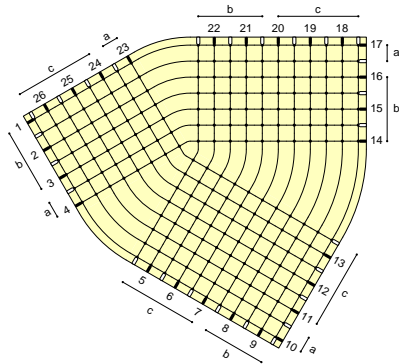
From Razumov-Stroganov on a domain Λ (with $2n$ black legs), we know that

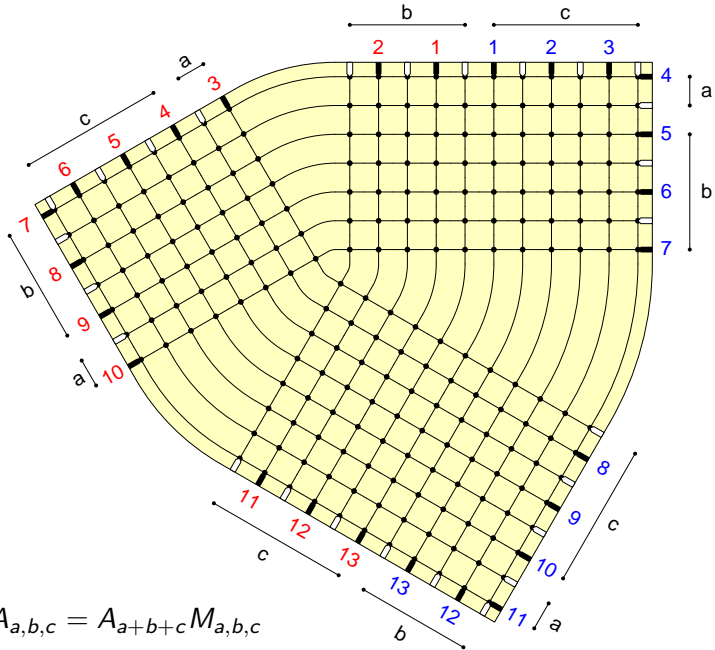
$$A_\Lambda = A_n K(\Lambda) \quad K(\Lambda) \in \mathbb{N}$$

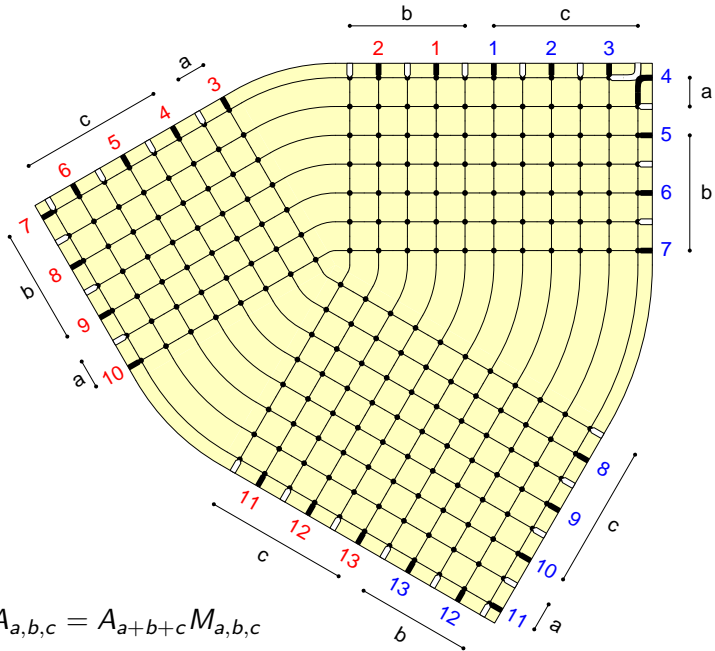
These numbers $K(\Lambda)$ are to be determined. We now do this for the “triangloid”, proving

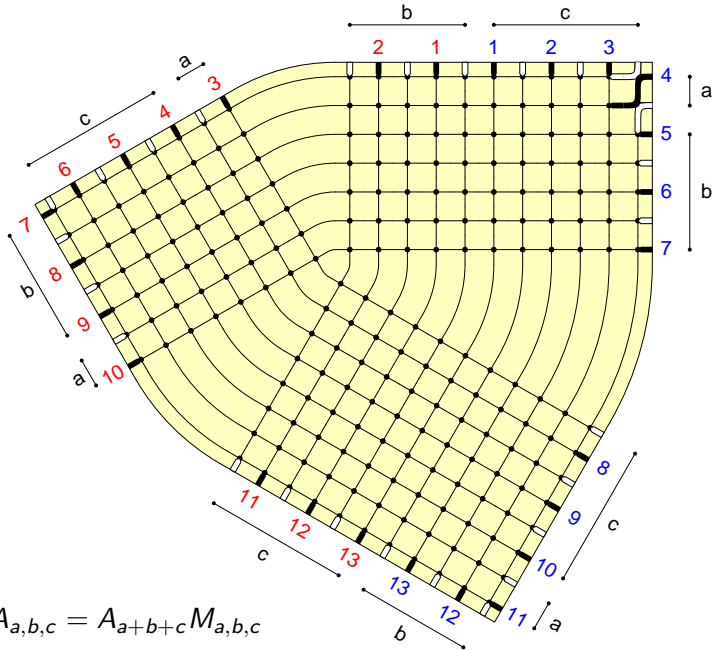
$$A_{a,b,c} = A_{a+b+c} M_{a,b,c}$$

(where $M_{a,b,c}$ is the number of Plane Partitions in the $a \times b \times c$ box, MacMahon 1915 formula)

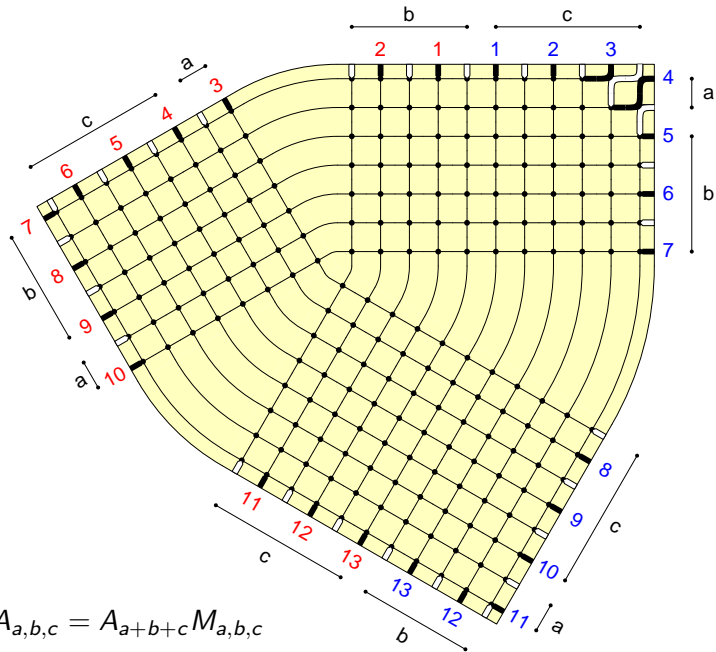




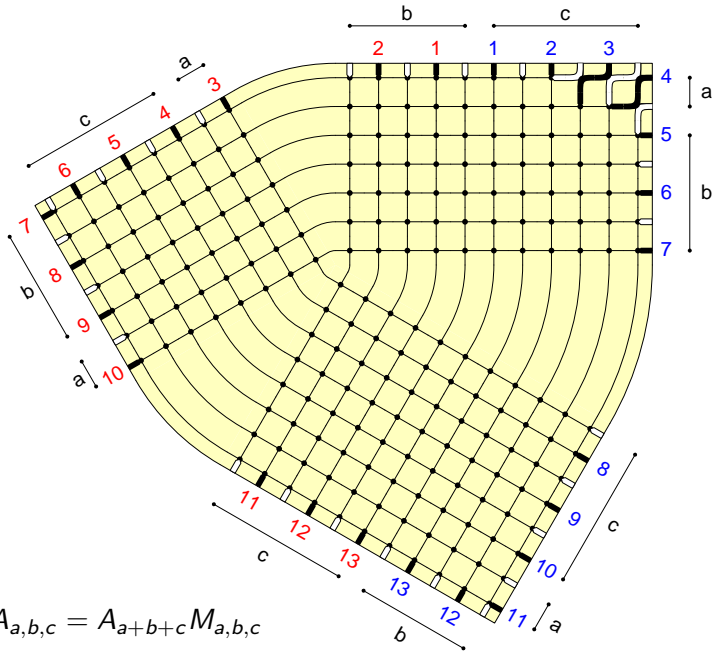




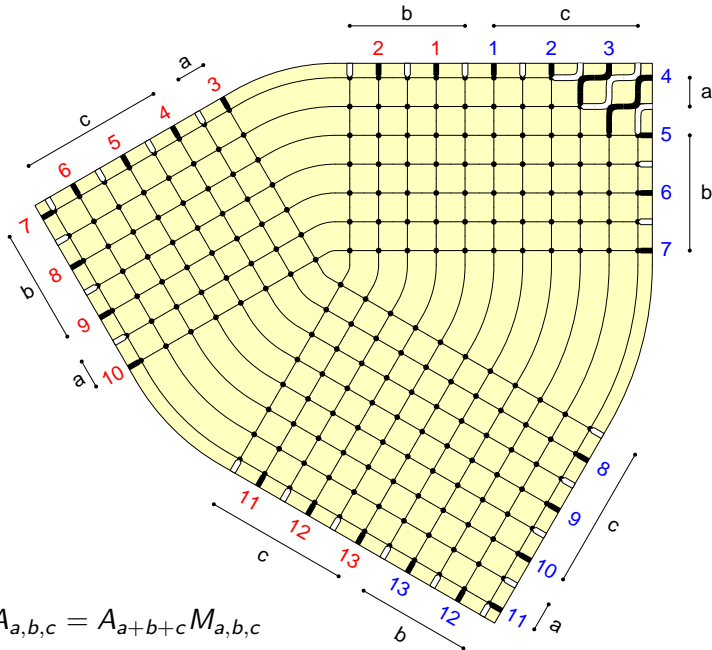
$$A_{a,b,c} = A_{a+b+c} M_{a,b,c}$$



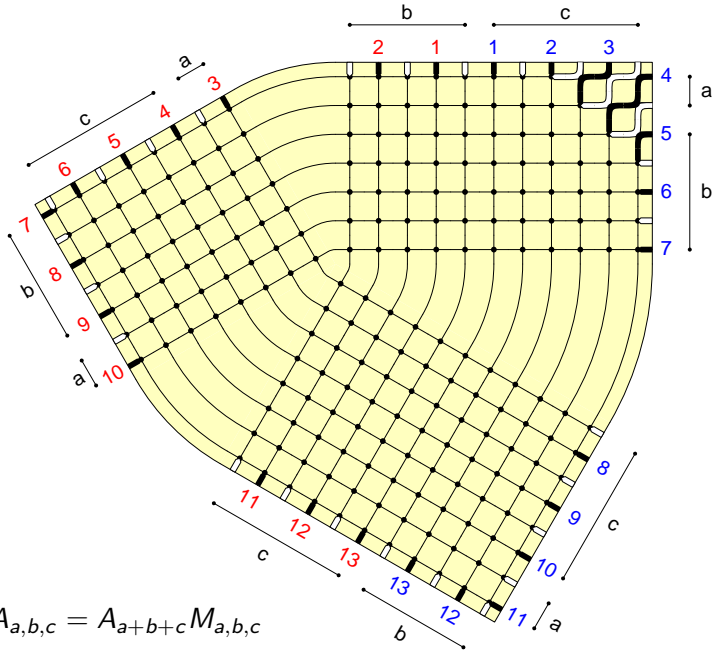
$$A_{a,b,c} = A_{a+b+c} M_{a,b,c}$$



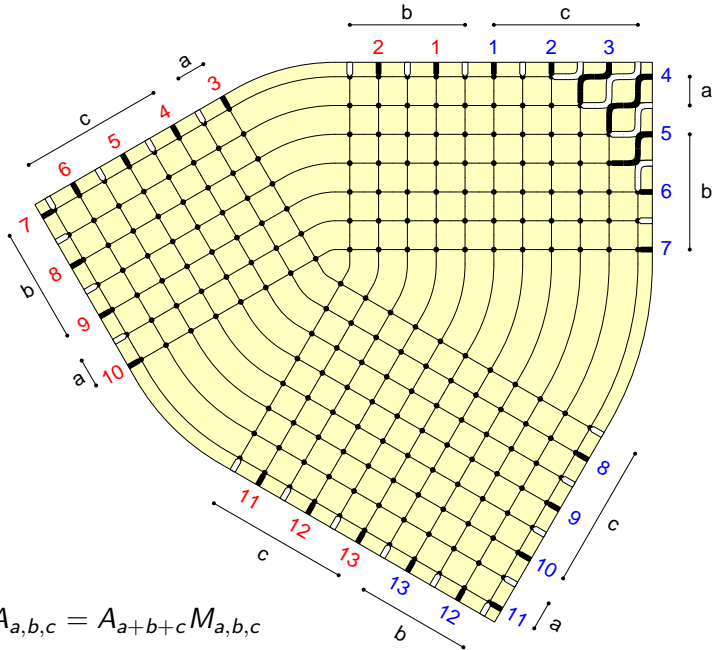
$$A_{a,b,c} = A_{a+b+c} M_{a,b,c}$$



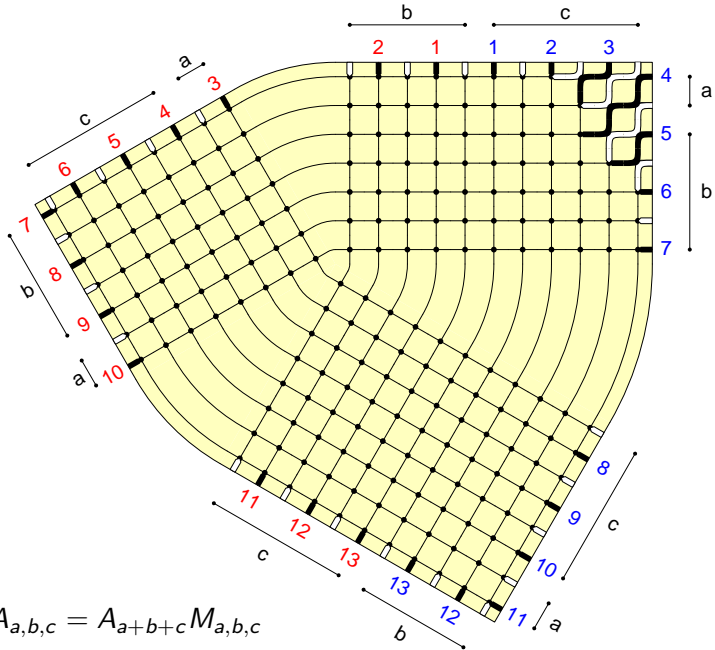
$$A_{a,b,c} = A_{a+b+c} M_{a,b,c}$$



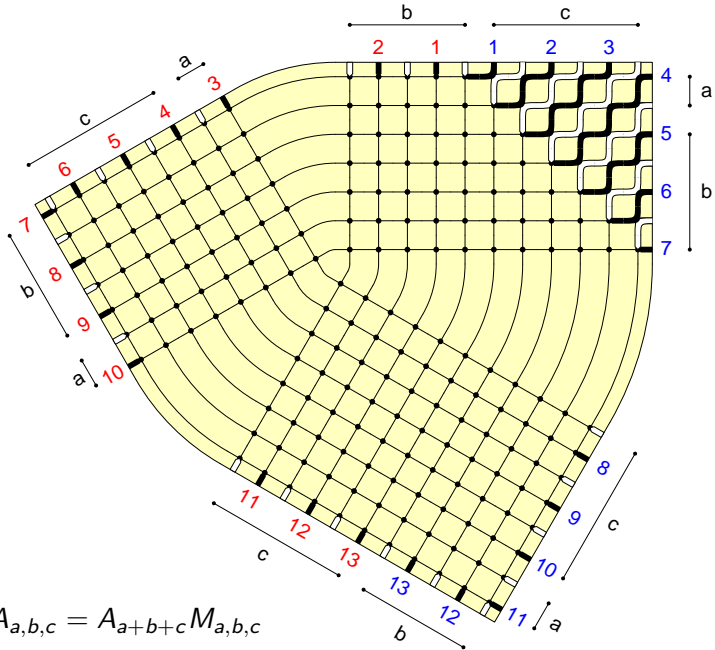
$$A_{a,b,c} = A_{a+b+c} M_{a,b,c}$$



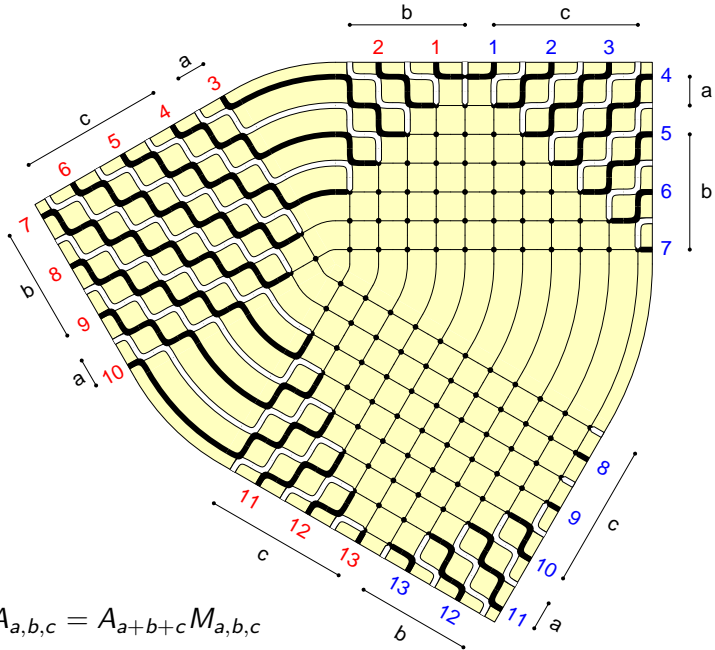
$$A_{a,b,c} = A_{a+b+c} M_{a,b,c}$$

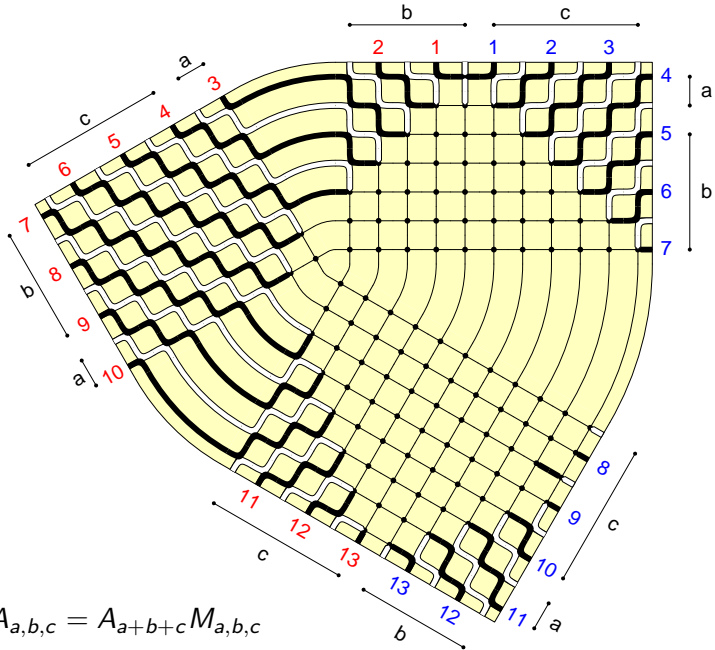


$$A_{a,b,c} = A_{a+b+c} M_{a,b,c}$$

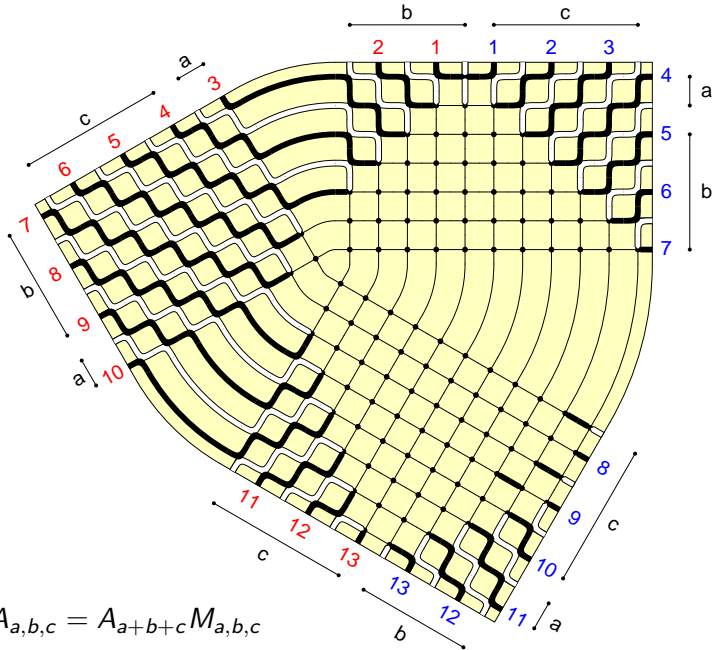


$$A_{a,b,c} = A_{a+b+c} M_{a,b,c}$$

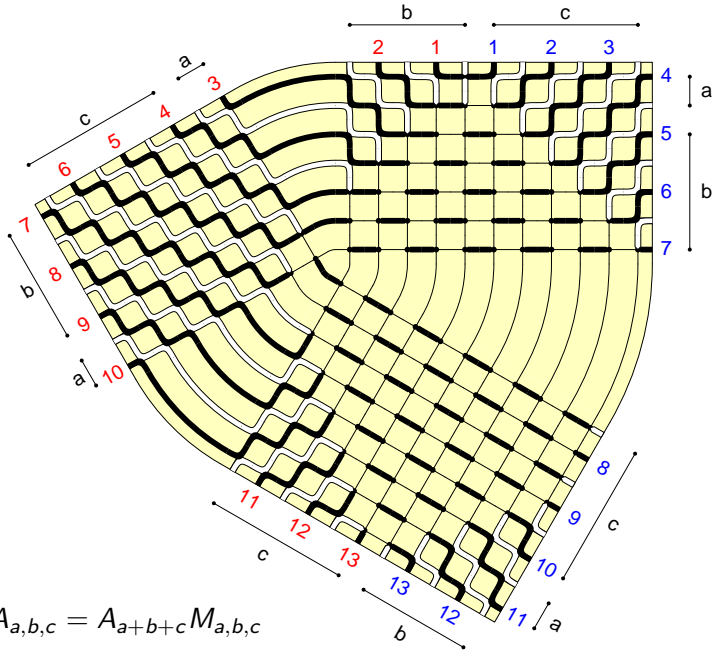




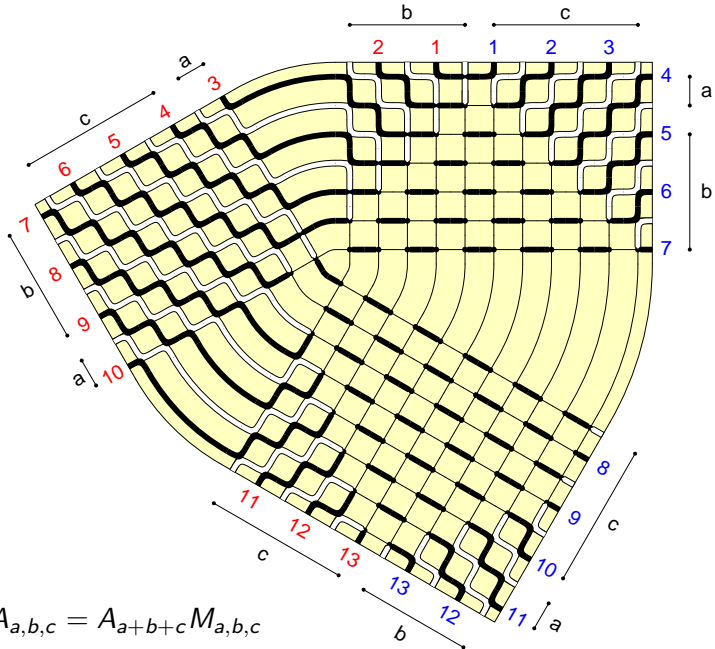
$$A_{a,b,c} = A_{a+b+c} M_{a,b,c}$$



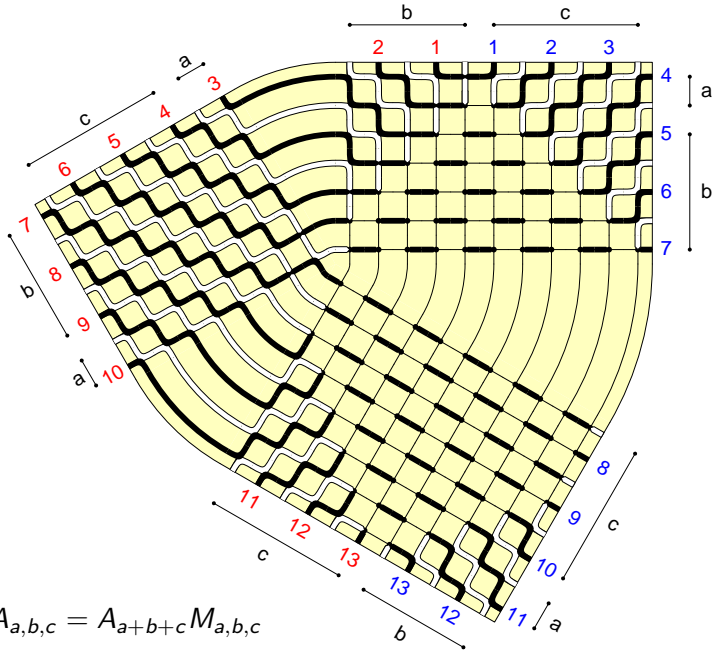
$$A_{a,b,c} = A_{a+b+c} M_{a,b,c}$$



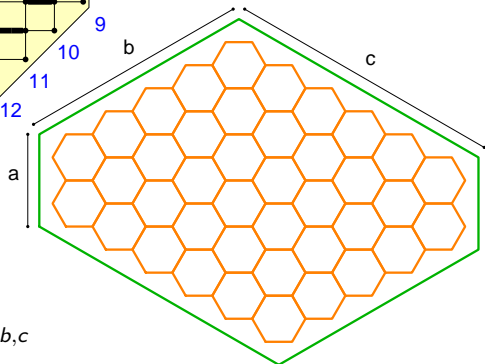
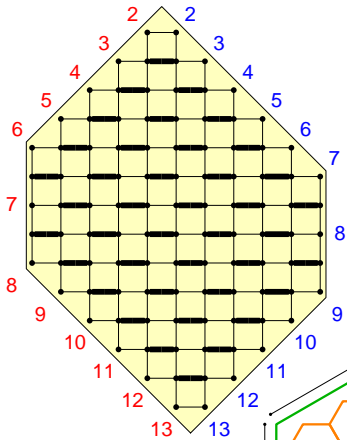
$$A_{a,b,c} = A_{a+b+c} M_{a,b,c}$$



$$A_{a,b,c} = A_{a+b+c} M_{a,b,c}$$



$$A_{a,b,c} = A_{a+b+c} M_{a,b,c}$$



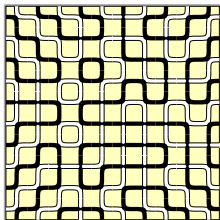
$$A_{a,b,c} = A_{a+b+c} M_{a,b,c}$$

THIS SHOULD BE THE END OF THE SECOND LECTURE...

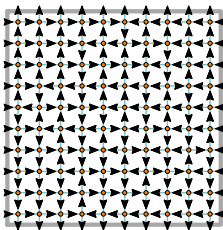
Lecture 3

Asymptotics of large Alternating Sign Matrices

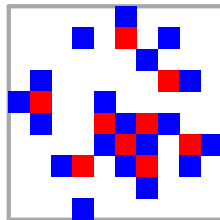
Reminder of local bijections for ASM



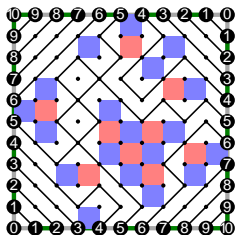
FPL



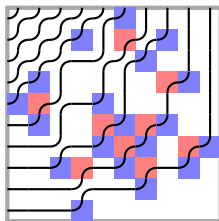
6-vertex



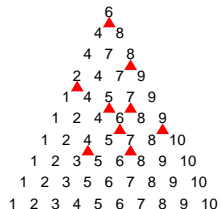
ASM



height function



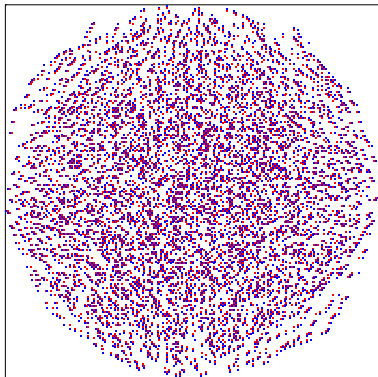
quasi-NILP



monotone triangle

Asymptotic shapes: the problem

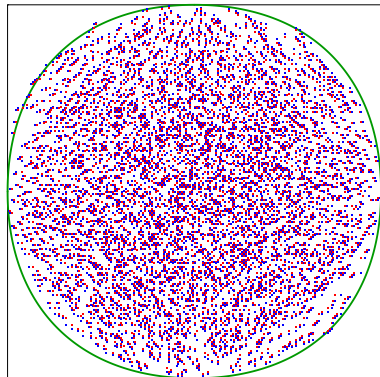
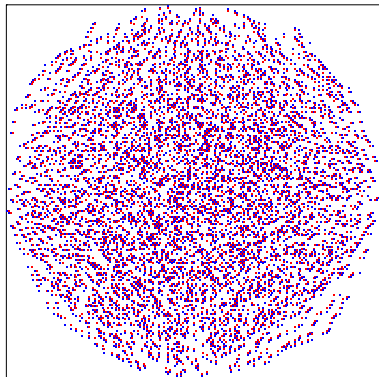
In **large** Alternating Sign Matrices you see the emergence of **frozen regions** and **limit shapes**...



The analytic determination of these curves is our subject today.

Asymptotic shapes: the problem

In **large** Alternating Sign Matrices you see the emergence of **frozen regions** and **limit shapes**...



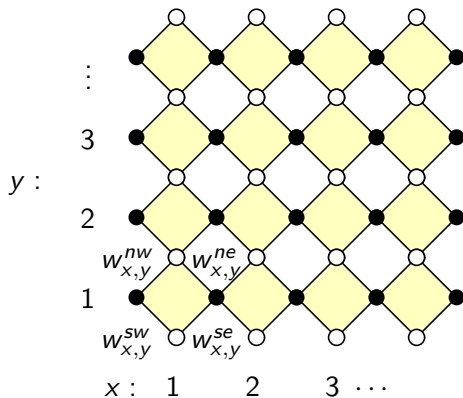
The analytic determination of these curves is our subject today.

Domino Tilings of the Aztec Diamond \rightarrow ASM at $\omega = 2$

weighted “Domino Tilings of the Aztec Diamond”

(a planar-graph dimer-covering problem,

thus a determinantal problem...)

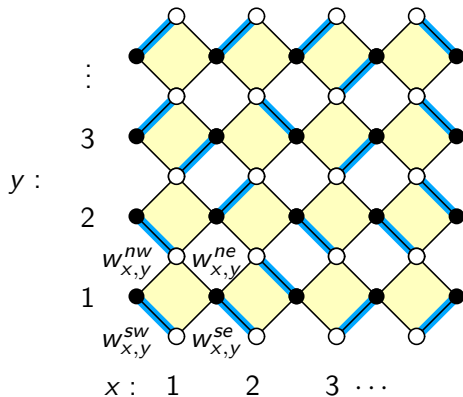


Domino Tilings of the Aztec Diamond \rightarrow ASM at $\omega = 2$

weighted “Domino Tilings of the Aztec Diamond”

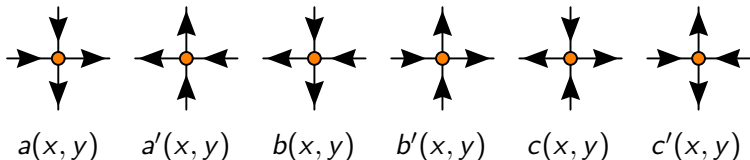
(a planar-graph dimer-covering problem,

thus a determinantal problem...)



Domino Tilings of the Aztec Diamond \rightarrow ASM at $\omega = 2$

Recall the 6-Vertex Model weights...



...and now consider the following map:

(note: $\Delta = 0$)

$$w_{x,y}^{sw} \quad w_{x,y}^{ne} \quad w_{x,y}^{se} \quad w_{x,y}^{nw} \quad 1 \quad w_{x,y}^{se} w_{x,y}^{nw} + w_{x,y}^{sw} w_{x,y}^{ne}$$

a

a'

b

b'

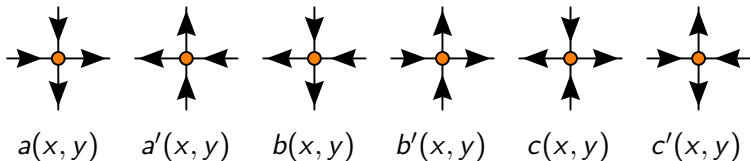
c

c'



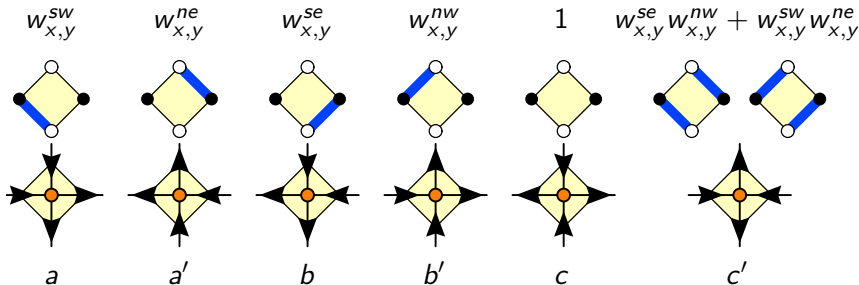
Domino Tilings of the Aztec Diamond \rightarrow ASM at $\omega = 2$

Recall the 6-Vertex Model weights...



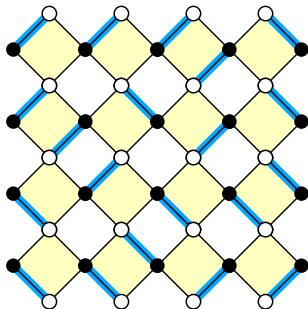
...and now consider the following map:

(note: $\Delta = 0$)



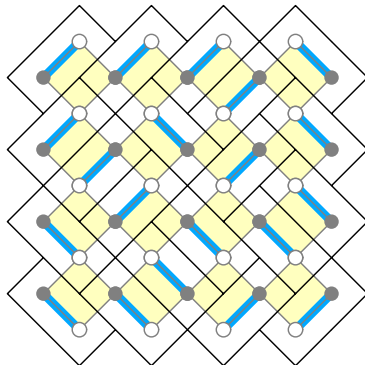
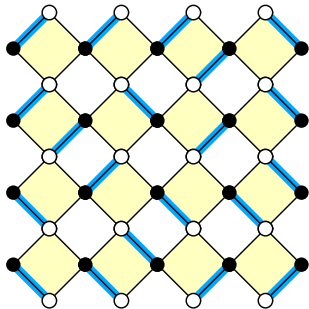
...they're also determinantal a'/a Gessel-Viennot...

The NILP construction for **Domino Tilings of the Aztec Diamond** is similar to the one for **Lozenge Tilings on the triangular lattice**, with **Motzkin** paths ($\{\pm 1, 0\}$) instead of ordinary $\{\pm 1\}$ lattice paths



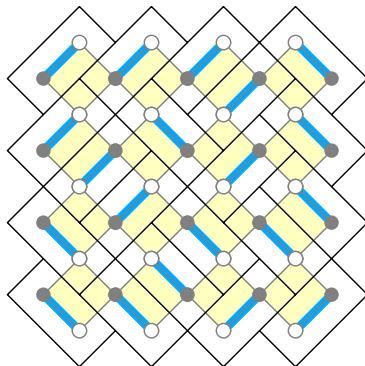
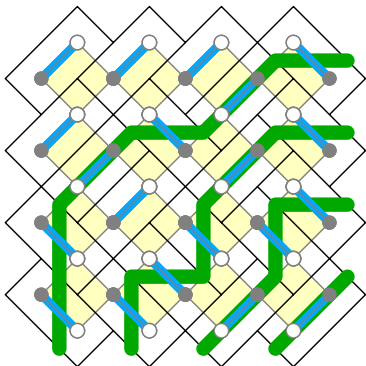
...they're also determinantal *a'la* Gessel-Viennot...

The NILP construction for **Domino Tilings of the Aztec Diamond** is similar to the one for **Lozenge Tilings on the triangular lattice**, with **Motzkin** paths ($\{\pm 1, 0\}$) instead of ordinary $\{\pm 1\}$ lattice paths

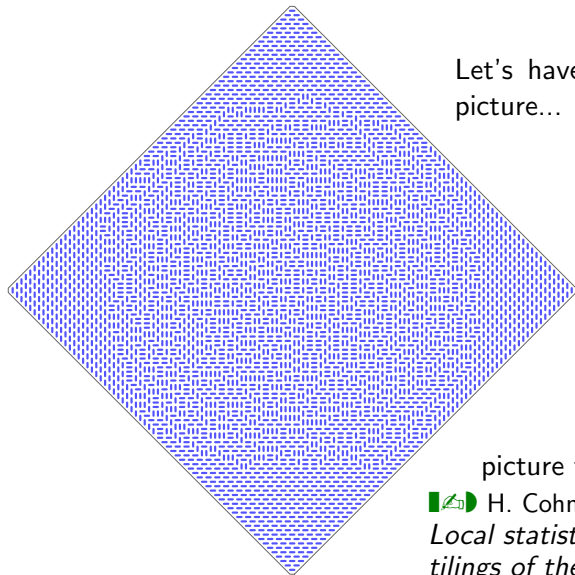


...they're also determinantal *a'la* Gessel-Viennot...

The NILP construction for **Domino Tilings of the Aztec Diamond** is similar to the one for **Lozenge Tilings on the triangular lattice**, with **Motzkin** paths ($\{\pm 1, 0\}$) instead of ordinary $\{\pm 1\}$ lattice paths




Domino Tilings of the Aztec Diamond: a bigger picture

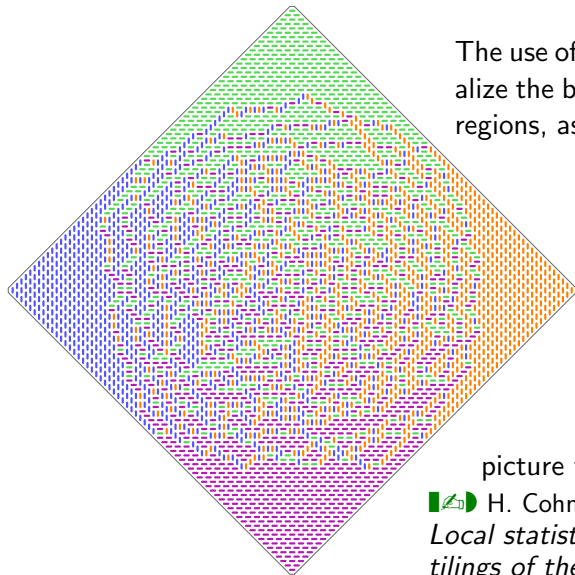


Let's have a look at a bigger picture... (here $L = 64$)

picture taken from:


 H. Cohn, N. Elkies and J. Propp,
*Local statistics for random domino
tilings of the Aztec diamond*, 1995

Domino Tilings of the Aztec Diamond: a bigger picture

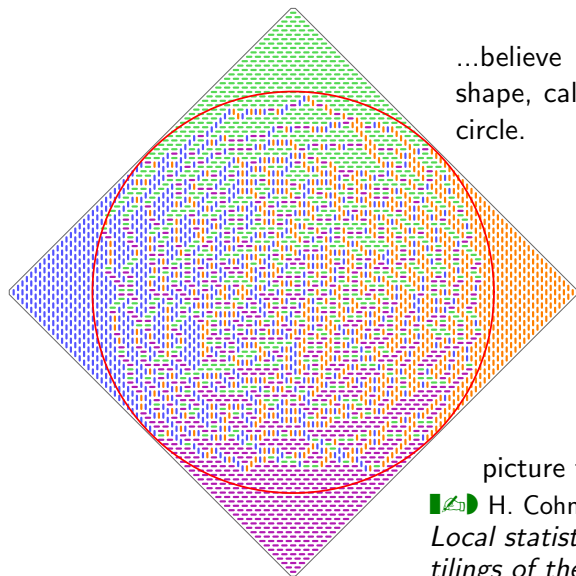


The use of colours allow to visualize the boundary of the frozen regions, as well as the NILP's...

picture taken from:


 H. Cohn, N. Elkies and J. Propp,
*Local statistics for random domino
tilings of the Aztec diamond*, 1995

Domino Tilings of the Aztec Diamond: a bigger picture



...believe it or not, the limit shape, called **Arctic curve**, is a circle.

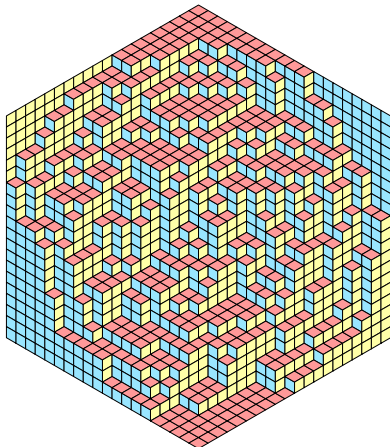
picture taken from:

 H. Cohn, N. Elkies and J. Propp,
*Local statistics for random domino
tilings of the Aztec diamond*, 1995

Arctic Circles in dimer-covering models...


A similar feature was also known to occur in lozenge tilings of a regular hexagon (the MacMahon $n \times n \times n$ “boxed” problem)

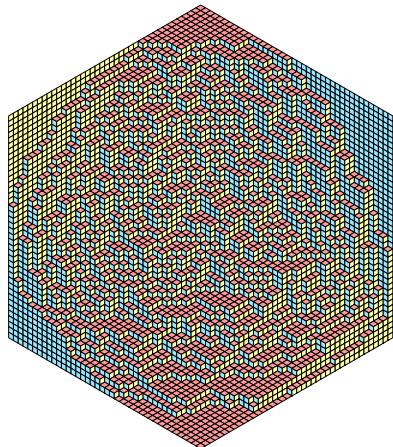
■📄 H. Cohn, M. Larsen and J. Propp, *The Shape of a Typical Boxed Plane Partition*, 1998



Arctic Circles in dimer-covering models...

A similar feature was also known to occur in lozenge tilings of a regular hexagon (the MacMahon $n \times n \times n$ “boxed” problem)

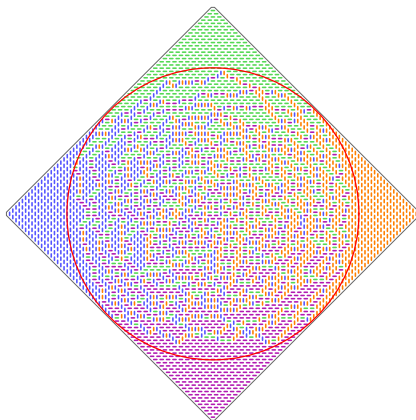
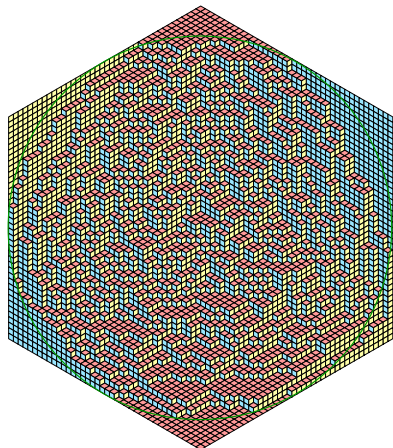
 H. Cohn, M. Larsen and J. Propp, *The Shape of a Typical Boxed Plane Partition*, 1998



Arctic Circles in dimer-covering models...

A similar feature was also known to occur in lozenge tilings of a regular hexagon (the MacMahon $n \times n \times n$ “boxed” problem)

■📄 H. Cohn, M. Larsen and J. Propp, *The Shape of a Typical Boxed Plane Partition*, 1998



dimer coverings of periodic planar bipartite graphs

So, we find similar features in [dimer coverings of periodic planar bipartite graphs](#), for different unit tiles. A general unified theory indeed exists:

📄 R. Kenyon, A. Okounkov, S. Sheffield, *Dimers and Amoebæ*, 2003

However, in this class of models, [lozenge tilings](#) are by far the most studied case, even more than the square lattice.


This because the [spectral curve](#) associated to this lattice (*sic!*) is the simplest possible: $P(z, w) = z + w - 1$.

This study culminates into

📄 R. Kenyon, A. Okounkov, *Limit shapes and the complex Burgers equation*, 2005

Semi-strict Gelfand Patterns


...but let's start with something more classic...

 H. Cohn, M. Larsen and J. Propp, *The Shape of a Typical Boxed Plane Partition*, 1998

Partial lozenge tilings (with a given string of defects on one boundary) are related to [Semi-strict Gelfand Patterns](#) (a version of monotone-triangle-like things, we already encountered for ASM's).

SSGP are counted by a \mathbb{Z} -valued Vandermonde:

$$\# \left\{ \begin{array}{c} x_1 \quad x_2 \quad \cdots \quad x_n \\ \text{tiling} \\ n \end{array} \right\} = \prod_{1 \leq i < j \leq n} \frac{x_j - x_i}{j - i}$$

 I.M. Gelfand and M.L. Tsetlin, *Finite-dimensional representations of the group of unimodular matrices*, 1950

A couple of remarks...

Remark 1: Interestingly, Semi-strict Gelfand Patterns “form bases of representations of $SL(n)$, and one can deduce the Gelfand-Tsetlin formula from this fact using the Weyl dimension formula” (but also derive it combinatorially).

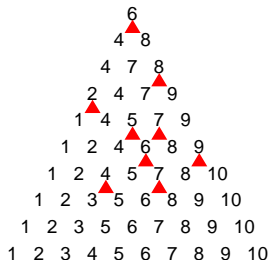
Remark 2: The Gelfand-Tsetlin formula also counts the very same monotone triangles T for ASM's, but with a factor $2^{-r(T)}$, where $r(T)$ is the number of entries of T that occur also in the preceding row. Thus, ASM at $\omega = 2$, the determinantal point.


 N. Elkies, G. Kuperberg, M. Larsen and J. Propp, *Alternating sign matrices and domino tilings*, 1991

A couple of remarks...


Remark 1: Interestingly, Semi-strict Gelfand Patterns “form bases of representations of $SL(n)$, and one can deduce the Gelfand-Tsetlin formula from this fact using the Weyl dimension formula” (but also derive it combinatorially).

Remark 2: The Gelfand-Tsetlin formula also counts the very same monotone triangles T for ASM's, but with a factor $2^{-r(T)}$, where $r(T)$ is the number of entries of T that occur also in the preceding row. Thus, ASM at $\omega = 2$, the determinantal point.



 N. Elkies, G. Kuperberg, M. Larsen and J. Propp, *Alternating sign matrices and domino tilings*, 1991


A too-short introduction to Kenyon-Okounkov Theory

 R. Kenyon, A. Okounkov, *Limit shapes and the complex Burgers equation*, 2005

How do you get the **arctic curve** for lozenge tilings in a fancy domain?

1. Think to your lozenge tiling as a plane partition, for which you want to determine the asymptotics of the **height function** $h(x, y)$. Here (x, y) are coordinates in the plane orthogonal to $(1, 1, 1)$. Call z and w the components of ∇h .
2. Recall that the spectral curve $P(z, w)$ pertinent to lozenges is $P(z, w) = z + w - 1$. It is a **Harnack curve** in general.


A too-short introduction to Kenyon-Okounkov Theory

 R. Kenyon, A. Okounkov, *Limit shapes and the complex Burgers equation*, 2005

How do you get the **arctic curve** for lozenge tilings in a fancy domain?

1. Think to your lozenge tiling as a plane partition, for which you want to determine the asymptotics of the **height function** $h(x, y)$. Here (x, y) are coordinates in the plane orthogonal to $(1, 1, 1)$. Call z and w the components of ∇h .
2. Recall that the spectral curve $P(z, w)$ pertinent to lozenges is $P(z, w) = z + w - 1$. It is a **Harnack curve** in general.

A too-short introduction to Kenyon-Okounkov Theory

 R. Kenyon, A. Okounkov, *Limit shapes and the complex Burgers equation*, 2005

How do you get the **arctic curve** for lozenge tilings in a fancy domain?

1. Think to your lozenge tiling as a plane partition, for which you want to determine the asymptotics of the **height function** $h(x, y)$. Here (x, y) are coordinates in the plane orthogonal to $(1, 1, 1)$. Call z and w the components of ∇h .
2. Recall that the spectral curve $P(z, w)$ pertinent to lozenges is $P(z, w) = z + w - 1$. It is a **Harnack curve** in general.

A too-short introduction to Kenyon-Okounkov Theory

3. Variational formulation \rightarrow Euler-Lagrange equations
 - \rightarrow complex inviscid Burgers eq. \rightarrow method of complex characteristics
 - \rightarrow find an analytic function $Q(z, w)$ (algebraic for slope- $k\pi/3$ domains) such that

$$\nabla h(x, y) = \begin{pmatrix} z(x, y) \\ w(x, y) \end{pmatrix} \leftrightarrow \begin{cases} P(z, w) = 0 \\ Q(z, w) = \left(xz \frac{\partial}{\partial z} + yw \frac{\partial}{\partial w} \right) P(z, w) \end{cases}$$

4. The arctic curve is the locus of double roots. Having P, Q algebraic, you get an algebraic $R(x, y) = 0$ from the discriminant.
5. Isolated higher order roots show up as cusps in the arctic curve.

A too-short introduction to Kenyon-Okounkov Theory

3. Variational formulation \rightarrow Euler-Lagrange equations
 \rightarrow complex inviscid Burgers eq. \rightarrow method of complex characteristics
 \rightarrow find an analytic function $Q(z, w)$ (algebraic for slope- $k\pi/3$ domains) such that

$$\nabla h(x, y) = \begin{pmatrix} z(x, y) \\ w(x, y) \end{pmatrix} \leftrightarrow \begin{cases} P(z, w) = 0 \\ Q(z, w) = \left(xz \frac{\partial}{\partial z} + yw \frac{\partial}{\partial w} \right) P(z, w) \end{cases}$$

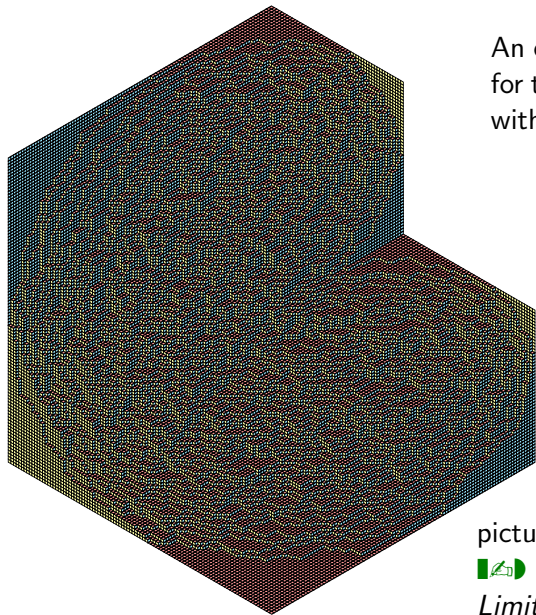
4. The arctic curve is the locus of double roots. Having P, Q algebraic, you get an algebraic $R(x, y) = 0$ from the discriminant.
5. Isolated higher order roots show up as cusps in the arctic curve.

A too-short introduction to Kenyon-Okounkov Theory

3. Variational formulation \rightarrow Euler-Lagrange equations
 \rightarrow complex inviscid Burgers eq. \rightarrow method of complex characteristics
 \rightarrow find an analytic function $Q(z, w)$ (algebraic for slope- $k\pi/3$ domains) such that


$$\nabla h(x, y) = \begin{pmatrix} z(x, y) \\ w(x, y) \end{pmatrix} \leftrightarrow \begin{cases} P(z, w) = 0 \\ Q(z, w) = \left(xz \frac{\partial}{\partial z} + yw \frac{\partial}{\partial w} \right) P(z, w) \end{cases}$$

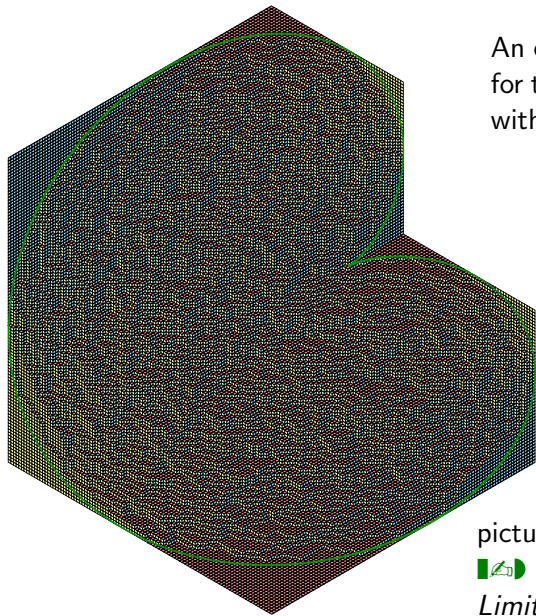
4. The arctic curve is the locus of double roots. Having P, Q algebraic, you get an algebraic $R(x, y) = 0$ from the discriminant.
5. Isolated higher order roots show up as cusps in the arctic curve.



An example: the cardioid
for the hexagonal domain
with a frozen corner


picture taken from:

 R. Kenyon, A. Okounkov,
*Limit shapes and the complex
Burgers equation*, 2005



An example: the cardioid
for the hexagonal domain
with a frozen corner

picture taken from:

 R. Kenyon, A. Okounkov,
*Limit shapes and the complex
Burgers equation*, 2005

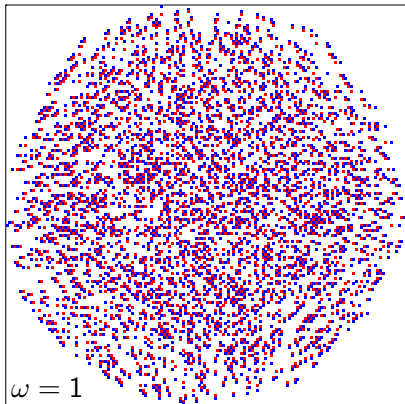
...and Yang-Baxter-integrable systems?...

All of this is beautiful, but planar dimer coverings are **determinantal**...

As we know, in various cases (included ω -enumerations of ASM) they are a special point on a **YB-integrable line** ($\omega = 2$ for ASM / domino tilings of the Aztec Diamond)

Numerical simulations (thanks CFTP!) seem to show that the arctic curve varies smoothly with ω , at least on some interval...

...but what is known theoretically?



from this point on, ASM pictures are produced with C code based on a version kindly provided by Ben Wieland

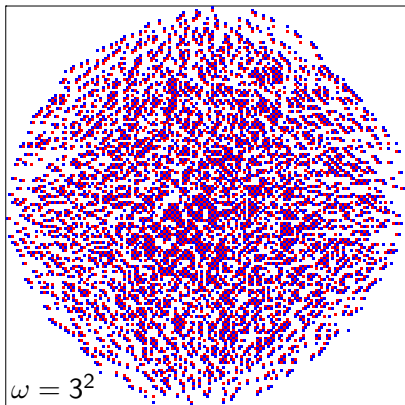
...and Yang-Baxter-integrable systems?...

All of this is beautiful, but planar dimer coverings are **determinantal**...

As we know, in various cases (included ω -enumerations of ASM) they are a special point on a **YB-integrable line** ($\omega = 2$ for ASM / domino tilings of the Aztec Diamond)

Numerical simulations (thanks CFTP!) seem to show that the arctic curve varies smoothly with ω , at least on some interval...

...but what is known theoretically?



from this point on, ASM pictures are produced with C code based on a version kindly provided by Ben Wieland

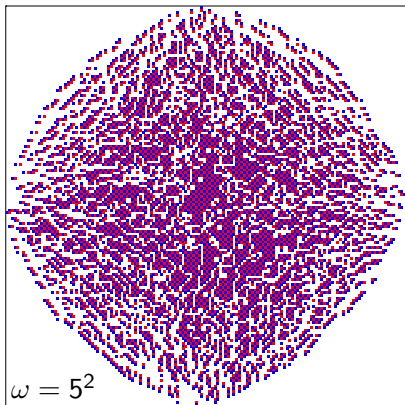
...and Yang-Baxter-integrable systems?...

All of this is beautiful, but planar dimer coverings are **determinantal**...

As we know, in various cases (included ω -enumerations of ASM) they are a special point on a **YB-integrable line** ($\omega = 2$ for ASM / domino tilings of the Aztec Diamond)

Numerical simulations (thanks CFTP!) seem to show that the arctic curve varies smoothly with ω , at least on some interval...

...but what is known theoretically?



from this point on, ASM pictures are produced with C code based on a version kindly provided by Ben Wieland

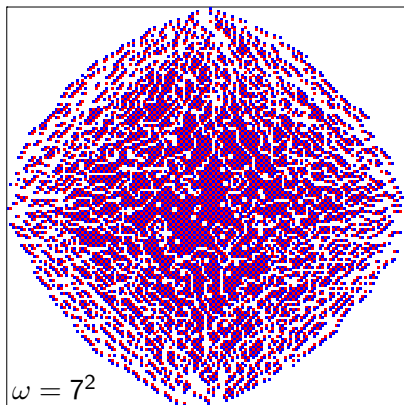
...and Yang-Baxter-integrable systems?...

All of this is beautiful, but planar dimer coverings are **determinantal**...

As we know, in various cases (included ω -enumerations of ASM) they are a special point on a **YB-integrable line** ($\omega = 2$ for ASM / domino tilings of the Aztec Diamond)

Numerical simulations (thanks CFTP!) seem to show that the arctic curve varies smoothly with ω , at least on some interval...

...but what is known theoretically?



from this point on, ASM pictures are produced with C code based on a version kindly provided by Ben Wieland


The Colomo-Pronko formula

...but what is known theoretically?

...this was almost nothing up to recent times...

Then Colomo and Pronko came with a series of papers in which:

- ▶ they found explicitly the Arctic Curve for $\omega = 1$ ASM;
- ▶ they found a formula for the Arctic Curve at generic ω , in terms of the refined enumerations $A_\omega(n; r)$;
- ▶ they found the necessary asymptotic properties of $A_\omega(n; r)$ using methods of Random Matrices, first for $\omega \leq 4$, and then, together with P. Zinn-Justin, also for $\omega > 4$ (where the corresponding 6-Vertex Model is “antiferromagnetic”);

 F. Colomo and A.G. Pronko,
The arctic circle revisited, 2007


The Colomo-Pronko formula

...but what is known theoretically?

...this was almost nothing up to recent times...

Then Colomo and Pronko came with a series of papers in which:

- ▶ they found explicitly the Arctic Curve for $\omega = 1$ ASM;
- ▶ they found a formula for the Arctic Curve at generic ω , in terms of the refined enumerations $A_\omega(n; r)$;
- ▶ they found the necessary asymptotic properties of $A_\omega(n; r)$ using methods of Random Matrices, first for $\omega \leq 4$, and then, together with P. Zinn-Justin, also for $\omega > 4$ (where the corresponding 6-Vertex Model is “antiferromagnetic”);

 F. Colomo and A.G. Pronko,

The limit shape of large alternating sign matrices, 2008


The Colomo-Pronko formula

...but what is known theoretically?

...this was almost nothing up to recent times...

Then Colomo and Pronko came with a series of papers in which:

- ▶ they found explicitly the Arctic Curve for $\omega = 1$ ASM;
- ▶ they found a formula for the Arctic Curve at generic ω , in terms of the refined enumerations $A_\omega(n; r)$;
- ▶ they found the necessary asymptotic properties of $A_\omega(n; r)$ using methods of Random Matrices, first for $\omega \leq 4$, and then, together with P. Zinn-Justin, also for $\omega > 4$ (where the corresponding 6-Vertex Model is “antiferromagnetic”);

 F. Colomo and A.G. Pronko,

The arctic curve of the domain-wall six-vertex model, 2009


The Colomo-Pronko formula

...but what is known theoretically?

...this was almost nothing up to recent times...

Then Colomo and Pronko came with a series of papers in which:

- ▶ they found explicitly the Arctic Curve for $\omega = 1$ ASM;
- ▶ they found a formula for the Arctic Curve at generic ω , in terms of the refined enumerations $A_\omega(n; r)$;
- ▶ they found the necessary asymptotic properties of $A_\omega(n; r)$ using methods of Random Matrices, first for $\omega \leq 4$, and then, together with P. Zinn-Justin, also for $\omega > 4$ (where the corresponding 6-Vertex Model is “antiferromagnetic”);

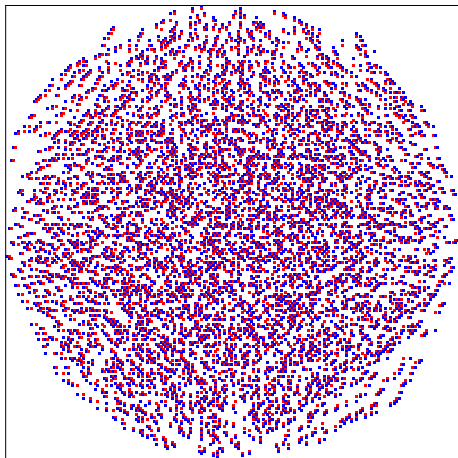
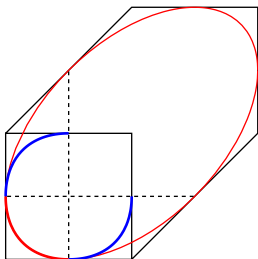
 F. Colomo, A.G. Pronko and P. Zinn-Justin, *The arctic curve of the domain-wall six-vertex model in its anti-ferroelectric regime*, 2010

The Colomo-Pronko formula: $\omega = 1$

Picture and formula for $\omega = 1$:

The South-West arc satisfies
 $x(1-x) + y(1-y) + xy = 1/4$
 $x, y \in [0, 1/2]$

(just a “+xy” modification
w.r.t. a circle)

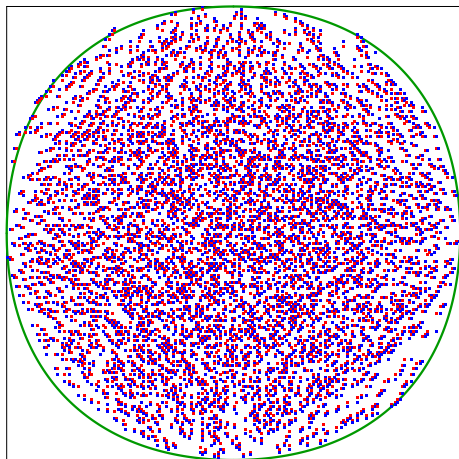
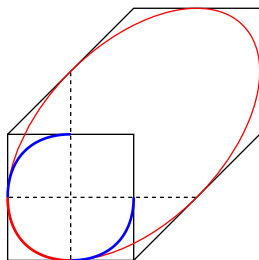


The Colomo-Pronko formula: $\omega = 1$

Picture and formula for $\omega = 1$:

The South-West arc satisfies
 $x(1-x) + y(1-y) + xy = 1/4$
 $x, y \in [0, 1/2]$

(just a “+xy” modification
w.r.t. a circle)



The Colomo-Pronko formula: generic ω

For ω -weighted ASM on the square, the arctic curve $\mathcal{C}(x, y)$, in parametric form $x = x(z)$, $y = y(z)$ on the interval $z \in [1, +\infty)$, is the solution of the system of equations

$$F(z; x, y) = 0; \quad \frac{\partial}{\partial z} F(z; x, y) = 0.$$

The function $F(z; x, y)$, that depends on x and y linearly, is

$$F(z; x, y) = \frac{1}{z}(x - 1) + \frac{\omega}{(z - 1)(z - 1 + \omega)}y + \lim_{n \rightarrow \infty} \frac{1}{n} \frac{\partial}{\partial z} \ln \left(\sum_{r=1}^n A_{\omega}(n, r) z^{r-1} \right).$$

$\mathcal{C}(x, y)$ is algebraic only at discrete special values of ω (including 0, 1, 2, 3).

Refined enumeration of ASM

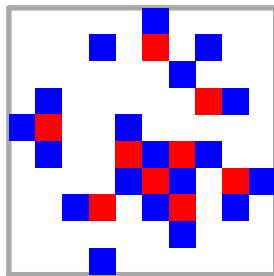
We call $A_\omega(n)$ the counting polynomial associated to ω -weighted ASM of size n :

$$A_\omega(n) = \sum_{A \in \mathcal{A}_n} \omega^{\#\{-1 \text{ in } A\}}$$

Thus $A_1(n) = \prod_{0 \leq j \leq n-1} \frac{(3j+1)!}{(n+j)!}$, the total number of size- n ASM (after Zeilberger and Kuperberg...)

Call $A_\omega(n, r)$ the counting polynomial associated to ω -weighted ASM of size n , such that the only $+1$ in the bottom row is at the r -th column (nice formula at $\omega = 1$, proven again by Zeilberger, in 1996...)

$n = 10, r = 4$



How to derive this?

Call $h_n(z) = \sum_{r=1}^n A_\omega(n, r) z^{r-1}$ (to conform to integrabilists')

Use fine techniques from Integrable Systems, in order to derive the **Emptiness Formation Probability**, $EFP(n; r, s)$: the probability that in the top-left $s \times r$ rectangle of the $n \times n$ ASM there are no ± 1 elements.

Clearly, $A(n; r) = EFP(n; r-1, 1) - EFP(n; r, 1)$.

But for $s \geq 2$ we do not see any simple property...

...however, integrability (at spectral parameters turned on) shows that also $EFP(n; r, s)$ is related to $h_n(z)$, through a **determinantal formula**.

For (r, s) crossing the Arctic Curve, $EFP(n; r, s)$ shows a 0-1 threshold transition, that you can study through saddle-point methods, helped by analogy with a Random Matrix Model.

How to derive this?

...in a few words, something very complicated already for the square.

And something relying deeply on “miracles” of **integrability methods**, that have no guarantee to occur in other domains.

Furthermore, the curve is **not** C_∞ at the tangence points on the boundary of the domain, already for $\omega = 1$, and is not even piecewise algebraic at generic ω ...

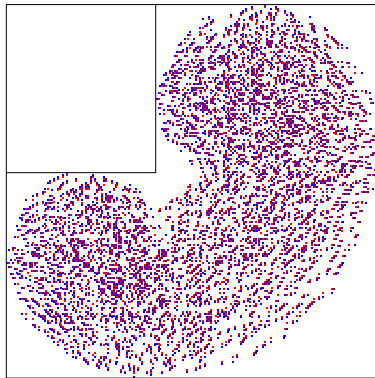
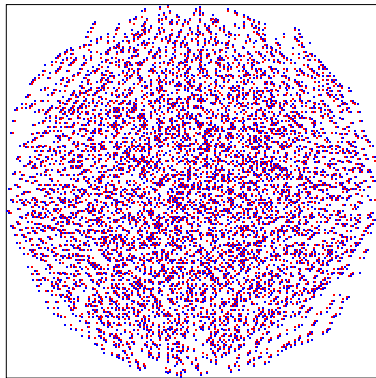
...how can we hope for an analogue of Kenyon-Okounkov Theory on the whole YB-integrable line for ω ?

Staying less ambitious, can we determine in ASM something like the KO cardioid for the hexagon with a frozen corner?


Emptiness Formation: typical configurations

...indeed, a typical configuration in the ensemble pertinent to $EFP(n; r, s)$, for (r, s) inside the arctic curve, shows the emergence of a new cardioid-like arctic curve (just like in Kenyon-Okounkov)

here $n = 200$, $(r, s) = (80, 90)$



A reminder on the basic theory of Plane Curves

 J. Dennis Lawrence, *A catalog of special plane curves*, Dover, New York, 1972

A *curve* \mathcal{C} will be represented either by the *Cartesian equation* $A(x, y) = 0$, or the *parametric equations* $x = f(t)$, $y = g(t)$.

It is constituted by the concatenation of a finite number of *arcs*.

An arc is a portion of the curve for which a “smooth” parametric presentation exists.

A curve is *algebraic* if the defining Cartesian equation $A(x, y) = 0$ is algebraic, otherwise it is *transcendental*.

A double point s.t. the two arcs passing through P have the same tangent is a *cusp*. A cusp is *of the first kind* if P is an endpoint of both arcs, and there is an arc of \mathcal{C} on each side of the tangent, and *of the second kind* if P is an endpoint of both arcs, and the two arcs lie on the same side of the tangent,

A reminder on the basic theory of Plane Curves

The *envelope* \mathcal{E} of a one-parameter family of curves $\{C_z\}_{z \in I}$ is the curve, minimal under inclusion, that is tangent to every curve of the family.

If the equation of the family $\{C_z\}$ is given in Cartesian coordinates by $U(z; x, y) = 0$, the non-singular points (x, y) of the envelope \mathcal{E} are the solutions of the system of equations

$$U(z; x, y) = 0; \quad \frac{d}{dz} U(z; x, y) = 0.$$

We call *geometric caustic* the envelope of a family of straight lines. In this case U is linear in x and y :

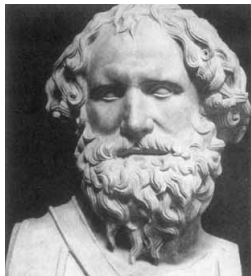
$$U(z; x, y) = x A(z) + y B(z) + C(z)$$

A reminder on the basic theory of Plane Curves

Caustics in optics are a special case of geometric caustics, in which the family of straight lines can be interpreted as the family of reflections of a beam of parallel rays from a curved mirror.

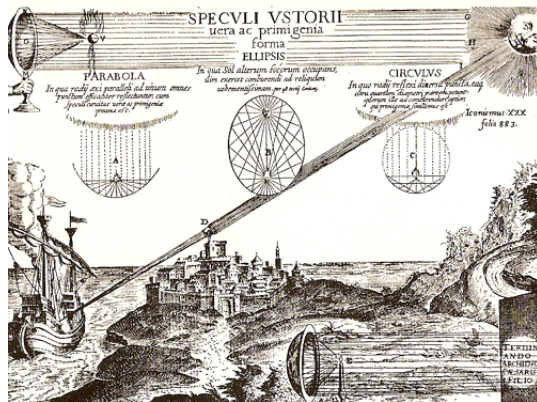
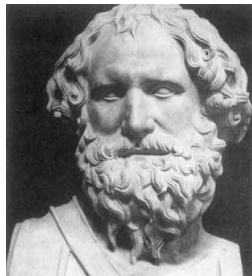
A reminder on the basic theory of Plane Curves

Caustics in optics are a special case of geometric caustics, in which the family of straight lines can be interpreted as the family of reflections of a beam of parallel rays from a curved mirror.



A reminder on the basic theory of Plane Curves

Caustics in optics are a special case of geometric caustics, in which the family of straight lines can be interpreted as the family of reflections of a beam of parallel rays from a curved mirror.



The Colomo-Pronko formula at generic ω – reloaded

For ω -weighted ASM on the square, the arctic curve $\mathcal{C}(x, y)$, in parametric form $x = x(z)$, $y = y(z)$ on the interval $z \in [1, +\infty)$, is the solution of the system of equations

$$F(z; x, y) = 0; \quad \frac{\partial}{\partial z} F(z; x, y) = 0.$$

The function $F(z; x, y)$, that depends on x and y linearly, is

$$F(z; x, y) = \frac{1}{z}(x - 1) + \frac{\omega}{(z - 1)(z - 1 + \omega)}y + \lim_{n \rightarrow \infty} \frac{1}{n} \frac{\partial}{\partial z} \ln \left(\sum_{r=1}^n A_{\omega}(n, r) z^{r-1} \right).$$

$\mathcal{C}(x, y)$ is algebraic only at discrete special values of ω (including 0, 1, 2, 3).

The Colomo-Pronko formula at generic ω – reloaded

For ω -weighted ASM on the square, the arctic curve $\mathcal{C}(x, y)$ is the **geometric caustic** of the family of lines, for z in the interval $z \in [1, +\infty)$,

$$F(z; x, y) = \frac{1}{z}(x - 1) + \frac{\omega}{(z - 1)(z - 1 + \omega)}y + \lim_{n \rightarrow \infty} \frac{1}{n} \frac{\partial}{\partial z} \ln \left(\sum_{r=1}^n A_{\omega}(n, r) z^{r-1} \right).$$

The Colomo-Pronko formula at generic ω – reloaded

For ω -weighted ASM on the square, the arctic curve $\mathcal{C}(x, y)$ is the **geometric caustic** of the family of lines, for z in the interval $z \in [1, +\infty)$,

$$F(z; x, y) = \frac{1}{z}(x - 1) + \frac{\omega}{(z - 1)(z - 1 + \omega)}y + \lim_{n \rightarrow \infty} \frac{1}{n} \frac{\partial}{\partial z} \ln \left(\sum_{r=1}^n A_{\omega}(n, r) z^{r-1} \right).$$

But this has not been derived geometrically!

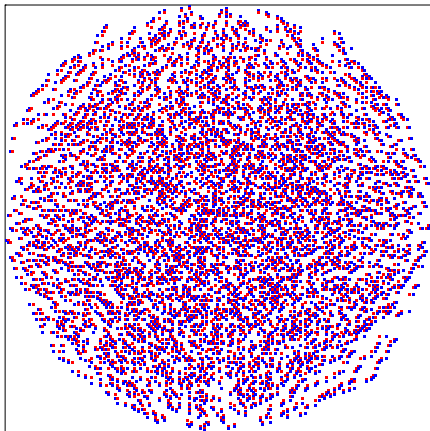
A quest for a new strategy...

So we would like a more **geometric strategy** for attacking this sort of questions...

Hopefully, with some luck, this could also be more generally applicable to **domains of different shape**...

Let's have a deeper look to the domain with a frozen rectangle...

$n = 200$, no frozen region



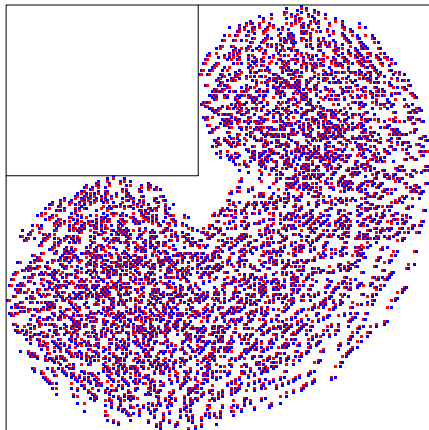
A quest for a new strategy...

So we would like a more **geometric strategy** for attacking this sort of questions...

Hopefully, with some luck, this could also be more generally applicable to **domains of different shape**...

Let's have a deeper look to the domain with a frozen rectangle...

$$n = 200, (r, s) = (90, 80)$$



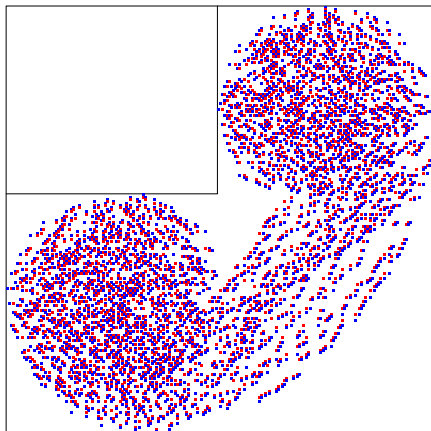
A quest for a new strategy...

So we would like a more **geometric strategy** for attacking this sort of questions...

Hopefully, with some luck, this could also be more generally applicable to **domains of different shape**...

Let's have a deeper look to the domain with a frozen rectangle...

$$n = 200, (r, s) = (99, 88)$$



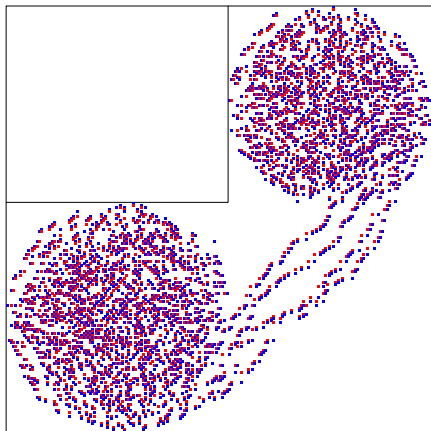
A quest for a new strategy...

So we would like a more **geometric strategy** for attacking this sort of questions...

Hopefully, with some luck, this could also be more generally applicable to **domains of different shape**...

Let's have a deeper look to the domain with a frozen rectangle...

$$n = 200, (r, s) = (104, 92)$$



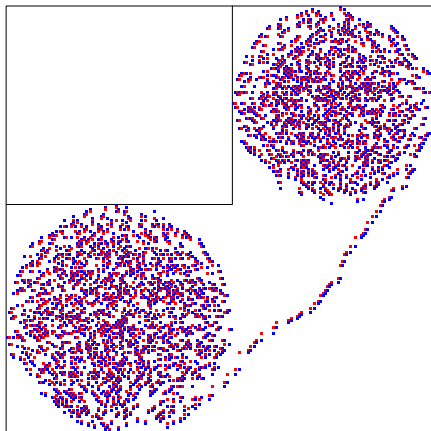
A quest for a new strategy...

So we would like a more **geometric strategy** for attacking this sort of questions...

Hopefully, with some luck, this could also be more generally applicable to **domains of different shape**...

Let's have a deeper look to the domain with a frozen rectangle...

$$n = 200, (r, s) = (106, 93)$$



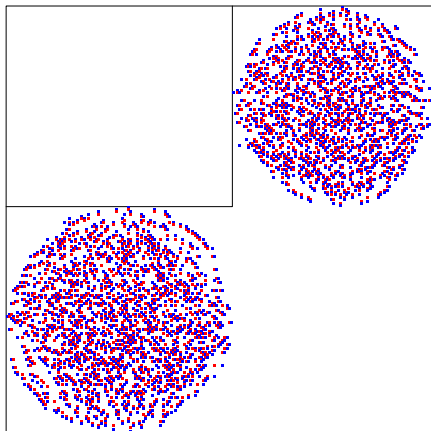
A quest for a new strategy...

So we would like a more **geometric strategy** for attacking this sort of questions...

Hopefully, with some luck, this could also be more generally applicable to **domains of different shape**...

Let's have a deeper look to the domain with a frozen rectangle...

$$n = 200, (r, s) = (106, 94)$$



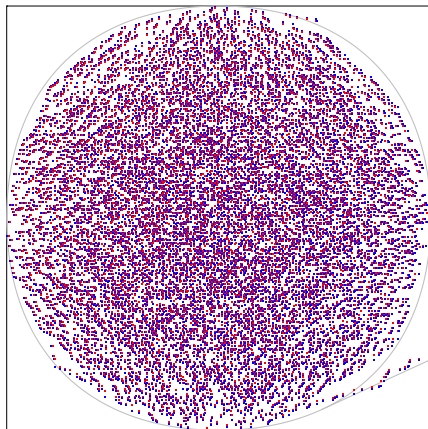
The structure of a typical refined ASM

...so this teaches us how does it look like a typical large ASM, of size n refined at r ...

It must be like a typical ASM, plus a **straight line** connecting $(0, r)$ to the Arctic Curve, and **tangent** to the Arctic Curve

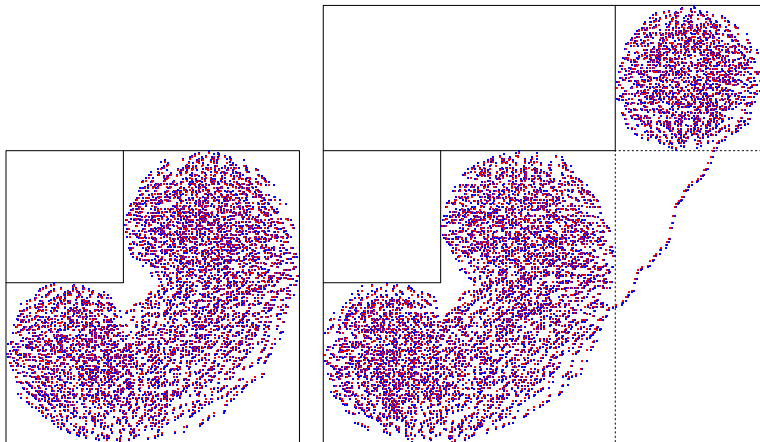
Indeed, this is what you see in a simulation...

$$n = 300, r = 250$$



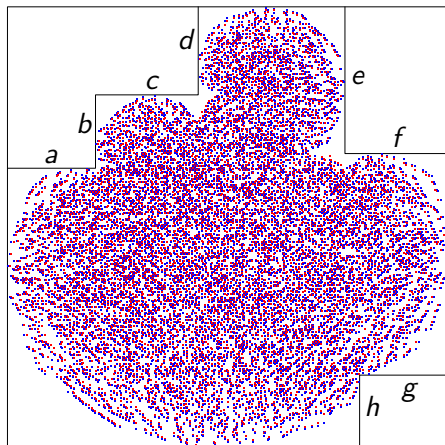
What about generic domains?

...our strategy has chances of working in general circumstances...



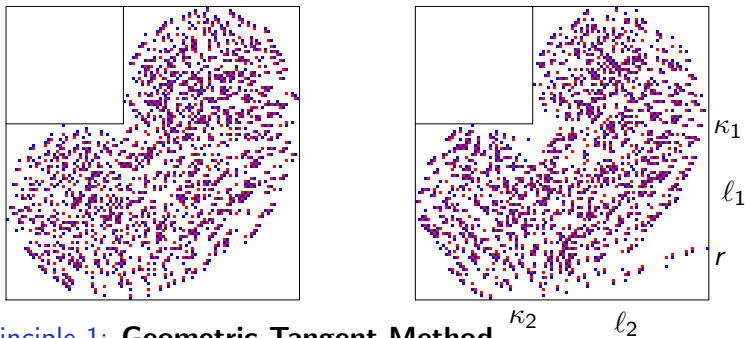
What about generic domains?

...our strategy has chances of working in general circumstances...



$$n = 300, \quad (a, b, \dots) = (60, 50, 70, 60, 100, 70, 60, 50)$$

The strategy: trying a precise statement

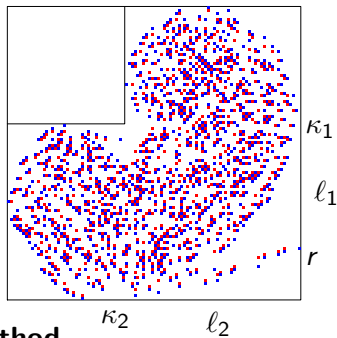
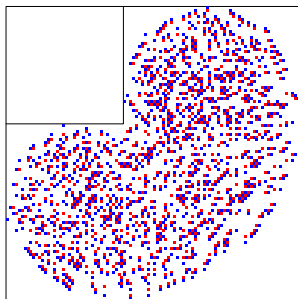


Principle 1: Geometric Tangent Method

Call Λ the domain shape, and \mathcal{C} the corresponding Arctic Curve.

In the large n limit, a typical refined ASM on Λ , for having a $+1$ at position r along l_1 , shows the Arctic Curve \mathcal{C} of unrefined ASM, plus a straight path from r to the tangent point on \mathcal{C} .

The strategy: trying a precise statement

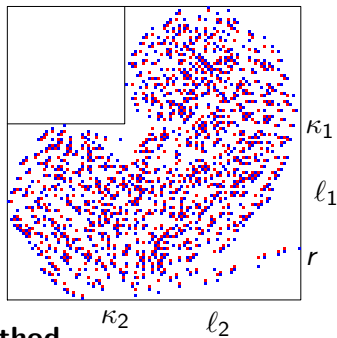
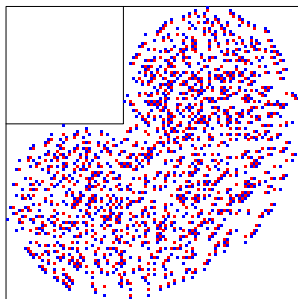


Principle 2: Entropic Tangent Method

Call Λ the domain shape, and \mathcal{C} the corresponding Arctic Curve.

Call Λ' the domain Λ minus one row/column along the sides containing κ_1 and κ_2

The strategy: trying a precise statement

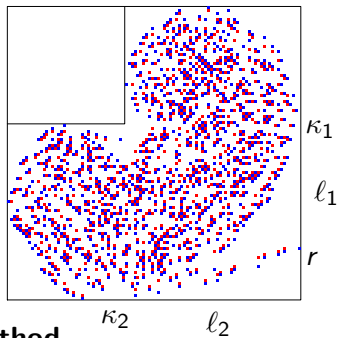
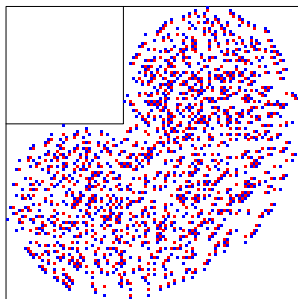


Principle 2: Entropic Tangent Method

Call $A(\Lambda)$ the number of ASM in Λ , and $A^{(1,2)}(\Lambda, r)$ the refined ASM enumerations along $\ell_{1,2}$.

Say $X(n) \sim Y(n)$ if $\lim_{n \rightarrow \infty} \frac{1}{n} \ln \frac{Y}{X} \sim \ln n$.

The strategy: trying a precise statement



Principle 2: Entropic Tangent Method

Then

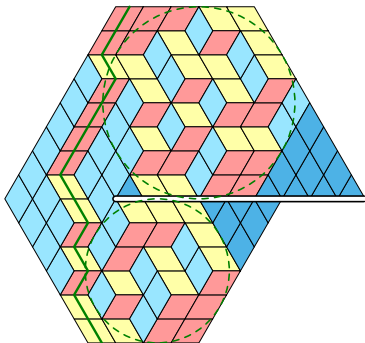
$$A^{(1)}(\Lambda, r)A^{(2)}(\Lambda, s) \sim A(\Lambda)A(\Lambda') \binom{r+s}{r}$$

If and only if the line $((0, r), (s, 0))$ is tangent to \mathcal{C} .

Does this really work?

① Yes, both methods, for the Arctic Circle in lozenge tilings of the regular hexagon

(hint: use the formula for Semi-strict Gelfand Patterns to deduce all the refined enumerations you may need)



Does this really work?

① Yes, both methods, for the Arctic Circle in lozenge tilings of the regular hexagon

(hint: use the formula for Semi-strict Gelfand Patterns to deduce all the refined enumerations you may need)

② Yes, both methods, for the Colomo-Pronko $\omega = 1$ Arctic Curve

Does this really work?

① Yes, both methods, for the Arctic Circle in lozenge tilings of the regular hexagon

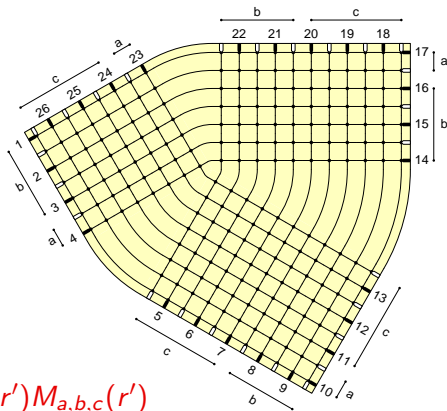
(hint: use the formula for Semi-strict Gelfand Patterns to deduce all the refined enumerations you may need)

② Yes, both methods, for the Colomo-Pronko $\omega = 1$ Arctic Curve

③ Yes, the “geometric method”, for deriving the Colomo-Pronko “caustic theorem” at generic ω (as it is harder, I did not try the entropic method)

Well ok... what about some new result?

The severe bottleneck for obtaining arctic curves in new geometries is the absence of exact formulas for the refined enumerations...
...but we have a nice candidate, our favourite triangloid domain!



Recall from yesterday:

$$A_{a,b,c} = A_{a+b+c} M_{a,b,c}$$

...but more is true!

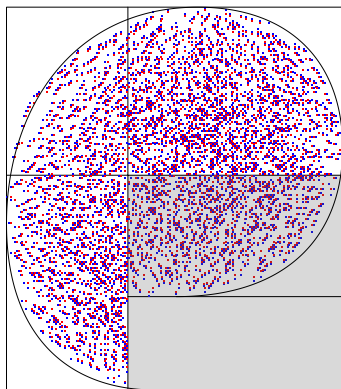
Call $n = a + b + c$,

$$A([a, b, c], r) = \sum_{r'} A(n, r - r') M_{a,b,c}(r')$$

The arctic curve for the triangoloid

Very easy to find the position of tangence points κ_j .
Then, finding the arc between two of these points is harder but feasible (through the entropic method)... finally you get a parametric expression (here $a = 1 - b - c$, $p \in [0, 1]$, $q = 1 - p$)

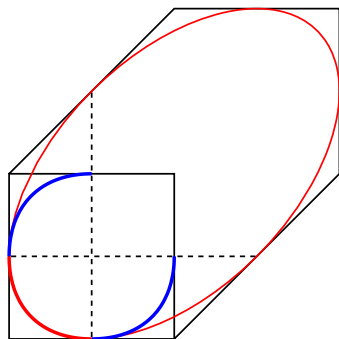
$$x(b, c, p) = \frac{3 - c}{2} - \frac{2 - p}{2\sqrt{1 - pq}}$$
$$- \frac{(1 - c)(1 - (pb + qc)) - 2pbc}{2\sqrt{(pb - qc)^2 - 2(pb + qc) + 1}};$$
$$y(b, c, p) = x(c, b, 1 - p).$$



Analytic continuation

The surprises are not over...

Just like the arc of the Colomo-Pronko Arctic Curve can be completed to a certain ellipse...



$$x(1-x) + y(1-y) + xy = 1/4$$

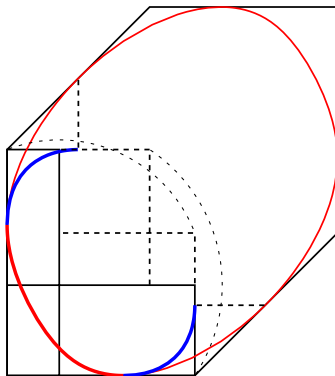
Analytic continuation

The surprises are not over...

Just like the arc of the Colomo-Pronko Arctic Curve can be completed to a certain ellipse...

...we can try to continue analytically our curve. We get a closed curve composed of 6 arcs, for the intervals $p \in (-\infty, 0], [0, 1], [1, +\infty)$, and a \pm -choice for square roots.

This curve is framed into a hexagonal box, with side-slopes $0, 1, \infty$ and nice rational tangence points.



The shear phenomenon

Fact:

Consider a given arc of the triangoloid arctic curve \mathcal{C} (the one “near vertex A ”)

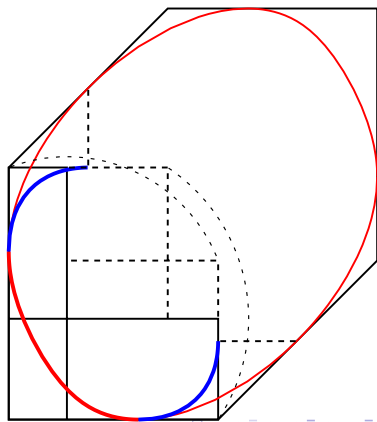
The two other arcs of \mathcal{C} (the ones “near vertices B and C ”) **do coincide** with the **45-degree shear** of the neighbouring arcs in the boxed analytic continuation of the first arc.

This fact is of course true also in Colomo-Pronko ellipse, but here it sounds much more striking: we have **two free parameters** (b/a and c/a), and the single arcs do not have a **polynomial Cartesian representation**

It is believable that this points towards the **universality** of the shear phenomenon, for any tangent point of the arctic curve \mathcal{C} on its boxing domain Λ , for $\omega = 1$ ASM.

The shear phenomenon

$$x(b, c, p) = \frac{3-c}{2} - \frac{2-p}{2\sqrt{1-pq}} - \frac{(1-c)(1-(pb+qc)) - 2pbc}{2\sqrt{(pb-qc)^2 - 2(pb+qc) + 1}};$$
$$y(b, c, p) = x(c, b, 1-p).$$



THIS SHOULD BE THE END OF THE THIRD LECTURE...